To nanu,

PEPTIDE THERAPEUTICS TO PREVENT PROTEIN AGGREGATION IN HUNTINGTON'S DISEASE

A THESIS SUBMITTED TO

THE GRADUATE SCHOOL OF ENGINEERING AND SCIENCE

OF BILKENT UNIVERSITY

IN PARTIAL FULFILLMENT OF THE REQUIREMENTS FOR THE

DEGREE OF
MASTER OF SCIENCE

IN
NEUROSCIENCE

BY

ANOOSHAY KHAN

SEPTEMBER 2022

PEPTIDE THERAPEUTICS TO PREVENT PROTEIN AGGREGATION
IN HUNTINGTON'S DISEASE

By Anooshay Khan

We certify that we have read this dissertation and that in our opinion it is fully adequate, in scope and in quality, as a thesis for the degree of Master of Science.

_____

Urartu Özgür Şafak Şeker(Advisor)

_____

Michelle Adams

_____

Gül Yalçın Çakmaklı.

Approved for the Graduate School of Engineering and Science:

_____

Ezhan Karaşan Director of the Graduate School

PEPTIDE THERAPEUTICS TO PREVENT PROTEIN AGGREGATION IN HUNTINGTON'S DISEASE

Anooshay Khan

M.SC in Neurosciences

Advisor: Urartu Özgür Şafak Şeker

September 2022

Huntington's disease is a progressive, autosomal dominant neurodegenerative disease caused by dramatic CAG repeat expansion in exon 1 of the Huntington (HTT) gene. More than 36 CAG repeats lead to the generation of mutant HTT (mHTT) fragments. These amino-terminal mutant HTT fragments result in misfolded proteins that give rise to oligomers and subsequent aggregate formation in relevant brain areas. Available therapies mainly focus on ameliorating the symptoms of the disease. Therefore, therapeutic interventions which can delay the onset of disease are imperative for halting disease progression. Peptide-based drug therapy provide such a platform. Previously in our lab, candidate ligand peptides were screened against both willd type (Htt-Q25) and mHTT fragments such as Htt-Q46, and Htt-Q103. This was done using different display technologies

This work focuses on the in vitro characterization of those selected peptides. Fibril formation was observed in real-time using Thiofllavin T assay. Selected peptides were added to check their effect on fibril formation by change in fluorescence signal. The effect of peptides on fibril formation was also studied using Atomic Force microscopy. 3 of the 6 selected peptides (HHGANSLSLVSQD), (HGLHSMHNKLTR) and (WMFPSLKLLDYH) successfully showed a blocking in aggregation. These s

tudies show that the selected peptides are affective for inhibiting the aggregation of fibrils in mHTT proteins.

Key words: Huntington's Disease, Peptide-based Drug therapy

ÖZET

HUNTINGTON HASTALIĞINDA PROTEİN AGREGASYONUNU ÖNLEMEK İÇİN PEPTİT TERAPİLERİ

Anooshay Khan

Nörobilim, Yüksek Lisans

Danışman: Urartu Özgür Şafak Şeker

eylül 2022

Huntington hastalığı, Huntington (HTT) geninin ekson 1'inde dramatik CAG tekrar genişlemesinin neden olduğu ilerleyici, otozomal dominant nörodejeneratif bir hastalıktır. 336'dan fazla CAG tekrarı, mutant HTT (mHTT) fragmanlarının üretilmesine yol açmaktadır. Bu amino-terminal mutant HTT fragmanları, ilgili beyin bölgelerinde oligomerlere ve müteakip agregasyon oluşumuna yol açan yanlış katlanmış proteinlerle sonuçlanır. Mevcut tedaviler esas olarak hastalığın semptomlarını iyileştirmeye odaklanır. Bu nedenle, hastalığın başlangıcını geciktirebilecek terapötik müdahaleler, hastalığın ilerlemesini durdurmak için zorunludur. Peptid bazlı ilaç tedavisi böyle bir platform sağlar. Daha önce laboratuvarımızda aday ligand peptitleri, hem doğal fenotipi (25Q-Htt) hem de 46Q-Htt ve 103Q-Htt gibi mHTT fragmanlarına karşı taranmıştı.

Bu çalışma, seçilen peptitlerin in vitro karakterizasyonuna odaklanmaktadır. Thioflavin T tahlili kullanılarak gerçek zamanlı olarak fibril oluşumu gözlemlenmiştir. Floresan sinyalindeki değişiklikle fibril oluşumu üzerindeki etkilerini kontrol etmek için seçilen

peptitler eklenmiştir. Peptitlerin kümelenme kinetiği üzerindeki etkisi Atomik Kuvvet mikroskobu kullanılarak da incelenmiştir. Seçilen 6 peptitten 3'ünün (HHGANSLSLVSQD, HGLHSMHNKLTR ve WMFPSLKLLDYH) agregasyonu başarılı bir şekilde bloke ettiğini gösterilmiştir. Bu çalışmalar, seçilen peptitlerin, mHTT proteinlerinde fibrillerin toplanmasını inhibe etmede etkili olduğunu göstermektedir.

Anahtar Kelimeler: HUNTINGTON HASTALIĞINDA, PEPTİT TERAPİLERİ

ACKNOWLEDGEMENTS

I would like to express my gratitude and thanks to my advisor Dr. Urartu Özgür Şafak Şeker. During my last three years at Dr. Sekers lab group, I learned a lot and explored different fields of synthetic biology. Coming from neurosciences department and having only verbose knowledge about synthetic biology, I had tremendous opportunity to grow and learn in the realms of synthetic biology by the constant guidance and mentorship of Dr. Seker.

I would like to thank Dr Esra Yuca, who guided me and helped me at every step. I am thankful to all my lab members, my collogues who made the lab pleasant environment to work in. I would especially like to thank Cemile Elif Ozcelik, for her kindness and patience and without whom this project wouldn't have been possible.

I would like to thank all the group members of Synthetic Biosystems Laboratory group members; Ahmet Hınçer, , Çisil Köksaldı, Dr. Ebru Aras, Dr. Ebru Şahin Kehribar, Eray Ulaş Bozkurt, Gozeel Binte Shadid, Julian Ostaku, Merve Erden Tüçer, Merve Yavuz Nedim Kurt, Recep Erdem Ahan, Sıla Köse, Ece Avici, and Suat Tüçer. It was a pleasure working with you all.

Lastly, I want to express my greatest gratitude to my family for their endless support and Love, to Mama and baba, to Danish and Tabish, to Ali, Mahnoor, Amina, Hira, Hani, Usama, Zain, Faaiz, Yusuf, Mayssam, Lidia, Salman, Loulwa, Sheila, my chosen family, to the Simpsons and to all the Yaars. Thank you for everything.

This study was supported by TUBITAK, project number 216S127

TABLE OF CONTENTS

CHAPTER 1 1

INTRODUCTION 1

1. 1.1. Huntington's disease (HD) background……1

   1.11 Epidemiology……1

   1.12 Molecular feature……...2

2. 1.2. Protein aggregation in HD.....2

   1.2.1 Etiology……..5

3. 1.3 Therapies for Huntington's Disease……5

   1.3.1 Specific and radical treatments for HD: molecular targets……..5

   1.3.2 Symptomatic and palliative therapies for HD……8

4. 1.4 Peptide-based therapeutics for HD……9
5. 1.5 Previously screened ligand peptide……9
6. 1.6 Aim of the study……. 9

CHAPTER 2 10

MATERIALS AND METHODS 10

1. 2.1. Plasmid Design, Cloning and Transformation..... 10

2. 2.2. GST-Htt protein Expression.....11
3. 2.3. SDS-PAGE and Western Blot for GST-Htt proteins..... 12
4. 2.4. Purification of GST-Htt proteins and Buffer Exchange……..13
5. 2.5 Removal of GST tag from GST-Htt proteins…….15
6. 2.6. Tev Reaction for Removal of GST Tag…….16
7. 2.7 Western Blot for GST removed Htt proteins with MW1 antibody……16
8. 2.8. Congo-Red Assay……17
9. 2.9 Peptide Synthesis……18
10. 2.10 Thioflavin (T) Assay……19
11. 2.11 Atomic Force Microscopy……20

CHAPTER 3..... 11

RESULTS AND DISCUSSION..... 28

3.1. Expression of GST-HTT(1) proteins and removal of GST tag.....28

3.1.1. Congo Red assay to visualize Htt amyloid fibril……30

3.1.2.Thioflavin T Assay…….. . 31

3.2... Atomic Force Microscopy for HTT (Q103)……..55

3.3 Atomic Force Microscopy for HTT (Q46)……58

3.4 Atomic Force Microscopy for HTT (Q25)…….60

CHAPTER 4 64

CONCLUSION 65

BIBLIOGRAPHY 66

APPENDIX A 78

Plasmids constructs used in this study 78

APPENDIX B 81

Inhibitory Peptide Alignment with Htt proteins 84

APPENDIX C 100

Buffers and Media used in this study 100

APPENDIX D 100

Concentration optimization for tht assay (Q103) 102

APPENDIX E..... 100

Concentration optimization for AFM (Q46)..... 103

List of tables

Table1. List of previously screened candidate ligand peptides……18

Table 2. Summarizes the increase or decrease in fluorescence detected after tht assay for all three Htt proteins, in the presence of all 6 peptides……54

Table C1. Lysogeny Broth recipe ……..81

Table C2. Autoinduction ZYM5052…….81

Table C3. Binding and elution buffer for HisPur Cobalt resin…..82

Table C4. Table C3 Binding and elution buffer for Ni-NTA column….82

List of Figures

Figure1. Schematics showing Molecular Pathology of HD…….3

Figure2. Schematic representation of the enzymatic activity of tev protease enzyme. Tev protease makes site specific cleavage at ENLYFQG between GST and Htt Protein……...22

Figure 3. Western blot analysis with MW1 antibody for Htt(Q25) for tev cleavage optimization……...23

Figure4. Western blot analysis with anti-His antibody for Htt(Q25) for tev cleavage optimization……...24

Figure 5. Western blot analysis with MW1 antibody for Htt(Q46) for tev cleavage optimization……...25

Figure 6. Western blot analysis with anti-His antibody for Htt(Q46) for tev cleavage optimization……...26

Figure 7. Western blot analysis by MW1 antibody for GST cleaved Htt proteins……28

Figure 8. Coomassie Blue staining for GST cleaved Htt proteins……29

Figure 9. Congo Red staining for Htt (Q103) fibrils……30

Figure 10. Aggregation kinetics for Htt(103Q) shown in real time by tht assay……..32

Figure11. Aggregation kinetics for Htt(Q103) shown in real time by tht assay with HHGANSLGLVQS…… 33

Figure12. Aggregation kinetics for Htt(Q103) shown in real time by tht assay with SWPLTPVRFMTE……34

Figure 13. Aggregation kinetics for Htt(Q103) shown in real time by tht assay with HGLHSMHNKLQD……35

Figure 14. Aggregation kinetics for Htt(Q103) shown in real time by tht assay with FQKEDAWEAVDIR……..36

Figure 15 Aggregation kinetics for Htt(Q103) shown in real time by tht assay with WMPSLKLLDYH …….37

Figure16 Aggregation kinetics for Htt(Q103) shown in real time by tht assay with HVTFKFQWDRES ……38

Figure17. Aggregation kinetics for Htt(Q46) shown in real time by tht assay with HHGANSLGLVQS……39

Figure18. Aggregation kinetics for Htt(Q46) shown in real time by tht assay with SWPLTPVRFMTE……40

Figure 19. Aggregation kinetics for Htt(Q46) shown in real time by tht assay with HGLHSMHNKLQD……41

Figure 20. Aggregation kinetics for Htt(Q46) shown in real time by tht assay with FQKEDAWEAVDIR……..42

Figure 21 Aggregation kinetics for Htt(Q46) shown in real time by tht assay with WMPSLKLLDYH …….43

Figure22 Aggregation kinetics for Htt(Q46) shown in real time by tht assay with HVTFKFQWDRES …….44

Figure23. Aggregation kinetics for Htt(Q25) shown in real time by tht assay with HHGANSLGLVQS…… 45

Figure 24. Aggregation kinetics for Htt(Q25) shown in real time by tht assay with SWPLTPVRFMTE……46

Figure 25. Aggregation kinetics for Htt(Q25) shown in real time by tht assay with HGLHSMHNKLQD……47

Figure 26. Aggregation kinetics for Htt(Q25) shown in real time by tht assay with FQKEDAWEAVDIR……..48

Figure 27 Aggregation kinetics for Htt(Q25) shown in real time by tht assay with WMPSLKLLDYH …….49

Figure 28 Aggregation kinetics for Htt(Q25) shown in real time by tht assay with HVTFKFQWDRES ……52

Figure 29. AFM images of aggregation kinetics of HttQ103……..55

Figure 30. Graphs of Aggregation kinetics HttQ103 (fibril length w.r.t time)…… ….57

Figure 29. AFM images of aggregation kinetics of HttQ46……..58

Figure 30. Graphs of Aggregation kinetics of HttQ46 (fibril length w.r.t.time)……60

Figure 29. AFM images of aggregation kinetics of HttQ25…….61

Figure 30. Graphs of Aggregation kinetics of HttQ25(fibrillength w.r.t.time)……63

CHAPTER 1

1 Introduction

A chronic neurological disorder that causes choreatic movements, behavioral disturbances, and dementia, Huntington's disease (HD) is caused by a malfunctioning nervous system [1]. Its an age-onset neurodegenerative disease, and has been a subject of scientific and medical fascination for decades [2].

1.1 Huntington's disease background

HD patients may experience subtle involuntary movements, executive function difficulties, and depression in the early stages [1]. In 1872, The classic description of HD by George Huntington (Huntington, 1872) sparked widespread interest. HD can still be diagnosed based on movement disorders, emotional disturbances, and cognitive impairment from a clinical trial that clarifies the familial basis and gives insight into the clinical trial findings. The majority of patients with this condition remain independent, but assistance becomes more necessary as the disease progresses. Due to their lack of voluntary motor control and uncontrollable involuntary movements, HD patients can become bedridden, require feeding tubes, and cannot speak [1]. As dementia progresses, it often affects all aspects of cognition at this stage in its progression [27]. The most common reason of death is infections, specifically aspiration pneumonia, which occurs 18 years after symptoms begin [28].

1.1.1 Epidemiology

Worldwide, every 2.7 per 100,000 people are directly affected by HD [25]. People from Western countries tend to have the highest prevalence rates, while those from Asian countries like Japan, Korea, Taiwan, and Hong Kong tend to have the lowest prevalence rates [30]. The HTT gene haplotypes could be responsible for these differences[31]. Since HD is an age onset

disease, the symptoms of these conditions often arise gradually and are insidious. Initially, the patient may not recognize them for several years before they are diagnosed [42].

1.1.2 Molecular Feature:

The HD gene on chromosome 4p16.3 [10] encodes Huntingtin, a protein of 3136 residues and a molecular weight of 360 kDa. An anonymous marker was first used to map HD in 1983 [2]. The molecular and cellular mechanisms underlying HD have made significant progress in recent years. The advancement of linkage analysis through molecular tools for predictive genetic testing [5].The CAG tri-nucleotide repeat expansion, the causative mutation, was identified after a decade-long struggle with positional cloning [10].

In HD, glutamine units (Gln) are repeated near the amino-terminus (beginning at residue 18) of huntingtin as a result of the unstable CAG trinucleotide expansion in the first exon [11]. The CAG/polyGln expansion of a normal individual varies from 6 to 39 units, whereas the expansion of a HD patient varies from 36 to 180 units[12]. PolyGln expansion overlaps between normal and pathological ranges, suggesting that HD has multiple causes or that some populations are incompletely affected. DNA replication may be disrupted by CAG repetitions by forming stable hairpin structures and mismatched duplexes, which may result in replication fork slippage [14][15]. Increasing CAG repeats are associated with disease progression, and paternal transmission tends to increase them [16].

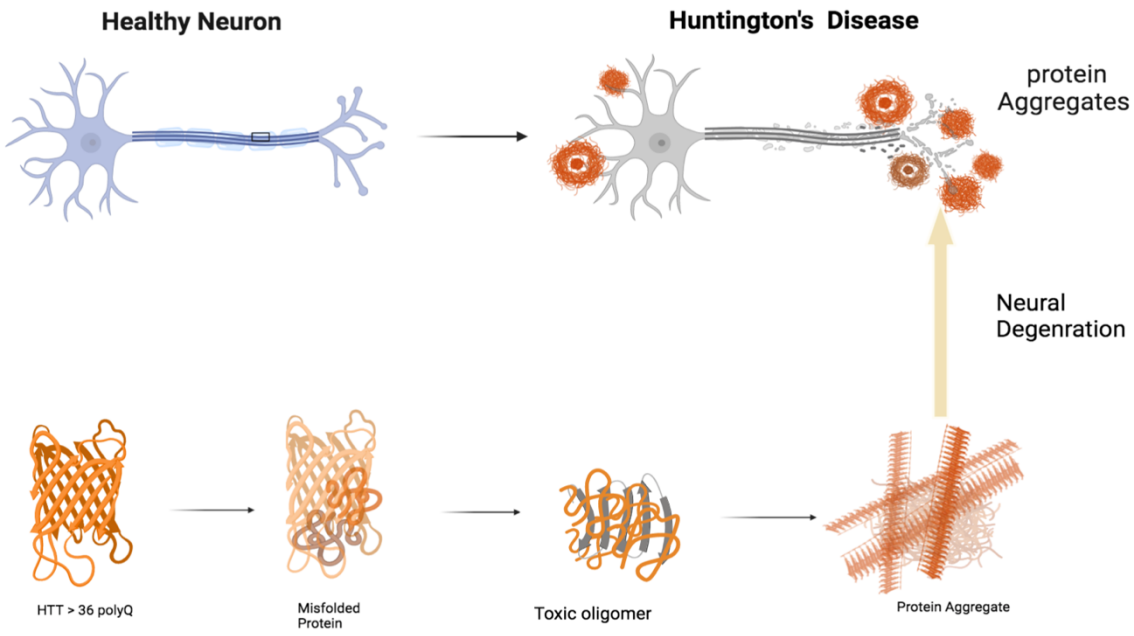

Figure1. Schematics showing Molecular Pathology of HD

1.2 Protein aggregation in Huntington disease

Inheritance of HD is autosomal dominant and located on chromosome 4 (4p16.3). In the HD gene coding region, the CAG repeat has expanded [10]. In the HD gene, huntingtin (HTT) protein is encoded; the protein is abundant throughout the body, but highest in the central nervous system (CNS). A variety of cellular events, including protein trafficking, transporting vesicles, and selective autophagy, have been proposed to rely on this protein. The function of this device has not yet been fully understood [33]. In subsequent generations, and particularly if they are passed down paternally, CAG sequences that exceed 6–26 repetitions may become unstable. Typically, individuals with the clinical phenotype have 27 to 35 repeats in their genome. It is commonly believed that HD can develop when 36 repeats or more are present, although full penetration does not occur until 40 repeats [35]. High CAG repeat counts have also been linked to an earlier onset, faster progression of disease, and an increase in severity of the disease [36]. A combination of predispositions to HD, as well as environmental factors, may contribute to its etiology and progression [37].

A number of neurodegenerative diseases are associated with CAG/polyglutamine expansions in coding regions of proteins, such as dentatorubral pallidoluysian atrophy, spinobulbar muscular atrophy, and spinocerebellar ataxias. Types 1, 2, 3, (Machado-Joseph disease) and types 6 and 7 are among them [17][18][19][20][21]. In these diseases, insoluble nuclear inclusions are formed in neurons, disrupting nuclear function and contributing to neurodegeneration. This suggests a common cellular basis for regional brain pathologies [22]. In the affected brain areas, these aggregates cause cell death and dysfunction, which eventually result in severe atrophy [40]. It appears that these aggregates primarily affect the striatum, which consists of the caudate nucleus, the putamen, the nucleus accumbens, and the olfactory tubercle. Neuronal intranuclear inclusions, or NIIs, have been observed post-mortem in both nuclei and cytoplasm of neurons [41]. HD is characterized by prominent striatal atrophy as a neuropathological hallmark. As well, select nuclei of the cerebral cortex, cerebellum, hypothalamus, hippocampal region, and brain stem have been reported to have atrophy[41].

Although the causal relationship between neuronal intranuclear inclusion formation and HD has not been proven, the gradual deposition of amyloids in neurons that degenerate in HD would be consistent with the late onset and progressive nature of symptoms. Therefore elucidation of underlying molecular mechanisms of amyloid formation and the explanation of why the huntingtin protein with an expanded poly(Q) stretch (38–100 and more residues), or an N-terminal fragment thereof, aggregates in diseased individuals, whereas the same protein with a poly(Q) tract in the normal range (6–37 residues) does not [56]; has attracted interest of scientist worldwide. It has been established that a nucleus that is formed before polymerization occurs predicts certain characteristics of the aggregation process, including (i) dependence on exceeding a critical protein concentration for the initial formation of aggregates and (ii) kinetics displaying a lag phase during which nuclei forms.

Formation of HDex1p Aggregates Is Nucleation-Dependent.

In a typical nucleation-dependent polymerization, polymer is not observed until the monomer concentration exceeds a certain critical concentration. Above that level, polymerization does not proceed immediately but after a defined time period, or lag time (Jarrett and Lansbury, 1993). Consistent with these predictions, it was revealed that the in vitro aggregation of poly(Q)-containing HDex1 peptides depends on both protein concentration and time [56].

1.1.2 Etiology

Protein encoded (HTT) by the gene that plays a role in synaptic function and post-embryonic development. In addition to having anti-apoptotic properties, it protects against toxic mutants of HTT. Mutant proteins may have both new and lost functions, according to some evidence. A number of brain areas contain intranuclear and intracytoplasmic inclusions. The inclusions themselves are unknown, however, as to whether they play a role in pathogenesis. Neuronal loss, particularly in the striatum, is well known to accompany brain atrophy [23].

Those with CAG repeats 36-55 are commonly carriers of the HTT allele. With juvenile-onset disease, CAG repeats usually exceed 60. There is no disease phenotype in patients with alleles between 27 and 35, but the patient is susceptible to repeat instability [1].

1.3 Huntington disease therapies

The therapeutic potential of HD

In spite of HD's rarity, it receives a great deal of examination attention, in part because it is more tractable than other neurodegenerative conditions due to its few features. Firstly, because the condition is autosomal dominant, it can be diagnosed almost definitively and even prior to death. In vitro and in vivo models can then be accurately developed, and patients can be assured that they suffer from a reasonably homogeneous condition. It is rarely possible to make a definitive diagnosis in other types of dementia, and autopsy analysis often reveals a mix of pathologies. It is also possible to diagnose the condition before symptoms appear, since it is

familial. The importance of early diagnosis is that it allows treatment to begin before significant neuronal damage occurs, which may make slowing progression even more difficult and make it impossible to correct existing deficits by that point in the illness [24].

Tremendous molecular research has been conducted for understanding the pathology of the disease. In laboratories around the world today, cell therapy and gene therapy of HD are not just a dream. As a result, it is pertinent to summarize the progress made, particularly in treating HD .

1.3.1 Specific and radical treatments for HD

Neuroprotective strategies

Neuroprotective therapies would be most effective in individuals with proven genetic risk before symptoms of HD appear because neurodegenerative processes begin long before symptoms appear (Hersch and Rosas, 2008). The treatment of mutant Htt itself seems to be an attractive therapeutic strategy. Bringing mutant Htt levels down may reduce aberrant protein interactions, reducing neurotoxicity in experimental disease models. It was initially shown that stopping mutant Htt expression could stop and even reverse HD progression in mice using a mutant Htt transgene model as a proof-of-concept [9].

Symptomatic and palliative therapies for HD

Drugs that are A receptor antagonists have shown to reduce choreographic movements and psychiatric disorders**.** [44].

Stereotaxic surgery for choreic movements

Ansa lenticularis, which is the origin of the common path, and globus pallidus (the internal segment) are generally targeted during HD surgery [46]. However In most cases, the outcome is not disappointing since the disease is highly progressive.

The aforementioned treatments mainly focus on ameliorating the symptoms of the disease but not the progression of the disease it-self. Recently Peptide based drug therapeutics that work towards halting the disease progression have come into light.

1.4 Peptide-based therapeutic approach

The peptide bond links amino acids together in small molecules called peptides. As a result of their targeted action and ability to reach difficult-to-reach locations in the body, these peptides are considered to have tremendous potential in disease-modifying treatments. Carnosine, a peptide found in nature, is currently being researched for treatment of Neurodegenerative Disorders (NDDs). Dementia, for example, is under intense research using peptide-based vaccines [58]. The use of peptides as therapeutics has a long and successful history in the management of disease. Bioactive peptides play a wide variety of roles in biological functions and contribute to human health. Antioxidants, antimicrobials, and antithrombotic effects are just a few of the therapeutic effects of peptides.

Peptide-based therapeutic for HD have shown promising results by hampering the progression of disease by preventing aggregation. Some of the highlighted studies in this regard as following,; An alpha-helix separated polyQ region (25Q) was found to colocalizes with polyQHtt protein aggregates and interacts with them. Drosophila HD models treated with this peptide were able to reduce and delay aggregate formation, increase survival, reduce degeneration and formation of eye aggregates, and inhibit brain aggregate formation in the presence of COR-1 hHtt17aa-103Q [47].

Polyglutamine binding peptide 1 (QBP1) was found to be particularly effective in binding abnormal polyQ molecules using combinatorial screening [48]. A Drosophila HD model showed that it improved survival, reduced aging, and reduced aggregate formation when it co-localized with aggregate formation, reducing aggregate formation in cultured cells [48]. In order to facilitate efficient delivery to cells, these short peptides of PTDs and CPPs have been

conjugated to QBP1[50]. When cells were internalized with HIV, a protein called TAT allowed them to access their cytoplasm and nucleus[51]. Antp-QBP1 significantly increased the bioavailability of the modified peptide in the MJD fly, a Drosophila model of polyQ-induced spinocerebellar ataxia 3. In addition, Antp-QBP1 significantly reduced the rate of premature death in PolyQ-MJD flies [52].

A caspase-6 inhibitor has also been developed and tested on the BACHD mouse model with full-length 97Q-mHtt mutations, which is an important step in HD development [54]. HTT competes with the caspase-6 active site for space, ED11 inhibited caspase-6 activity in cells and enhanced cell penetration using HIV TAT-derived peptides. There was a selective interference effect of caspase 6 with only minor effects on caspase 1 and 10. ED11 administered continuously under the skin with a minipumps resulted in a reduction in depressive behavior, weight loss, and improved cognitive performance at the presymptomatic stage. Postsymptomatic ED11

administration improved motor performance, cognition, and depression. BACHD mice transgenic with hHtt-97Q showed no sign of atrophy or aggregation. This makes it impossible to evaluate ED11's effectiveness on these features. Neither mice nor cells showed toxicity after prolonged administration[54].

These all peptides demonstrated a considerable decrease in the aggregation of HD.

1.5 Previously screened ligand peptide

Our group member Cemile Elif Ozcelik in her master's thesis screened candidate ligand peptides screened against both wild type (25Q-Htt) and mHTT fragments such as Htt(Q46),

and Htt(Q103). This was done using display technologies such as yeast surface display system and M13 phage display library. The monomers of Htt were displayed on the surface of yeast and candidate inhibitory peptides were selected by phage display library. The candidate peptides were selected after 4 rounds of biopanning and the model of their interaction with proteins were predicted by online tools.

1.6 Aim of the study

Available therapies for HD mainly focus on ameliorating the symptoms of the disease. Therefore, therapeutic interventions which can delay the onset of disease are imperative for halting disease progression. Peptide-based drug therapy provide such a platform. As described above, Inhibitory peptides that interact with the mutant Huntington fibrils at early stages can block aggregation. This work focuses on the *in vitro* characterization of previously screened ligand peptides. The aim of this study was to evaluate whether the screened peptides interacted with the mHtt proteins to inhibit the fibril formation in mHTT proteins.

Chapter 2 Materials and methods

2.1 Designs and Cloning

6His-GST-htt-(Q25), 6His-GST-htt-(Q46) and 6His-GST-htt-(Q103) were designed and cloned in PET22b (+) ampR vector by our lab member Cemile Elif Ozcelik. Tev cleavage site was designed between the 6His-GST and Htt proteins and the construct was cloned downstream to T7 promoter region. The sequence was verified by (NGS) sequencing

2.Transformation

Sequence verified PET22b 6His-GST-htt-protein plasmids were then chemically transformed in *E. coli* BL21 (DE3) strain for protein expression. For the preparation of chemical competent cells, *E. coli* BL21 (DE3) cell stock stored previously at -80 was inoculated and grown in Lysogeny Broth (LB) media for 16hours at 37C. The following day, cells were diluted in fresh LB with a dilution factor of 1:100. The cells were then grown till the OD600 reached 0.3. Cells were placed on ice and cooled for 10 minutes. After this, the cells were centrifuged at 1000 x g for 10 minutes. The supernatant was discarded and the cell pellet was resuspended in TSS Buffer. The volume of TSS buffer was 1:10 of the original cell growth media. The cells were then aliquoted as 100µl in 1.5 ml micro-centrifuge tubes and were then stored in -80℃.

To perform transformation, chemically competent *E. coli* BL21 (DE3) cell stock were thawed on ice for 20 minutes. 100 ng of isolated plasmid was then mixed into the thawed cells. The cell-plasmid mixture was incubated again on ice for 15 minutes. After this the cells were heat shocked by placing them on heat block at 42℃ for 45 seconds. Immediately after this the cells were incubated on ice for 2 minutes. 450µl of LB was then added on the cells and the cells were incubated at 37℃ for 45 minutes in shaking incubator (200rpm) for cell recovery. The cells were then centrifuged at 4500rpm for 5 minutes. 300ul of supernatant was then discarded and the cell pellet was resuspended in the remaining 150ul media. The cells were

then spread onto ampicillin resistant LB-agar plates. The agar plates were incubated at 37C overnight.

Protein Expression

Next day, a single colony from each transformed plate was inoculated in LB containing 100mg/ml ampicillin. The cells were then grown at 37C, 200rpm in the shaking incubator overnight. For the production of 6His-GST-htt-exon1 (Q103), the overnight culture was diluted in LB with 1:100 ratio and grown in 37C shaking incubator till the OD600 reached 0.4-0.6 (mid-log phase), the expression of 6His-GST-htt-exon1 (Q103) was induced by the addition of 1mM of IPTG (isopropyl β- D-1-thiogalactopyranoside). The cells were then grown at three different conditions. These were 37C for 4 hours, 30C for 8 hours and 16C for 18 hours. Best growth condition at 37C for 4 hours was selected for protein expression after SDS-PAGE and Western blot analysis.

6His-GST-htt-(Q46) and 6His-GST-htt-(Q25) were expressed using ZYM5052 autoinduction media. The overnight cultures grown in LB were diluted in autoinduction media in 1:100 ratio and grown at 37C for 20-24 hours.

SDS-PAGE and Western Blot

Following the induction, 20ul cells from each sample were centrifuged. The supernatant was discarded and the pellet was resuspended in 20ul of ddH_2O. 4ul of 6X SDS loading dye was added. The samples were then boiled at 95C for 5minutes for SDS-PAGE analysis. The samples were loaded on 12% SDS-PAGE gel and 80V was applied until the samples passed through the stacking gel. As the samples reached the separating gel, the voltage was increased to 120V and the gel was ran for 1.5 hours in 1x SDS running buffer.

For SDS-PAGE analysis, the gel was transferred to Coomassie blue staining dye and was heated for 30 seconds in the microwave. The gel was then incubated for 10 minutes at room temperature by gentle shaking. Following this, the excess dye was washed off by water and the gel was transferred into destaining buffer composed of 30% methanol, 10% acetic acid and 60% water. The gel was incubated in destaining buffer at room temperature over night by gentle shaking. Once the proteins bands were visible the destaining dye was removed and the gel was visualized by Fusionâ Software of Vilber Lourmat imaging system.

Western Blotting for 6His-GST-Htt proteins

For the detection of the desired proteins by western bot analysis, the gel was subjected to semi-wet protein transfer onto a polyvinylidene difluoride (PVDF) membrane (Thermo Fisher Scientific). The activation of PVDF membrane was done by placing the membrane in methanol for 2 minutes and then equilibrating it in Turbo Transfer buffer (Bio-Rad). Meanwhile two watt man filter papers were soaked in into Turbo Transfer buffer as well. One filter paper was placed on the cathode of the transfer cassette, followed by the PVDF membrane, the gel was placed and lastly the other filter paper was placed on top. The cassette was tightly closed and semi-dry transfer protocol from the Transblot Turbo Transfer System was selected. The transfer of proteins from the gel to the membrane was completed in 7 minutes after which the membrane was placed in the blocking solution (comprising of 1x Tris Buffer Saline Tween (TBS-T (0.1%)) and 5% skimmed milk) for 1 hour at room temperature. This was done to prevent any unspecific binding. After the blocking, primary antibody incubation was performed. The membrane was incubated in His-Tag Mouse McAB (Proteintech Europe) antibody, diluted at 1:10000 in %5 milk powder and TBS-T. The incubation was performed at +4 overnight. The membrane was then washed in TBS-T for once for 5 minutes, then twice for 10 minutes each. After this the membrane was incubated in

secondary antibody (comprising HRP conjugated goat anti-mouse antibody) (Abcam) in 1:10000 blocking solution) for 1 hour at room temperature. The membrane was again washed in TBST by the same way as described above. After this the membrane was visualized using Enhanced chemiluminescence (ECL) (Bio-Rad) solution. This was prepared by mixing equal volumes of Clarity Western Luminol/Enhancer Reagent and Clarity Western Peroxide Reagent. The solution was poured over the membrane which was then incubated in dark for 2 minutes. The membrane was visualized by Fusionâ Software of Vilber Lourmat imaging system.

Purification of 6His-GST-Htt proteins

All three 6His-GST-htt-(Q103), (Q46), (Q25) proteins were induced in 200ml media as described above. The cell culture was then centrifuged at 8000 rpm for 5 minutes and the supernatant was discarded. The cell pellet was resuspended in 20ml binding buffer (20 mM sodium phosphate, 0.5 M NaCl, 20 mM imidazole, pH 7.4). For cell lysis, 200ul of 1mM of PMSF and 40ul of 100 µg/µl of lysozyme was added. Immediately after this the cells were frozen in liquid nitrogen followed by thawing in water bath (55C). The cells were lysed by 3 rounds of this freeze and thaw and then were subjected to lysis by sonication. Sonication was performed at 30% Amp, with 10seconds pulse on and 10 seconds pulse off for 5 minutes at 4C. Cells were then centrifuged at 13000rpm for 1 hour, 4C. The supernatant was collected and filtered using 0.45um filters. Fast protein liquid chromatography (FPLC) was used to purify the his tagged proteins from the whole cell lysate. The proteins were purified using Ni-NTA column in AKTA start and were eluted in imidazole elution buffer(20 mM sodium phosphate, 0.5 M NaCl, 500 mM imidazole, pH 7.4).

Buffer Exchange

AKTA start and Hi-Trap Desalting column (5ml) was used for buffer exchange. Proteins in Imidazole Elution buffer were desalted in tev reaction buffer. For this purpose, the Hi-Trap column was first washed with 25ml of filtered and degassed water at the flow rate of 5ml/min. The column was then equilibrated in 1X tev reaction buffer (50mM tris-HCl (pH8.0) and 0.5mM EDTA). The flow rate was then reduced to 1ml/min and 1.5ml of protein was manually added to the column. 2ml of buffer exchanged protein was then collected protein quantification was performed using BCA assay (Thermo Fisher Scientific). Protein standards for BCA were prepared 2000u/ml of BSA solution. The working reagent for BCA was prepared by adding Reagent A and Reagent B in 50:1 ratio respectively. 200ul of this working solution was added to 10ul of both the standards and protein samples in 96 well plate. 10ul of tev reaction buffer was used as blank. The plate was incubated for 30minutes at 37C in dark. The absorbance was then measured at 540 nm using spectraMax M5 Microplate Reader spectrophotometer (Molecular Devices). Each measurement was done in duplicates and the mean OD of standards was plotted against their concentrations. The standard curve was created and the concentration of the proteins were extrapolated from the equation of the curve.

.

Removal of GST tag from GST-Htt proteins

Tev reaction optimization

Tev protease was added to purified proteins, to remove the GST tag. One unit of tev protease was added per 50g of protein and 1mM DTT was added. The reaction was performed at rtp and samples were every collected after 3,4,6,8,12 and 18 hours. 4ul of 6X SDS loading dye was added to the sample to stop the reaction and the sample was stored immediately at -20C. Once all samples were collected, they were loaded on 12% SDS PAGE gel for Coomassie blue and western blot analysis. Wester blot was performed both with anti-his antibody and anti-polyQ (MWI) antibody.

Tev Reaction for Removal of GST Tag

After the optmisation, of tev cleavage reaction, 12 hours at rtp was selected for the future experiments. GST-Htt Exon1 (Q25), GST-Htt Exon1 (Q46), GST-Htt Exon1 (Q103) were purified as described above. Tev : Protein was kept (1:50). The reaction was set up for 12 hours after which 20ul sample was mixed with 6X SDS loading dye.

6His-GST was removed from the reaction by batch purification with HisPur™ Cobalt Resin. Since both tev protease used in the reaction and GST had 6 his tag fused. HisPur™ Cobalt Resin was preferred for batch purification.

1ml of cobalt resin was added to a 15ml falcon tube. The tube was centrifuged for 2 minutes at 700 × g and the supernatant was removed. 1ml of Wash Buffer (50mM sodium phosphate, 300mM sodium chloride, 10mM imidazole; pH 7.4) was added to the resin and the mixture was centrifuged for 2 minutes at 700 × g. The supernatant was removed. sample for purification was prepared by mixing the 1ml of protein in 1ml of Wash Buffer. The prepared protein solution was added to the resin tube and was mixed on an end-over-end rotator at rtp for 30 minutes. After this The tube was centrifuged for 2 minutes at 700 × g. The supernatant containing unbound proteins was collected. The resin was then washed with 1ml of Wash Buffer and centrifuged for 2 minutes at 700 × g. This step was repeated again. All unbound fractions were collected and concentrated in thermofisher scientific protein concentrator with

10K cutoff at 1500g for 30 mins. Once the protein was concentrated to >1ml, 1ml of PBS was added and centrifuged again for 10 mins. This was repeated twice to perform buffer exchange. The protein concentration was then calculated with BCA kit as described above. Since HTT proteins aggregates soon after the removal of GST tag, the samples were loaded on 8% SDS PAGE gel.

For SDS-PAGE analysis, the gel was transferred to Coomassie blue staining dye. No heating was applied. The gel was incubated for 16 hours at room temperature by gentle shaking. Following this, the excess dye was washed off by water and the gel was transferred into destaising buffer composed of 30% methanol, 10% acetic acid and 60% water. The gel was incubated in destaining buffer at room temperature over night by gentle shaking. Once the proteins bands were visible the distaining dye was removed and the gel was visualized by Fusionâ Software of Vilber Lourmat imaging system.The stacking gel was not removed.

Western Blot with MW1 (anti-polyQ) antibody

For the detection of the GST cleaved Htt exon1(proteins) by western bot analysis, the 8% SDS-PAGE gel was subjected to semi-wet protein transfer onto a polyvinylidene difluoride (PVDF) membrane (Thermo Fisher Scientific). The activation of PVDF membrane was done by placing the membrane in methanol for 2 minutes, followed by incubation in water for two minutes and then equilibrating it in 1X towbin buffer (Bio-Rad) for 10 minutes. Meanwhile two wattman filter papers were soaked in into 1X Towbin Transfer buffer as well. The gel was equilibrated in 1X Towbin Transfer buffer for 10 minutes. One filter paper was placed on the cathode of the transfer cassette, followed by the PVDF membrane, the gel was placed and lastly the other filter paper was placed on top. The cassette was tightly closed and semi-dry transfer was done with 1.3A 25V for 30 minutes. Once the transfer of proteins from the gel to the membrane was completed the membrane was placed in the blocking solution (comprising of 1x Tris Buffer

Saline Tween (TBS-T (0.1%)) and 5% skimmed milk) for 1 hour at room temperature. This was done to prevent any unspecific binding. After the blocking, primary antibody incubation was performed. The membrane was incubated in MWI (ms anti-polyQ) antibody (Mecrk) , diluted at 1:10000 in %5 milk powder and TBS-T. The incubation was performed at +4 overnight. The membrane was then washed in TBS-T for once for 5 minutes, then twice for 10 minutes each. After this the membrane was incubated in secondary antibody (comprising HRP conjugated goat anti-mouse antibody) (Abcam) in 1:10000 blocking solution) for 1 hour at room temperature. The membrane was again washed in TBST by the same way as described above. After this the membrane was visualized using Enhanced chemiluminescence (ECL) (Bio-Rad) solution. This was prepared by mixing equal volumes of Clarity Western Luminol/Enhancer Reagent and Clarity Western Peroxide Reagent. The solution was poured over the membrane which was then incubated in dark for 2 minutes. Fusionâ Software of Vilber Lourmat imaging system.

Congo Red Assay

Congo red dye was used to visualize fibril aggregation in Htt exon1 (Q103) protein. For this the GST-Htt exon1 (Q103) was purified as described above.

1ml of Tev cleavage reaction was set up with 600ug/ml protein for 12 hours at rtp. After this batch purification with HisPur^{TM} Cobalt Resin was performed as described above. The purified protein in PBS which was free of Tev protease and GST tag was then incubated at rtp for 5 days.

After 5 days, 4ul of 50X Congo red dye was added to 200ul pf protein and was centrifuged at 11000rpm for 10 minutes.

Peptide Synthesis

The peptides were produced by solid state synthesis and were purchased from Peptiteam.

The following peptides were used in the experiments.

INHIBITORY PEPTIDE
1. **HHGANSLGLVQS**
2. **SWPLTPVRFMTE**
3. **HGLHSMHNKLQT**
4. **FQKDAWEAVDIR**
5. **WMFPSLKLLDYH**
6. **HVTFKFQWDRES**

Table1. List of previously screened candidate ligand peptides

Thioflalvin T Assay

All three Htt proteins; 6His-GST-htt-(Q25), 6His-GST-htt-(Q46) and 6His-GST-htt-(Q103); were purified and quantified by the methods described above.

600ug/ml of purified 6His-GST-htt-(Q103) and 1.5mg/ml of purified 6His-GST-htt-(Q25) and 6His-GST-htt-(Q46) were completed to the final concentration of 7uM and put into each well. 3ul of 1000ug/ml tev protease was added to remove 6His-GST and initiate fibril formation. 7uM of each peptide was then added to the peptide treated groups. The reaction was completed to 200ul by tev reaction buffer and 0.5ul of 25uM tht was added. The 96-microwell plate was then sealed by adhesive tape to prevent evaporation and incubated in dark at 37°C .The ThT fluorescence intensity of each sample was recorded by spectraMax M5 Microplate Reader spectrophotometer (Molecular Devices) with 438/495-nm excitation/emission filters at cutoff at 475nm after every 10 minutes for 16-20 hours. Each reading was preceded by 5 s for orbital agitation. To study the effect of ligand peptides fibril kinetics of Htt exon 1 proteins, 4 experimental groups were set up. These were GST-Htt proteins (Q25)(Q46) and (Q103), GST-Htt proteins (Q25)(Q46) and (Q103) with tev protease (to remove GST). Peptide effect was evaluated on both GST removed and GST fused Htt proteins.

All samples were repeated three times. The ThT data were normalized as described earlier (65). and percentage fluorescence was plotted against time.

2.5 Atomic Force Microscopy

The effect of inhibitory peptides on the aggregation kinetics of Huntingtin exon1 was studied using 6His-GST-htt-exon 1-(Q25), 6His-GST-htt-exon 1-(Q46) and 6His-GST-htt-exon 1-(Q103) . GST fusion proteins were purified quantified by the aforementioned methods. In order to remove any pre-existing aggregates, the proteins were centrifuged at 18000 x g for 20 minutes.

6His-GST-htt-exon 1-(Q103) was diluted to a final concentration of 10μM in 1X tev reaction buffer (pH 8.0); 4.2μl of 1000μg/ml Tev Protease was added to remove 6His-GST and initiate the aggregation. 500ul reaction volumes were incubated at room temperature. 2 hours after addition of tev protease; at t=0, 10μM peptide was added. Following this 5μl of samples were aliquoted after 2,4,8,10,12 and 24 hours from both peptide treated and non-treated htt-exon-1(Q103) for AFM deposition. For taking the topographic images in air, 5μl sample was deposited on SiO2 wafers. After two minutes the wafer was rinsed with ultrapure water and was argon dried.

For studying the effect of inhibitory peptides on 6His-GST-htt-exon 1-(Q46) and 6His-GST-htt-exon 1-(Q25), the purified proteins were diluted to a final concentration of 30μM in 1X tev reaction buffer (pH 8.0); 12.6μl of 1000μg/ml Tev Protease was added to remove 6His-GST and initiate the aggregation. 1ml reaction volumes were incubated at room temperature. 2 hours after addition of tev protease; at t=0, 30μM peptide was added. Following this 5μl of samples were aliquoted after 4,8 and 24 hours from both peptide treated and non-treated htt-exon-Q25 and htt-exon-Q46 experimental groups. The sample deposition for AFM was performed in a similar fashion as described above.

AFM Imaging

AFM surface topography images were obtained with an Oxford Instruments MFP-3D Origin in the Tapping mode which uses the air topography technique. Beam-shaped AFM probes of 300 kHz resonance frequency with 40 N/m spring constant from Budget Sensors are used for the measurements. Samples are scanned with 1.2Hz to 2.2Hz, depending on the scan area dimensions. AFM measurements are performed under the ambient at room temperature. Collected AFM images are then analyzed and corrected for scan artifacts in the Gwyddion v2.60 program

Matlab FiberApp was used to measure the fibril length of each data set. Fibril length of both peptide treated htt-exon 1 proteins and untreated htt-exon 1 proteins were compared by using the 2 way-Anova statistic test.

RESULTS

1. Expression of 6HisGST-HTT(1) proteins and removal of GST tag

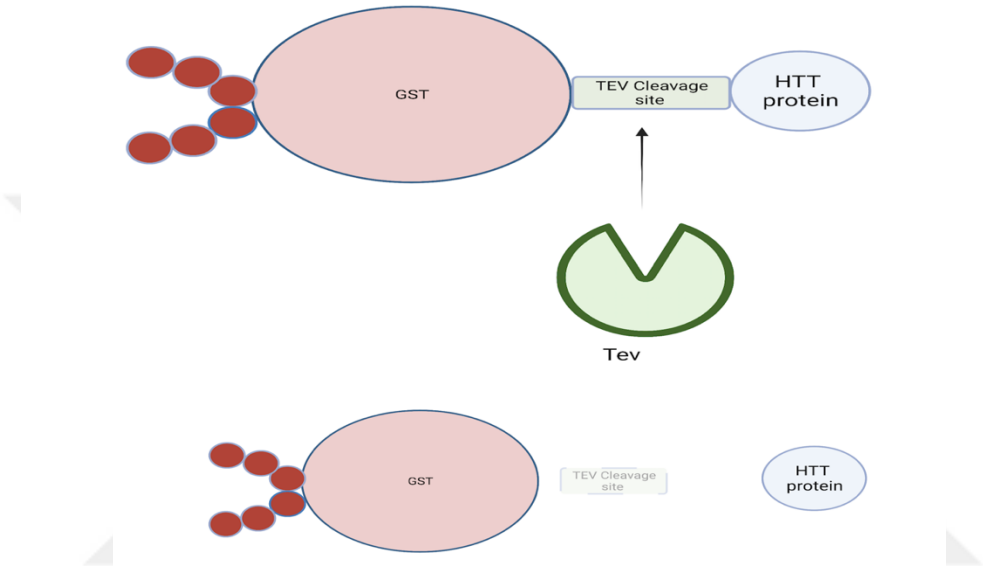

Figure2 . Schematic representation of the enzymatic activity of tev protease enzyme. Tev protease makes site specific cleavage at ENLYFQG between GST and Htt protein, releasing the Htt monomer free.

All three proteins were expressed and purified and Following buffer exchange in tev reaction buffer, Tev cleavage reaction optimization was carried out as described in chapter 2.

Optimisation of tev cleavage reaction for Htt (Q25)

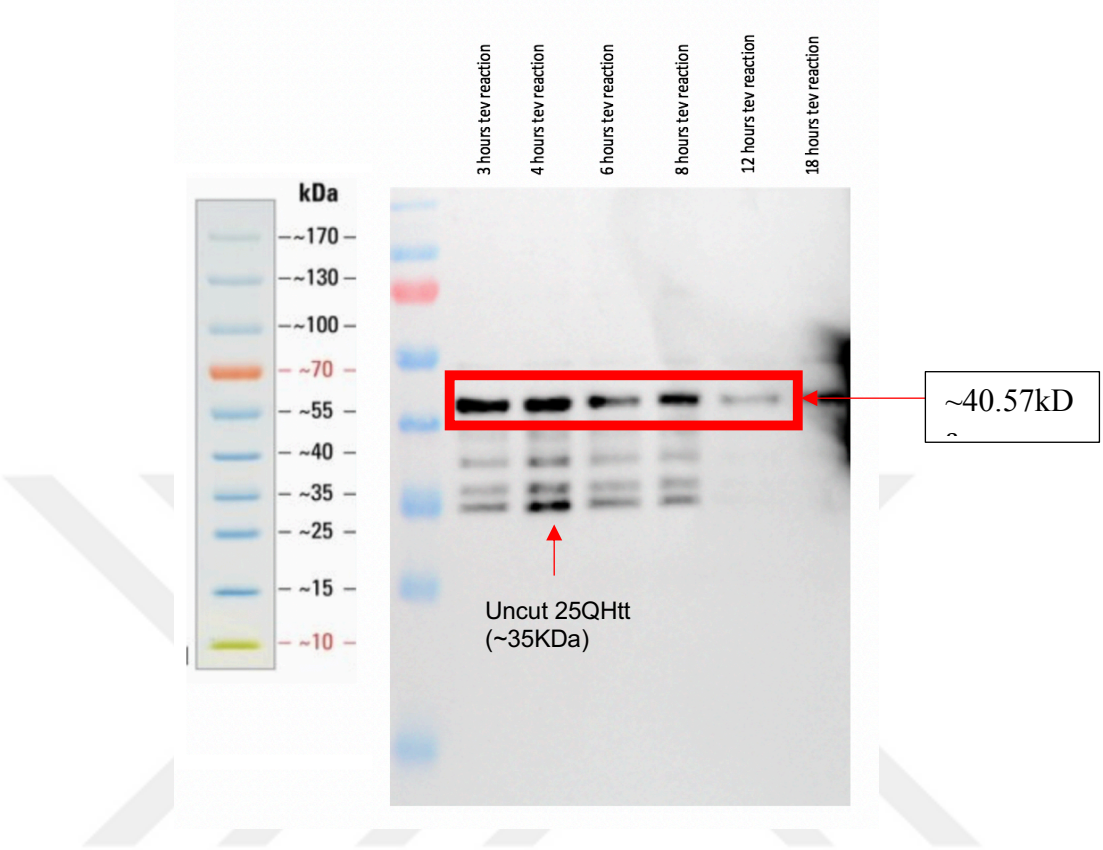

Figure 3) Western blot analysis with MW1 antibody for Htt(Q25) treated with tev protease for different time points. The lanes are annotated with corresponding time point after initation of tev cleavage reaction at which the sample was taken.

The gel was ran on 12% SDS PAGE gel

After the cleavage of GST by tev protease, the monomers of Htt Q25 form polymers of different sizes like 20.24kDa , 30.36kDa, 40.57kDa. Polymerization can be observed at these sizes as shown above at different time points after tev cleavage reaction as indicated above.

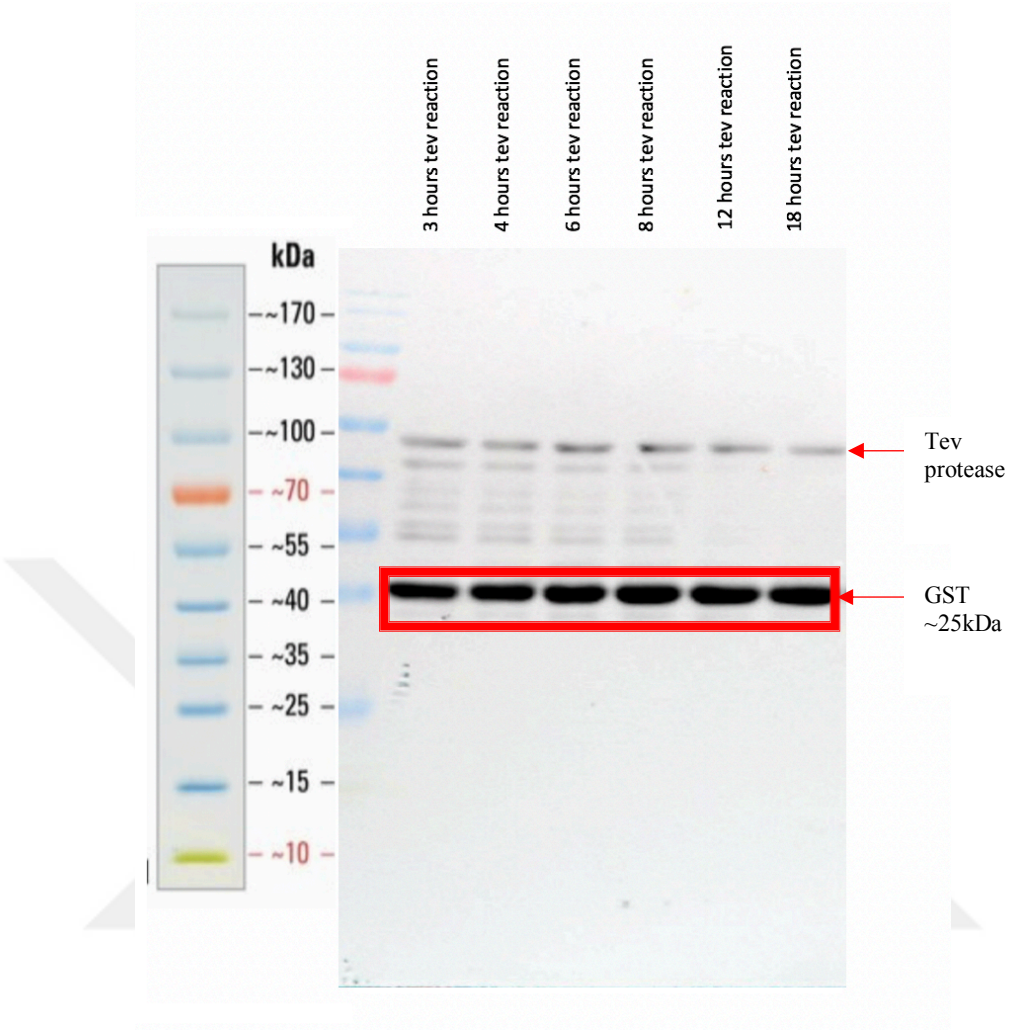

Figure 4) Western blot analysis with anti-His antibody for Htt(Q25) treated with tev protease for different time points. The lanes are annotated with corresponding time point after initation of tev cleavage reaction at which the sample was taken.

The gel was ran on 12% SDS PAGE gel

Uncut GST-Htt Q25 at 35kDa were visible till 8th hour. After which bands for uncut protein were not observed, marking possible completion of the reaction.

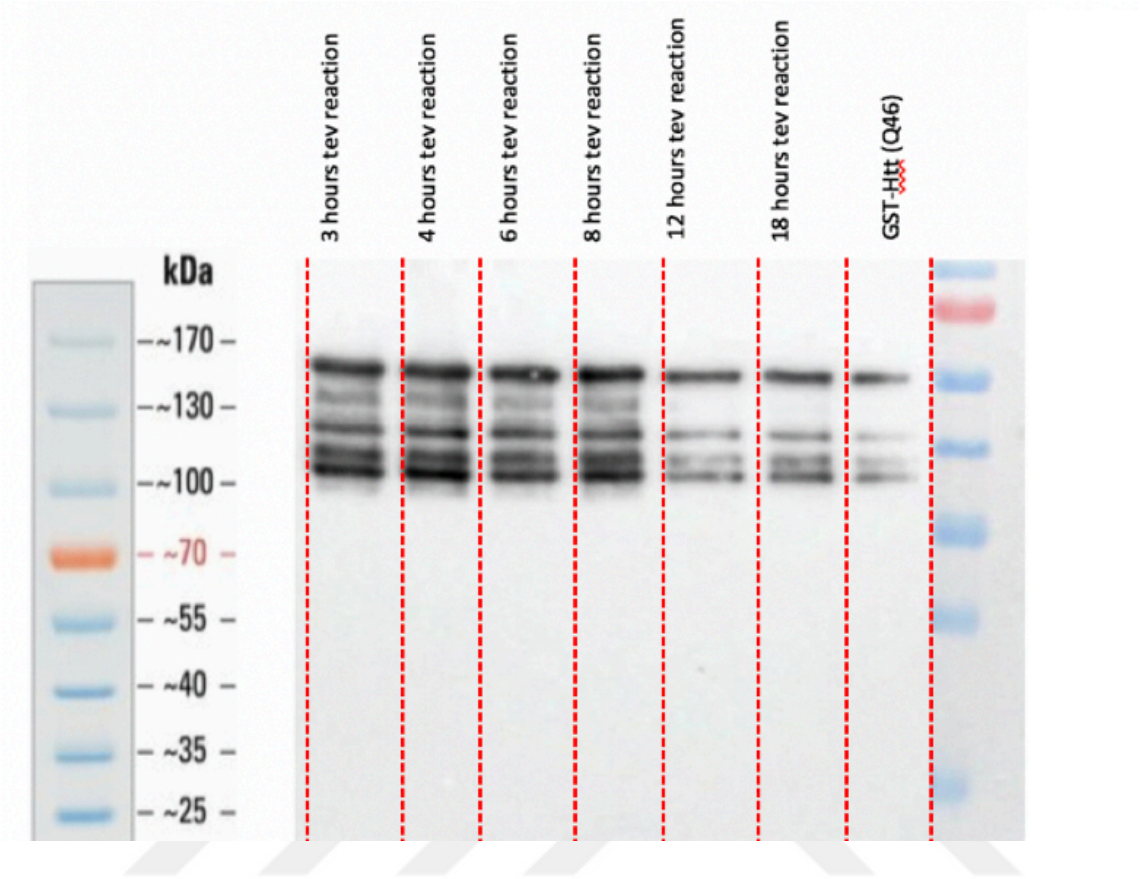

Figure 5) Western blot analysis with MW1 antibody for Htt(Q46) treated with tev protease for different time points. The lanes are annotated with corresponding time point after initation of tev cleavage reaction at which the sample was taken.

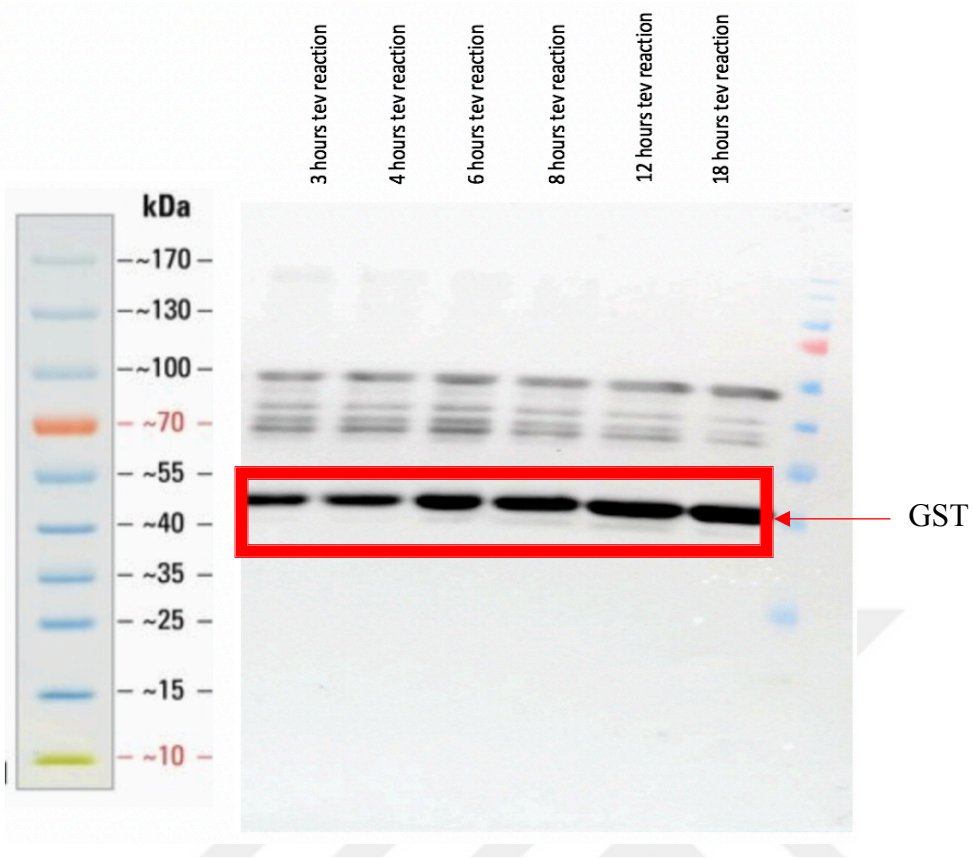

Figure 6) Western blot analysis Anti-His antibody for Htt(Q46) treated with tev protease for different time points. The lanes are annotated with corresponding time point after initiation of tev cleavage reaction at which the sample was taken. The gel was ran on 12% SDS PAGE gel

After the cleavage of GST by tev protease, the monomers of Htt Q46 (12.43kDa) form rapid polymers of different sizes like (24.86kDa 35.07kDa 47.50kDa). Polymerization can be observed at these sizes as shown above at different time points after tev cleavage reaction as indicated by the arrows. However the monomers were not seen either of the proteins.

For Htt (Q103) bands were not observed (data not shown here).

Form the above data and the AFM analysis of aggregation kinetics of GST-cleaved Htt proteins (discussed in detail below). It was observed that 12 hours at rtp was sufficient for tev protease reaction.

As reported earlier, GST tag increase the solubility of Htt proteins and prevents aggregation. This can be owed to the property of GST for existing as a dimer. As per this model GST-Htt fusion protein form stable hairpins around GST dimer, and consists of antiparallel β strands held together by hydrogen bonds. These GST bound protein are not accessible for protein interactions with other Htt proteins, However once GST is removed by Tev cleavage reaction, these proteins are made accessible for polyQ interact to form stable β sheet fibrils. These then immediately start polymerization(66). And as seen above the Htt proteins go under rapid aggregation, it seemed a better idea to carry out the SDS-PAGE analysis on 8% SDS-PAGE gel. All three GST fused Htt proteins were purified as mentioned above. The proteins were desalted in tev reaction buffer and tev cleavage reaction was set up for 12 hours. Following this, GST tag was removed by HisPur Cobalt Resin. The unbound protein fractions were concentrated in PBS and were analysed by 8% SDS -PAGE gel. The figure below shows the Western blot result carried out by immunoblotting MW1 anti polyQ anti body.

Western blot with MW1 antibody

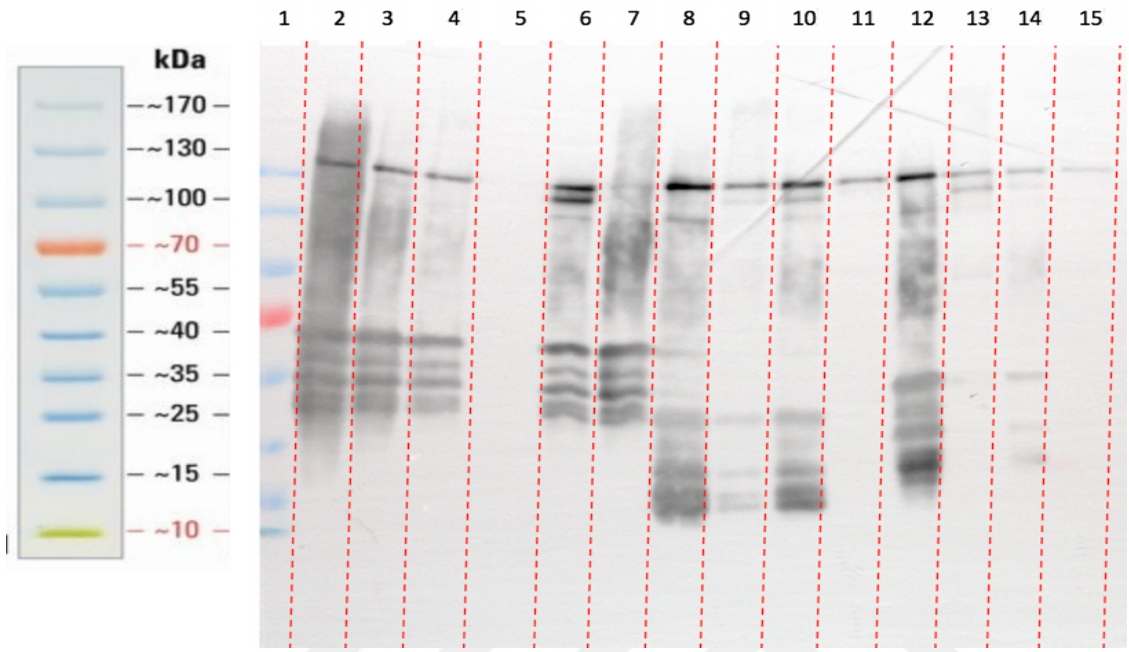

Figure . 7) Western blot analysis results by MW1 antibody. The wells were loaded in the following order. Lane1= page ruler, lane 2=GST-Htt (Q103), lane3= GST-Htt (Q103) with tev protease (12 hours after GST removal reaction), lane 4= Htt (103Q) purified by removal of GST and tev protease. Lane5= Htt (Q103) in PBS. Lane 6= 5 days old Htt (103Q) pellet. Lane 7 = 5 days old Htt (103Q) supernatant.

Lane8= GST-Htt (Q46), lane9= 5 days old Htt (46Q) pellet. Lane 10 = 5 days old Htt (46Q) supernatant. Lane 11= Htt (Q46) in PBS.

Lane12= GST-Htt (Q25), lane13= 5 days old Htt (25Q) pellet. Lane 14 = 5 days old Htt (25Q) supernatant. Lane 14= Htt (Q25) in PBS.

Coomassie blue staining

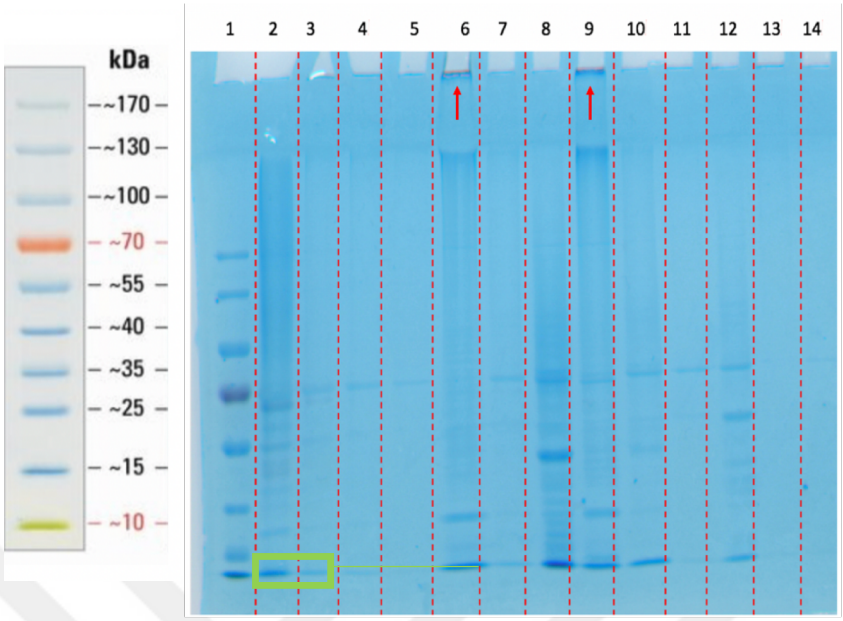

Figure . 8) Coomassie blue staining on 8% SDS-PAGE gel. The wells were loaded in the following order. Lane1= page ruler, lane 2=GST-Htt (Q103), lane3= GST-Htt (Q103) with tev protease (12 hours after GST removal reaction), lane 4= Htt (103Q) purified by removal of GST and tev protease. Lane5= Htt (Q103) in PBS. Lane 6= 5 days old Htt (103Q) pellet. Lane 7 = 5 days old Htt (103Q) supernatant.

Lane8= GST-Htt (Q46), lane9= 5 days old Htt (46Q) pellet. Lane 10 = 5 days old Htt (46Q) supernatant. Lane 11= Htt (Q46) in PBS.

Lane12= GST-Htt (Q25), lane13= 5 days old Htt (25Q) pellet. Lane 14 = 5 days old Htt (25Q) supernatant. Lane 14= Htt (Q25) in PBS.

Both Western blot analysis and Commassie blue staining showed higher molecular mass proteins. Lane1 and 2, the green box shows GST tag. The arrow indicates insoluble high-molecular-weight aggregates stuck in stacking gel. Lane 6 and Lane 9, both show protein in the well. These are fibrils of Htt Q103 and Htt Q46 respectively.

Next we wanted to confirm the presence of fibrils in HttQ103 (one week old) reaction in PBS. For that Congo Red dye was used as described in the material and method section.

Congo Red assay to visualize Htt amyloid fibrils

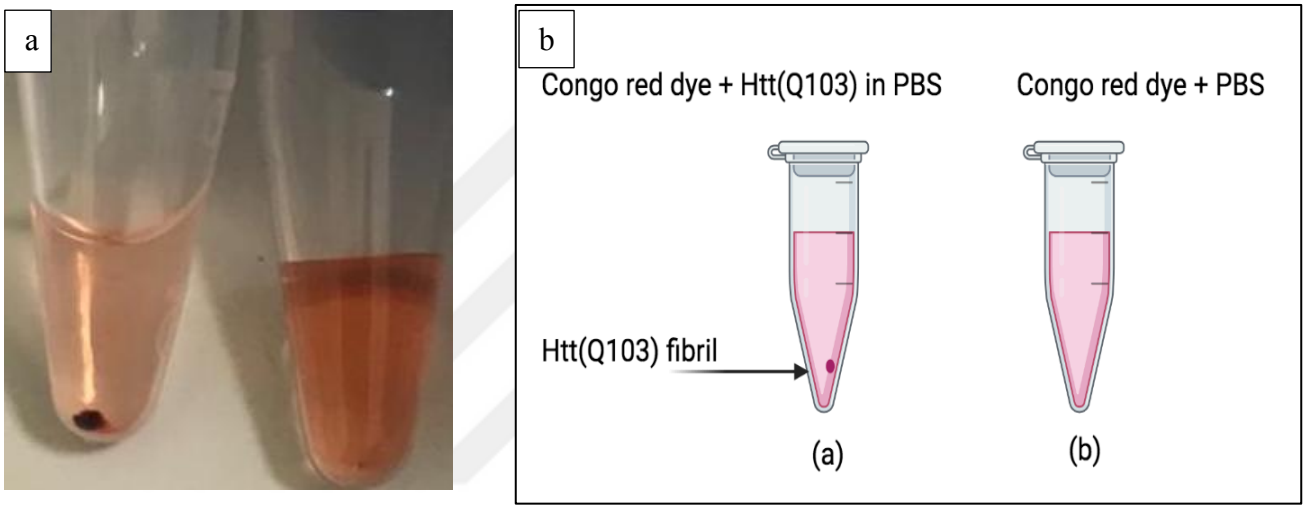

Figure 9. a) Congo Red staining for Htt (Q103) fibrils
b)Schematic representation of Congo Red staining for Htt (Q103) fibrils

Congo Red dye has been extensively used for detecting amyloid fibrils both *in-vivo and in-vitro.* Congo red high binding affinity towards the beta-sheet rich regions of amyloid fibrils (66) makes it an excellent candidate for quick detection of the presence of aggregates in isolated Htt proteins. Here Congo red dye was used to detect the presence of fibrils in Htt(Q103), 5 days after its purification.

In the figure above, 4ul of 50X Congo Red dye was added to 200ul protein sample. A red pellet was observed after centrifugation, showing the presence of fibrils in in Htt(Q103). B was PBS control, upon adding congo red and centrifugation no pellet was observed as per expectation.

Thioflavin T (ThT) Assay

Thioflavin T (ThT) dye is a fluorescence dye which has been widely used quantify fibril kinetics in real-time. Tht dye binds to β-sheet quaternary structure of amyloid fibrils and gives off fluorescent signal with excitation at ~440nm and emission at ~490nm. Owing to this property, tht assay has been widely used to quantify both the formation and inhibition of amyloid fibrils *in vitro*.

Herein THT assay was used to quantify the effects of candidate ligand peptides on fibril formation and subsequent aggregation in Htt proteins.

THT ASSAY FOR HTT (Q103)

The fibril formation in real-time was evaluated by Tht assay. Tev protease was added to one experimental group to initiate GST removal process just before adding tht dye. Tht measurements for both for GST cleaved Htt protein and GST fused proteins were measured. 7uM protein was used in all experiments. The effect of inhibitory peptide on fibrilization process was evaluated by adding 7uM peptide to the protein. Peptide was added both to the GST cleaved Htt protein and GST fused proteins.

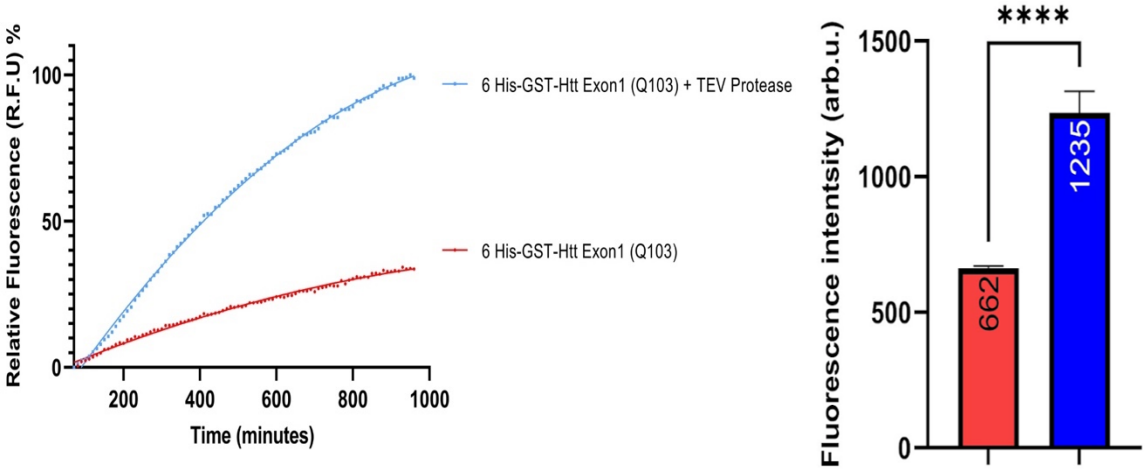

Figure 10. Aggregation kinetics for Htt(exon1)103Q shown in real time by tht assay. The measurement were taken for the interval of 16 hours. Site specific GST cleavage was done by adding tev protease. The GST cleaved Htt-103Q exhibited 1.8 fold increase in fluorescence as compared to the GST intact protein.

a) The fluorescence intensity was normalized and plotted as a standard curve.

b) The measurements were taken as triplicates. The bar represents the mean fluorescence intensity of the end point fluorescence value and the error bars show the standard deviation of the triplicates.

Student t- test was performed to check the significance in the fluorescence

As seen in the figure above, the binding of tht dye to the β-sheet-rich amyloid structures in the presence of GST is significantly reduced as expected. To quantify the effect of the candidate inhibitory peptide on fibril formation. Equimolar (7uM) of peptide was added at the beginning of tht assay. The fluorescence was then recorded for over the interval of 16 hours. Figure 4 shows that fluorescence intensity was decreased in the peptide treated groups; the observance was relevant for both in GST cleaved and GST fused Htt-(Q103).

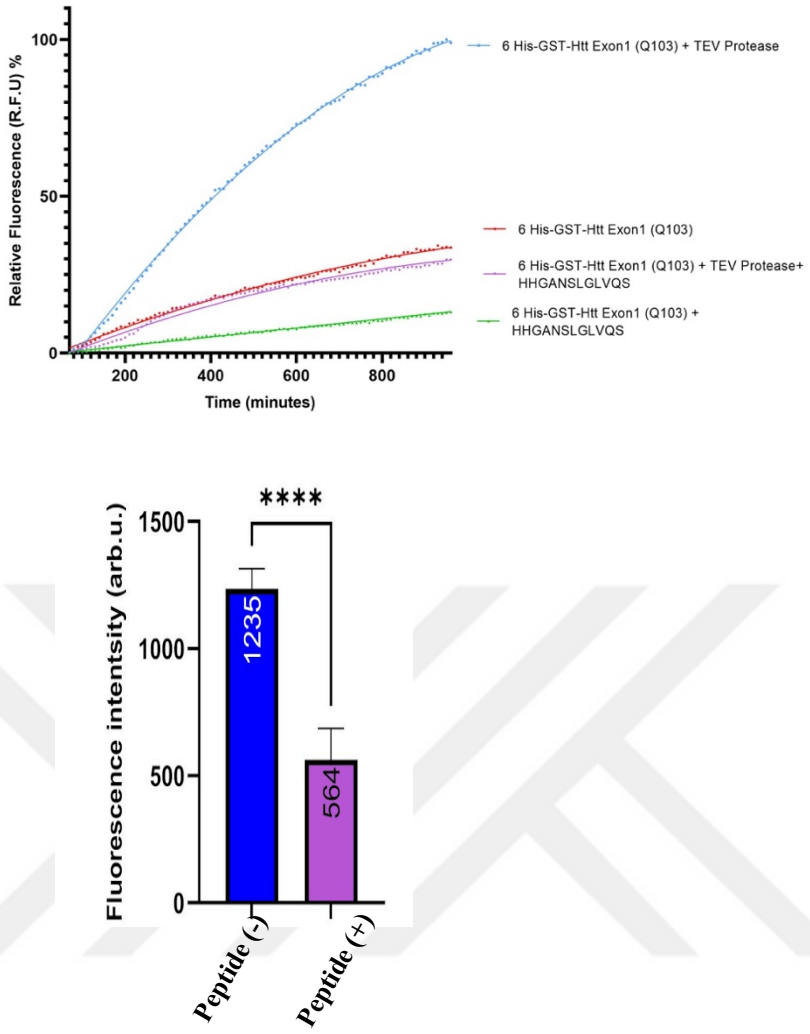

Figure11. Aggregation kinetics for Htt-(Q103) with the addition of peptide HHGANSLGLVQS shown in real time by tht assay.

a) The fluorescence intensity was normalized against GST cleaved Htt-(Q103) and plotted as a standard curve.

b) The fluorescence decreased by 53% GST cleaved Htt-(Q103) in presence of the peptide.The bar represents mean fluorescence intensity of the end point fluorescence value and the error bars show the standard deviation of the triplicates. Student t-test was performed to check the significance in the fluorescence difference between the groups. (p= <0.0001).

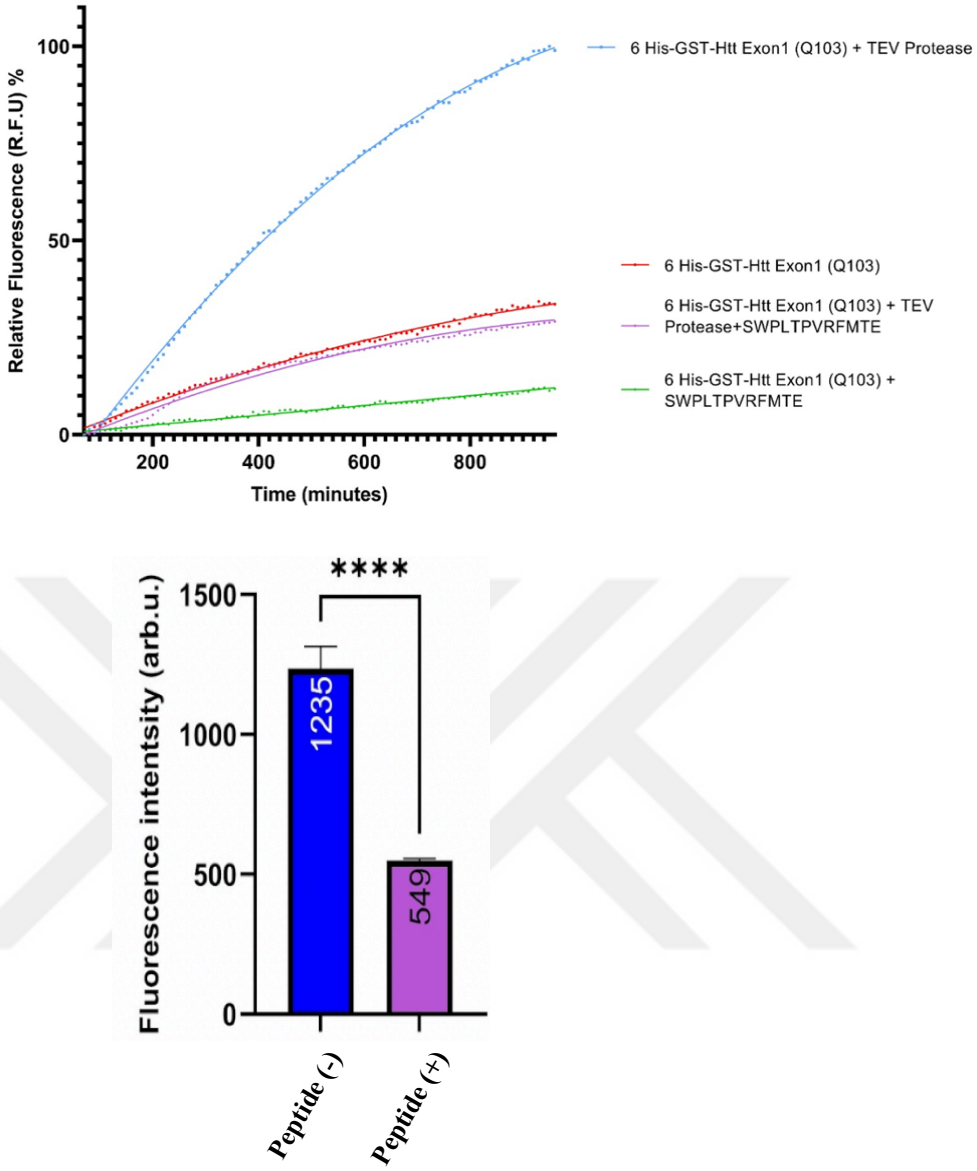

Figure12. Aggregation kinetics for Htt exon1(Q103) with the addition of peptide SWPLTPVRFMTE shown in real time by tht assay.

a) The fluorescence intensity was normalized against GST cleaved Htt-(Q103) and plotted as a standard curve.

b) The fluorescence decreased by 55.5% GST cleaved Htt-(Q103) in presence of the peptide. The bar represents mean fluorescence intensity of the end point fluorescence value and the error bars show the standard deviation of the triplicates. Student t-test was performed to check the significance in the fluorescence difference between the groups. ($p = <0.0001$).

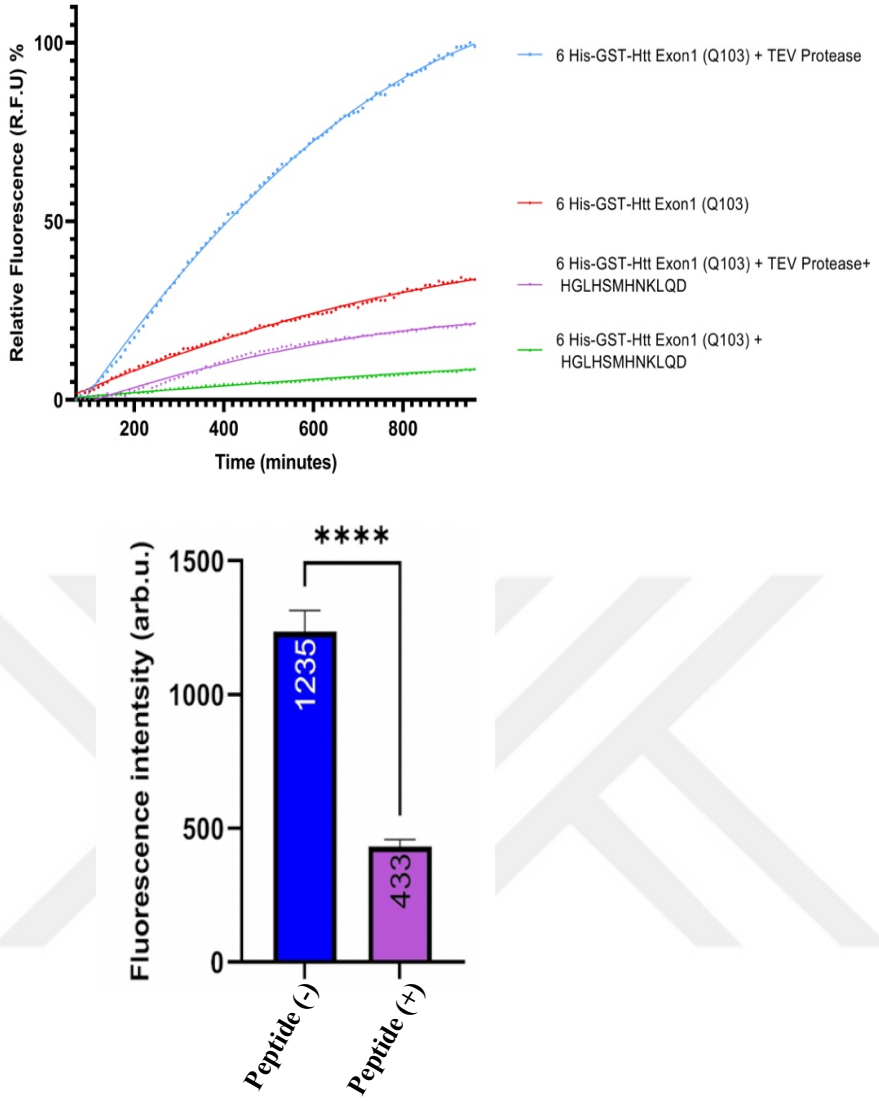

Figure13. Aggregation kinetics for Htt exon1(Q103) with the addition of peptide HGLHSMHNKLQD shown in real time by tht assay.

a) The fluorescence intensity was normalized against GST cleaved Htt-(Q103) and plotted as a standard curve.

b) The fluorescence decreased by 64.9% in GST cleaved Htt-(Q103) in the presence of the peptide. The bar represents mean fluorescence intensity of the end point fluorescence value and the error bars show the standard deviation of the triplicates. Student t-test was performed to check the significance in the fluorescence difference between the groups. (p= <0.0001).

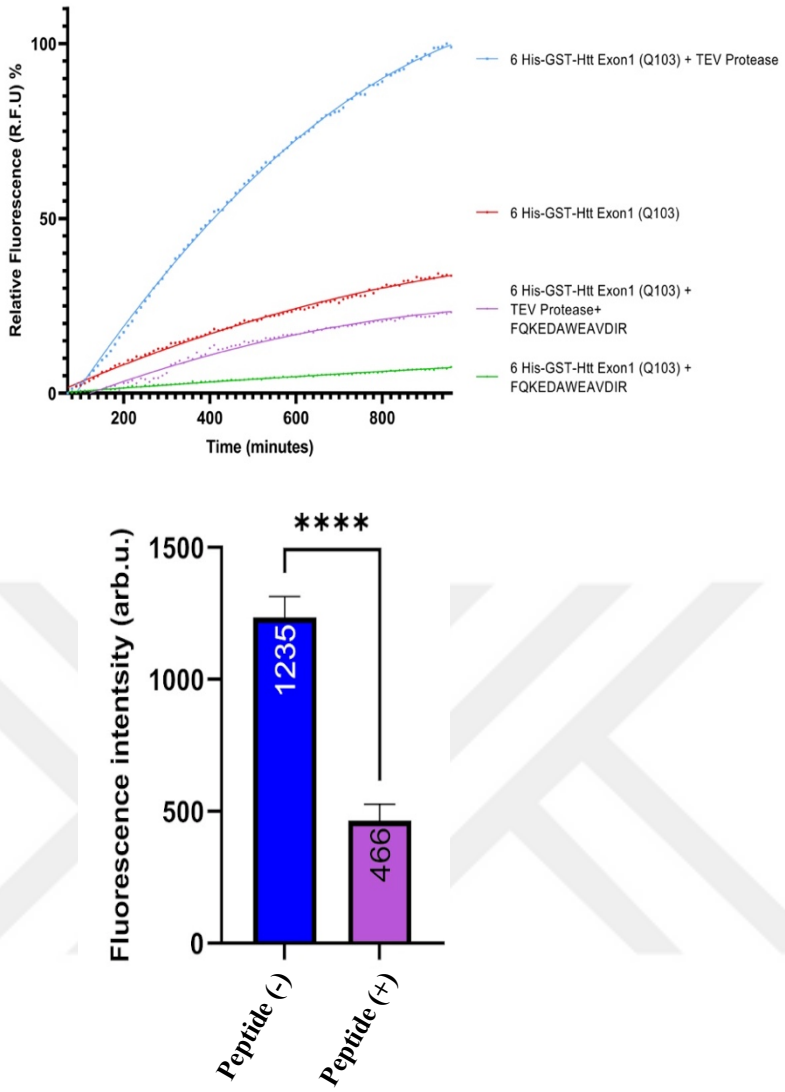

Figure14. Aggregation kinetics for Htt exon1(Q103) with the addition of peptide FQKEDAWEAVDIR shown in real time by tht assay.

a) The fluorescence intensity was normalized against GST cleaved Htt-(Q103) and plotted as a standard curve.

b) The fluorescence decreased by 62.3% in GST cleaved Htt-(Q103) in the presence of the peptide. The bar represents mean fluorescence intensity of the end point fluorescence value and the error bars show the standard deviation of the triplicates. Student t-test was performed to check the significance in the fluorescence difference between the groups. ($p = <0.0001$).

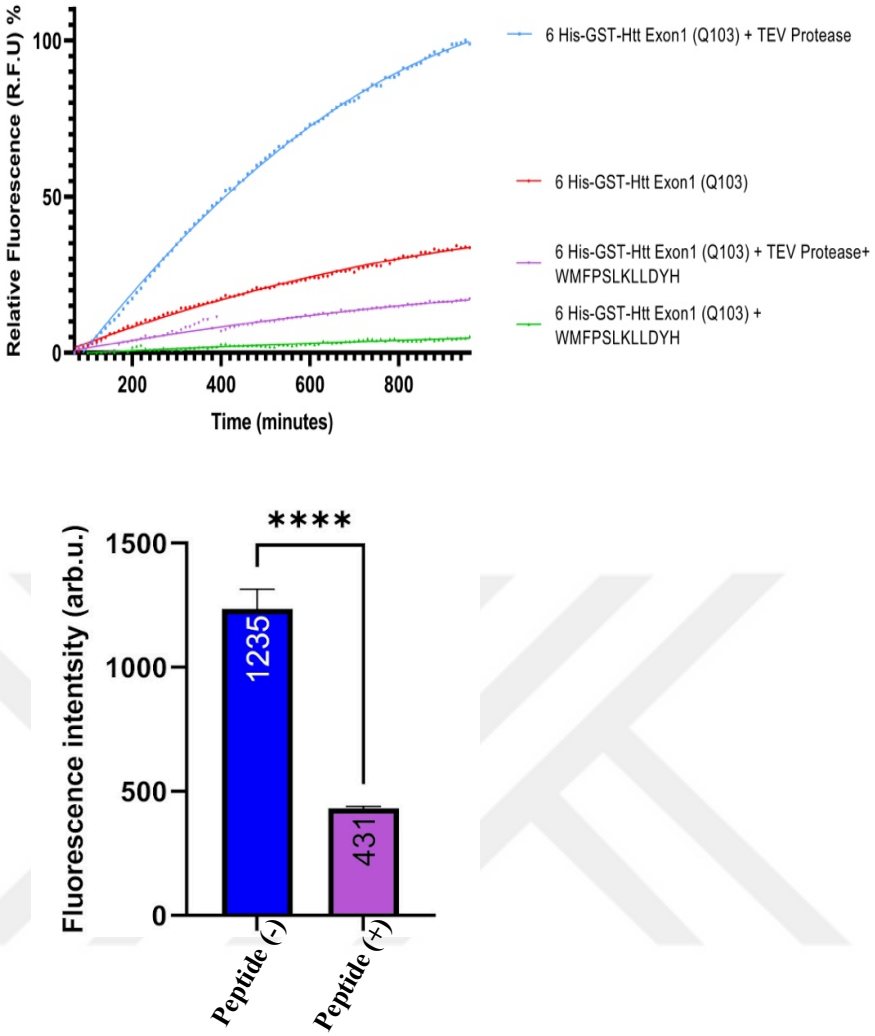

Figure 15. Aggregation kinetics for Htt exon1(Q103) with the addition of peptide WMPSLKLLDYH shown in real time by tht assay.

a) The fluorescence intensity was normalized against GST cleaved Htt-(Q103) and plotted as a standard curve.

b) The fluorescence decreased by 65.1% in GST cleaved Htt-(Q103) in the presence of the peptide. The bar represents mean fluorescence intensity of the end point fluorescence value and the error bars show the standard deviation of the triplicates. Student t-test was performed to check the significance in the fluorescence difference between the groups. ($p = <0.0001$).

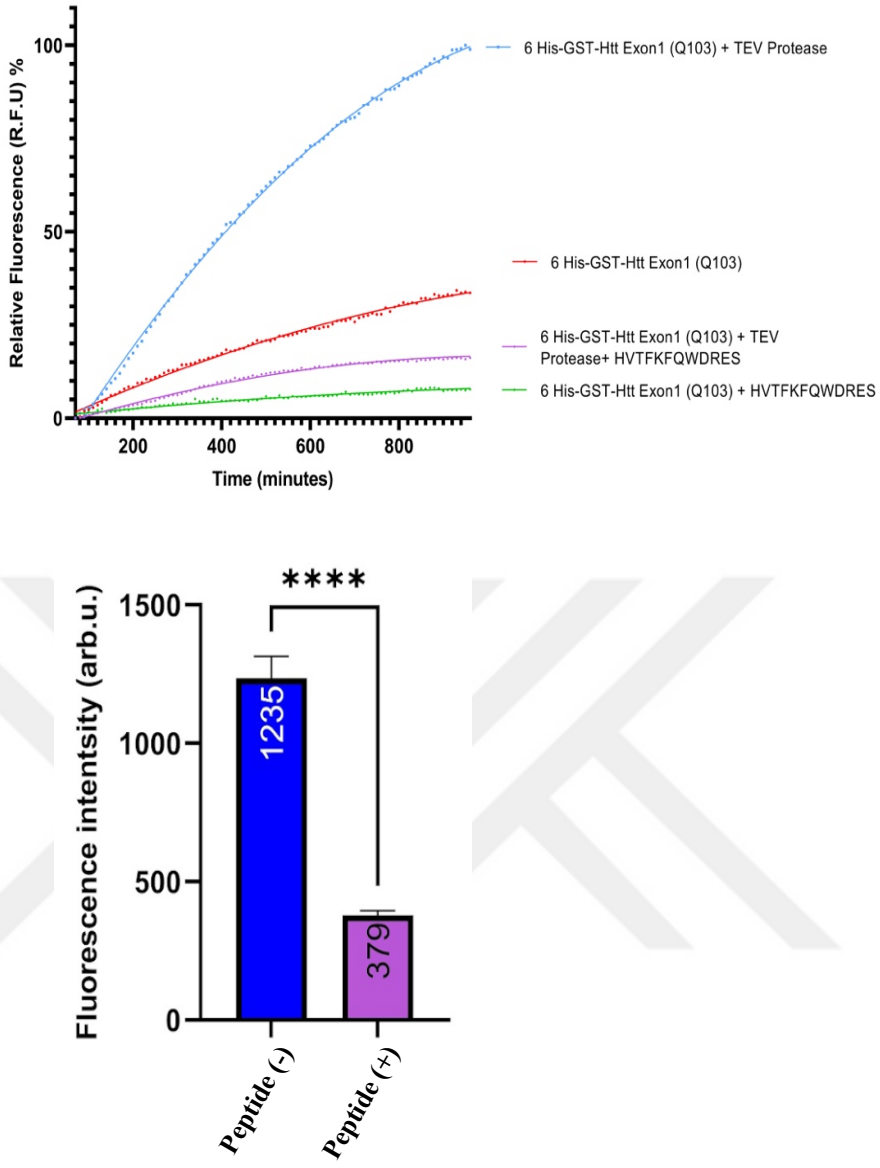

Figure16. Aggregation kinetics for Htt exon1(Q103) with the addition of peptide HVTFKFQWDRES shown in real time by tht assay.

a) The fluorescence intensity was normalized against GST cleaved Htt-(Q103) and plotted as a standard curve.

b) The fluorescence decreased by 69.3% in GST cleaved Htt-(Q103) in the presence of the peptide. The bar represents mean fluorescence intensity of the end point fluorescence value and the error bars show the standard deviation of the triplicates. Student t-test was performed to check the significance in the fluorescence difference between the groups. (p= <0.0001).

All six candidate ligand peptides showed a significance decrease in fluorescent signal. Since fluorescence signal, in tht assay, is a measure of aggregation kinetics of amyloid fibrils; From the above data It is fair to say that the peptides caused inhibition and blocking in this aggregation process.

THT ASSAY FOR HTT EXON1 (Q46)

Aggregation kinetics were also studied for Htt-(Q46) protein both in the presence and absence of the inhibitory peptides. The tht assay was set up as described in chapter 2. As seen previously with Htt-(Q103). GST-fused Htt-(Q46) showed lower fluorescence signal as compared to the when GST was cleaved.

All six peptides were tested in the similar fashion. The results are shown the figures below.

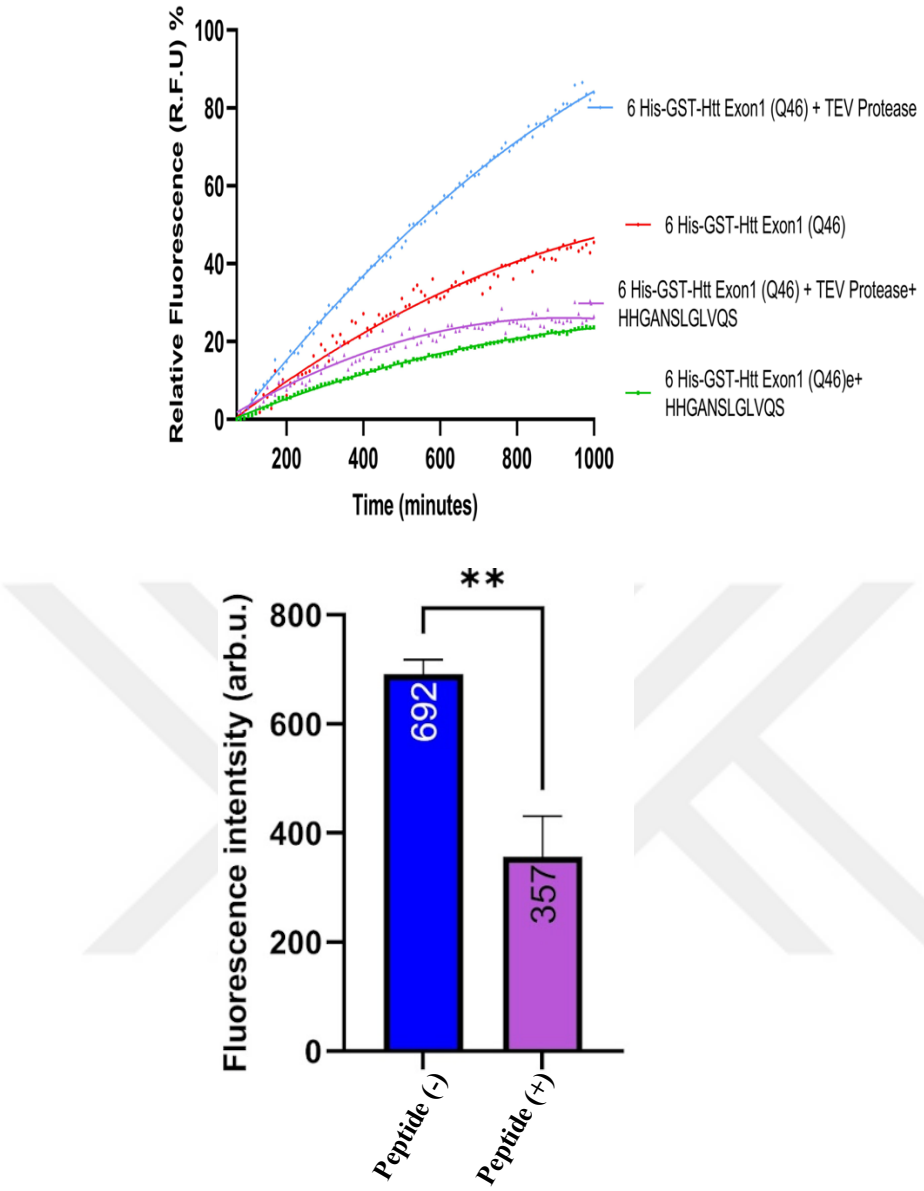

Figure17. Aggregation kinetics for Htt-(Q46) with the addition of peptide HHGANSLGLVQS shown in real time by tht assay.

a) The fluorescence intensity was normalized against GST cleaved Htt-(Q46) and plotted as a standard curve.

b) The fluorescence decreased by 48.4% in GST cleaved Htt-(Q46) in the presence of the peptide. The bar represents mean fluorescence intensity of the end point fluorescence value and the error bars show the standard deviation of the triplicates. Student t-test was performed to check the significance in the fluorescence difference between the groups. (p= <0.0001).

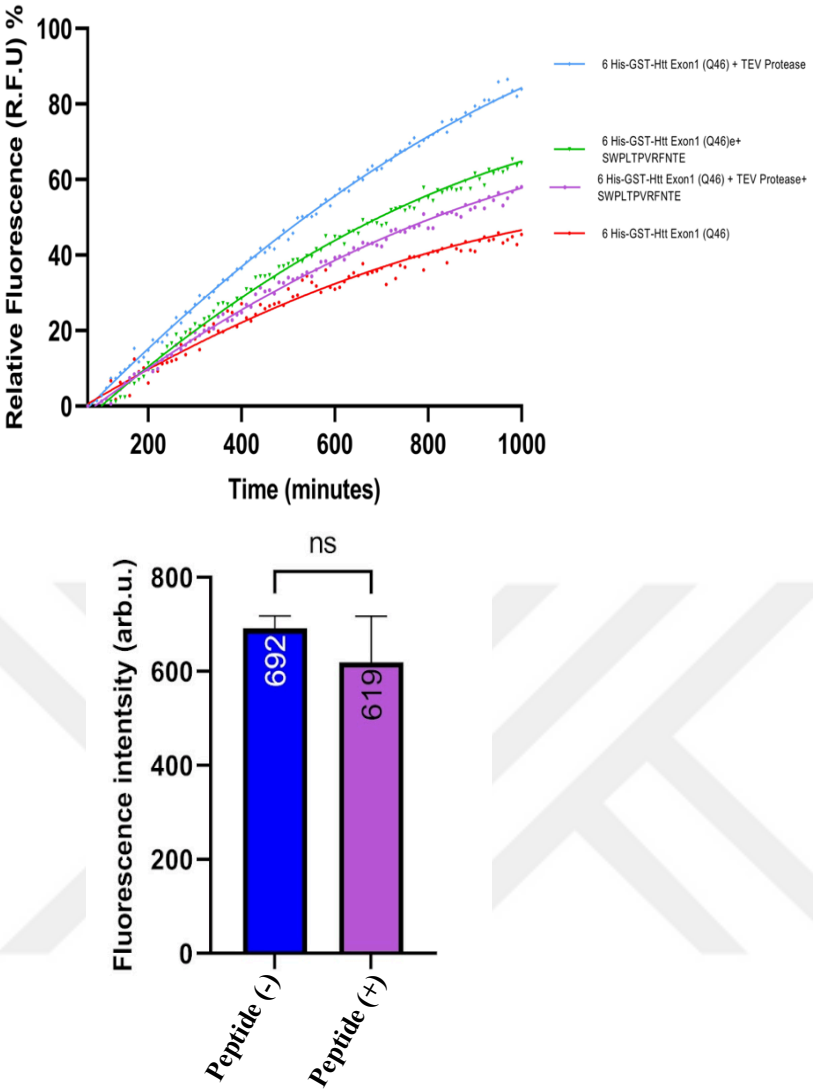

Figure18. Aggregation kinetics for Htt exon1(Q46) with the addition of peptide SWPLTPVRFMTE shown in real time by tht assay.

a) The fluorescence intensity was normalized against GST cleaved Htt-(Q46) and plotted as a standard curve.

b) The fluorescence decreased by 10.5% in GST cleaved Htt-(Q46) in the presence of the peptide. The bar represents mean fluorescence intensity of the end point fluorescence value and the error bars show the standard deviation of the triplicates. Student t-test was performed to check the significance in the fluorescence difference between the groups. (p= <0.0001).

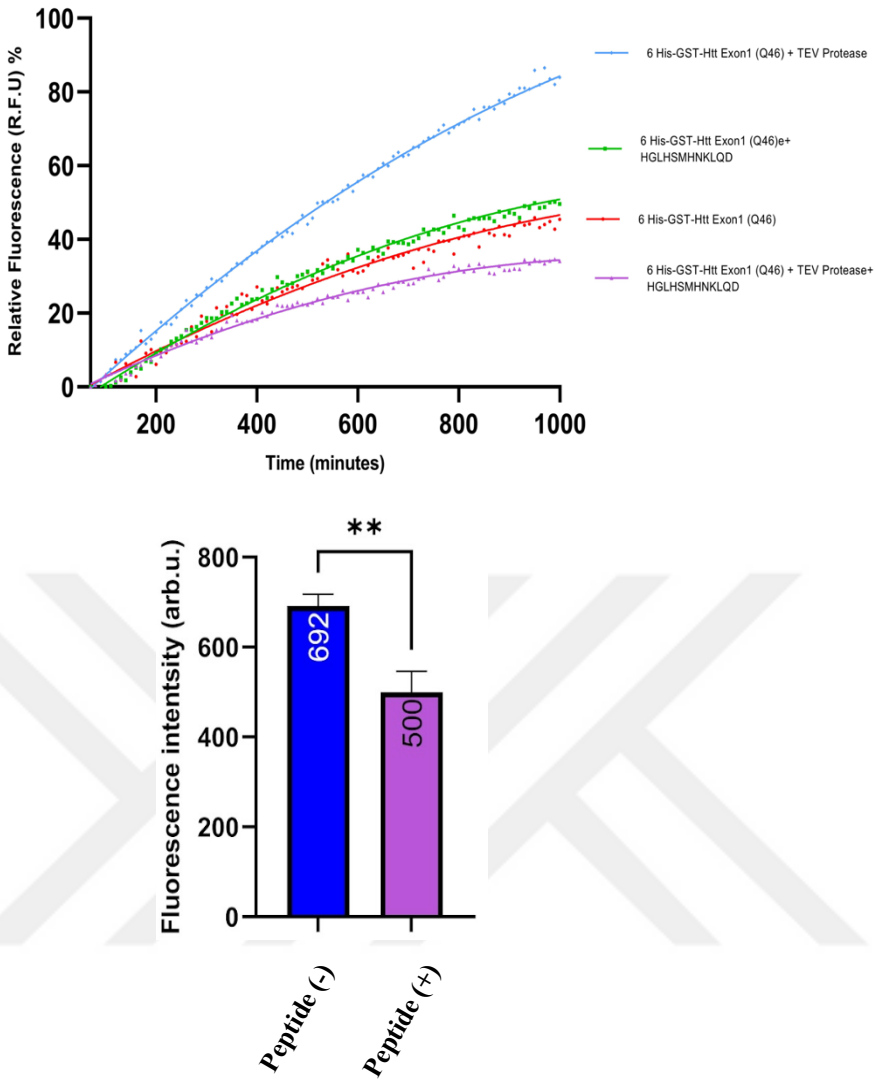

Figure19. Aggregation kinetics for Htt exon1(Q46) with the addition of peptide HGLHSMHNKLQD shown in real time by tht assay.

a) The fluorescence intensity was normalized against GST cleaved Htt-(Q46) and plotted as a standard curve.

b) The fluorescence decreased by 27.7% in GST cleaved Htt-(Q46) in the presence of the peptide. The bar represents mean fluorescence intensity of the end point fluorescence value and the error bars show the standard deviation of the triplicates. Student t-test was performed to check the significance in the fluorescence difference between the groups. (p= <0.0001).

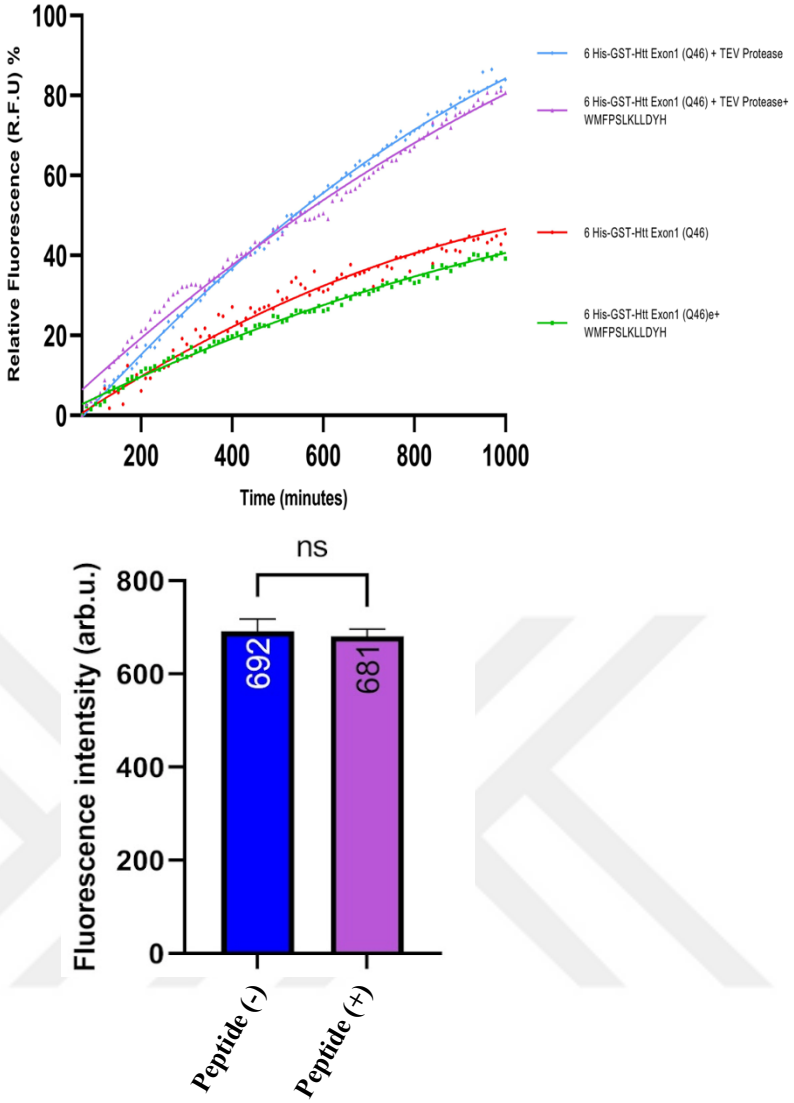

Figure20. Aggregation kinetics for Htt exon1(Q46) with the addition of peptide WMFPSLKLLDYH shown in real time by tht assay.

a) The fluorescence intensity was normalized against GST cleaved Htt-(Q46) and plotted as a standard curve.

b) The fluorescence decreased by 1.6% in GST cleaved Htt-(Q46) in the presence of the peptide. The bar represents mean fluorescence intensity of the end point fluorescence value and the error bars show the standard deviation of the triplicates. Student t-test was performed to check the significance in the fluorescence difference between the groups. (p= <0.0001).

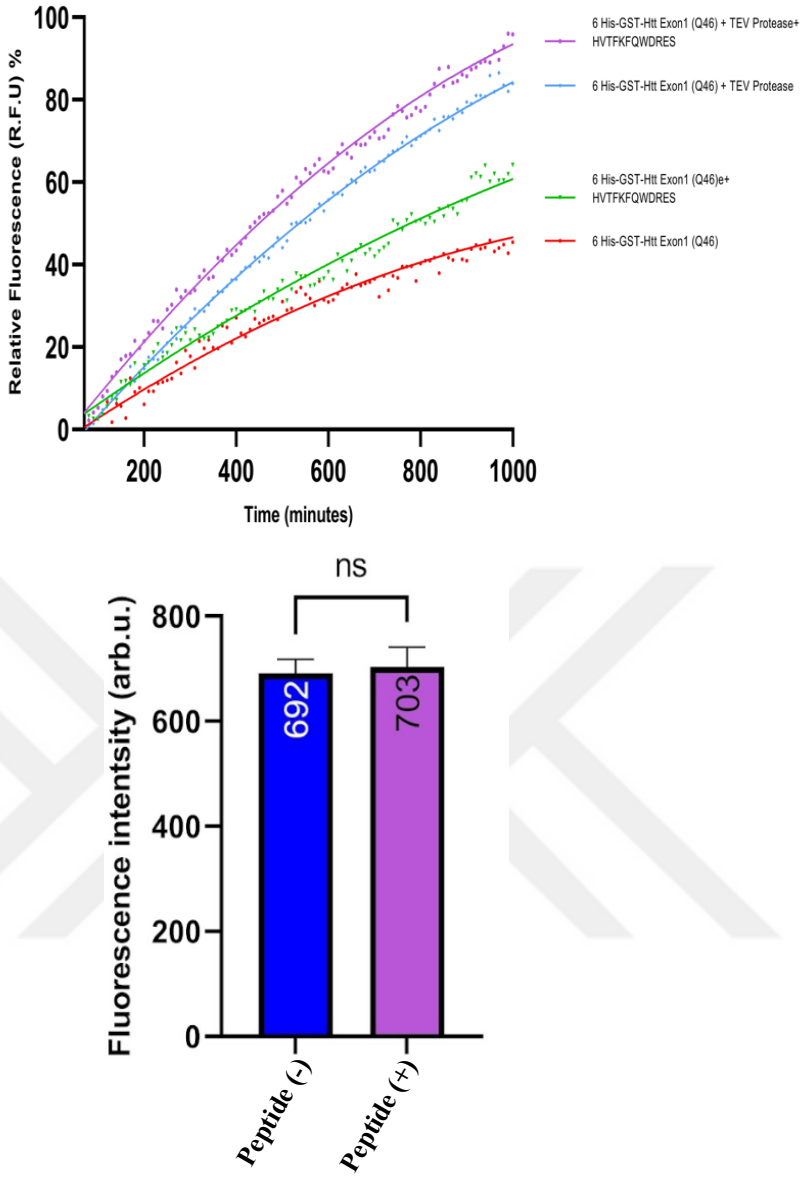

Figure21. Aggregation kinetics for Htt exon1(Q46) with the addition of peptide HVTFKFQWDRES shown in real time by tht assay.

a) The fluorescence intensity was normalized against GST cleaved Htt-(Q46) and plotted as a standard curve.

b) The fluorescence increase by 1.6% in GST cleaved Htt-(Q46) in the presence of the peptide. The bar represents mean fluorescence intensity of the end point fluorescence value and the error bars show the standard deviation of the triplicates. Student t-test was performed to check the significance in the fluorescence difference between the groups. (p= <0.0001).

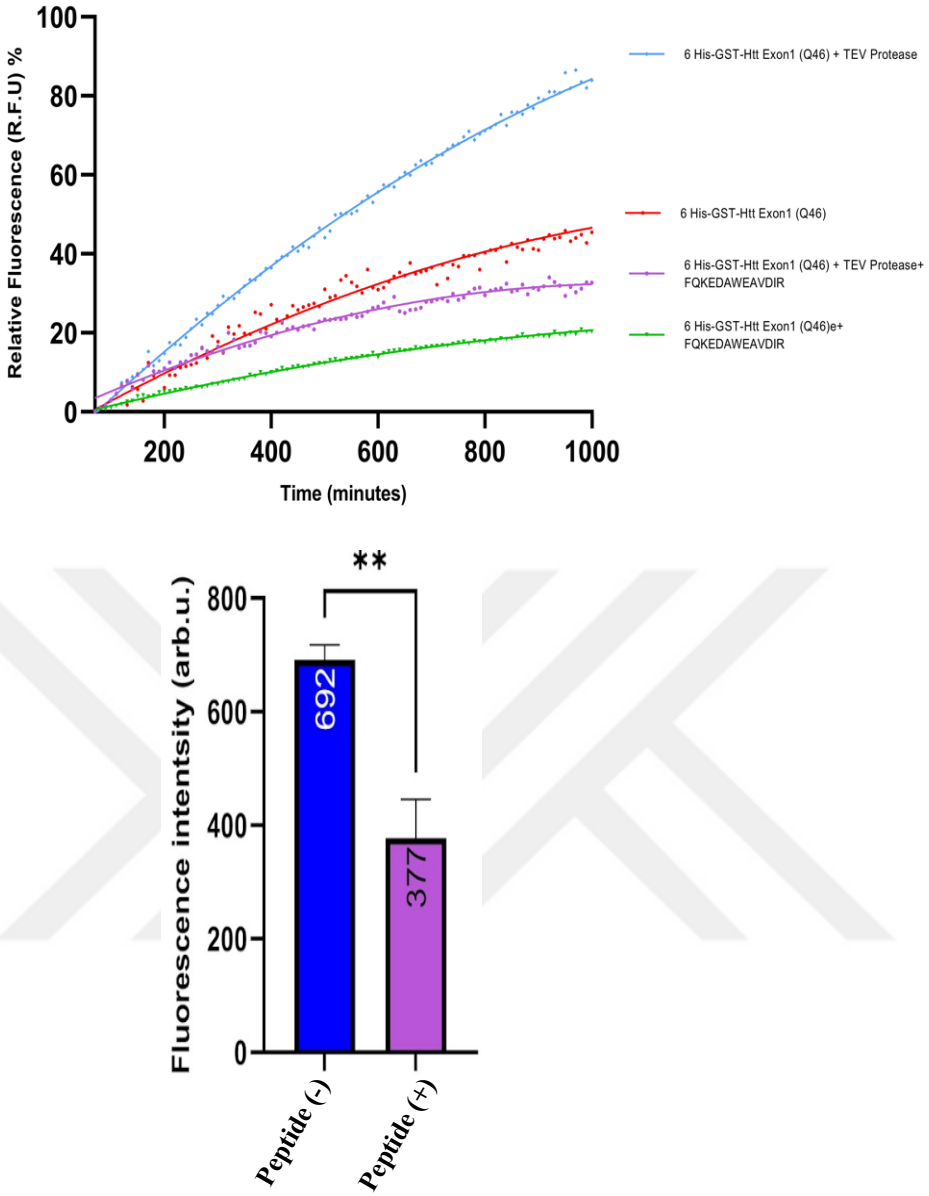

Figure 22. Aggregation kinetics for Htt exon1(Q46) with the addition of peptide FQKDAWEAVDIR shown in real time by tht assay.

a) The fluorescence intensity was normalized against GST cleaved Htt-(Q46) and plotted as a standard curve.

b) The fluorescence decreased by 45.5% in GST cleaved Htt-(Q46) in the presence of the peptide. The bar represents mean fluorescence intensity of the end point fluorescence value and the error bars show the standard deviation of the triplicates. Student t-test was performed to check the significance in the fluorescence difference between the groups. (p= <0.0001).

THT ASSAY FOR HTT EXON1 (Q25)

In comparison with the mutant Htt exon1 fragments, the wildypye Htt with less than 36 polyQ repeats do not form insoluble aggregates, but soluble aggregates are present in Htt Q25(69).

Both GST cleaved and fused protein did not vary in terms of fluorescence intensity. As expected. However baseline fluorescence was observed for both, this is due to the presence of Beta sheets (although of shorter length and less cross linked) are still present. Since the screened peptides were screed against all three Htt (Q25), (Q46) and (Q103) proteins, The effect of the candidate inhibitory peptides was also studied on HttQ25.

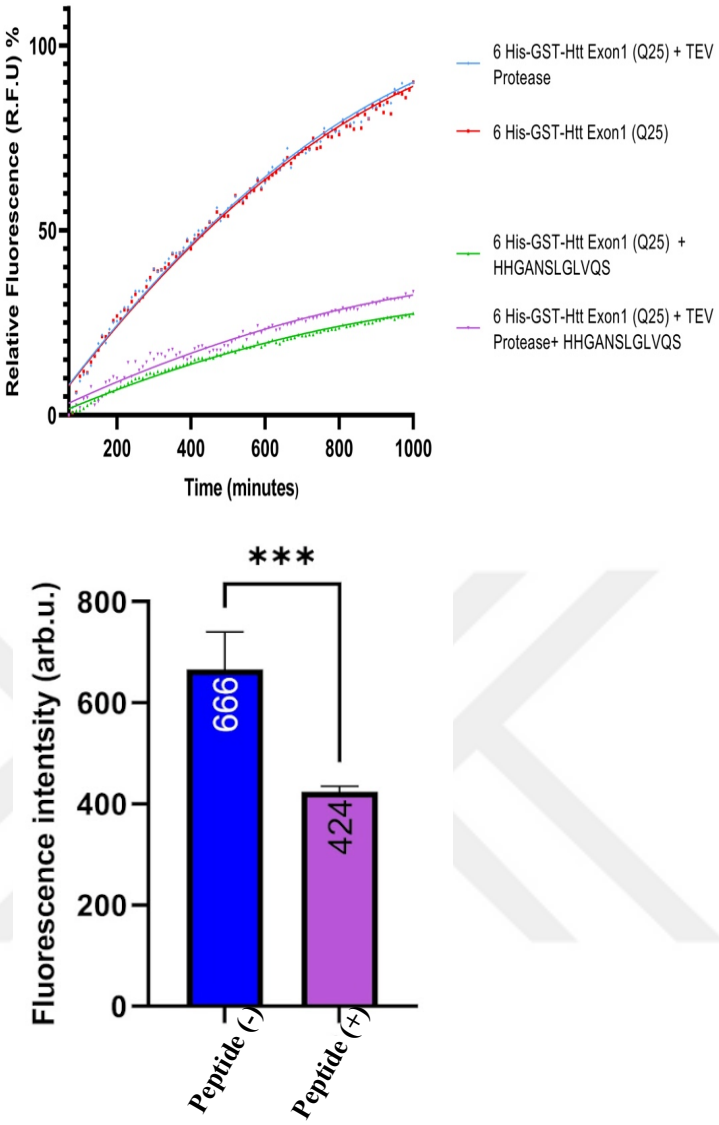

Figure 23. Aggregation kinetics for Htt-(Q25) with the addition of peptide HHGANSLGLVQS shown in real time by tht assay.

a) The fluorescence intensity was normalized against GST cleaved Htt-(Q25) and plotted as a standard curve.

b) The fluorescence decreased by 36.3% in GST cleaved Htt-(Q25) in the presence of the peptide. The bar represents mean fluorescence intensity of the end point fluorescence value and the error bars show the standard deviation of the triplicates. Student t-test was performed to check the significance in the fluorescence difference between the groups. ($p = <0.0001$).

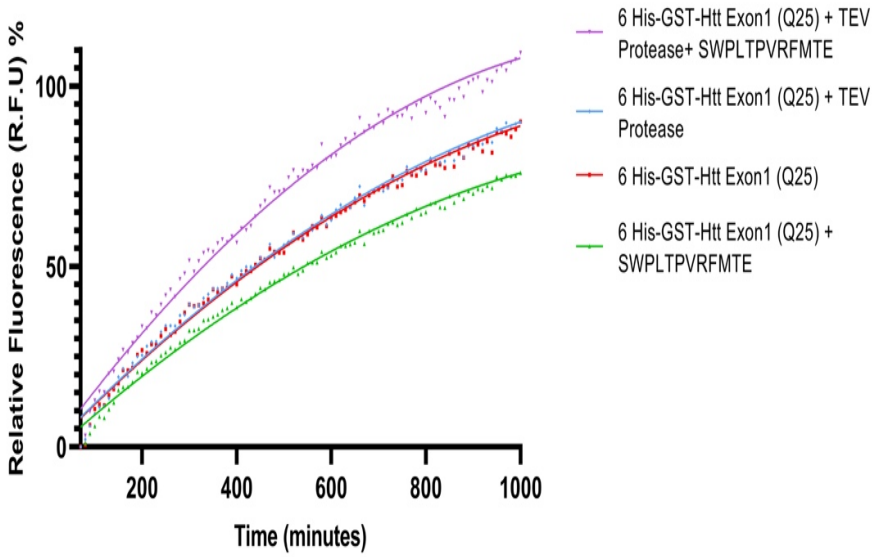

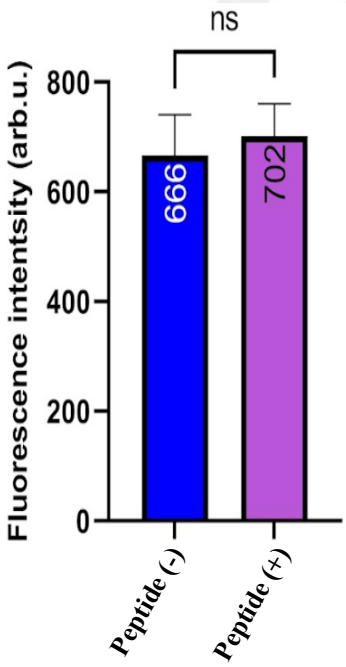

Figure24. Aggregation kinetics for Htt-(Q25) with the addition of peptide SWPLTPVRFMTE shown in real time by tht assay.

a) The fluorescence intensity was normalized against GST cleaved Htt-(Q25) and plotted as a standard curve.

b) The fluorescence increased by 5.4% in GST cleaved Htt-(Q25) in the presence of the peptide. The bar represents mean fluorescence intensity of the end point fluorescence value and the error bars show the standard deviation of the triplicates. Student t-test was performed to check the significance in the fluorescence difference between the groups. ($p = <0.0001$).

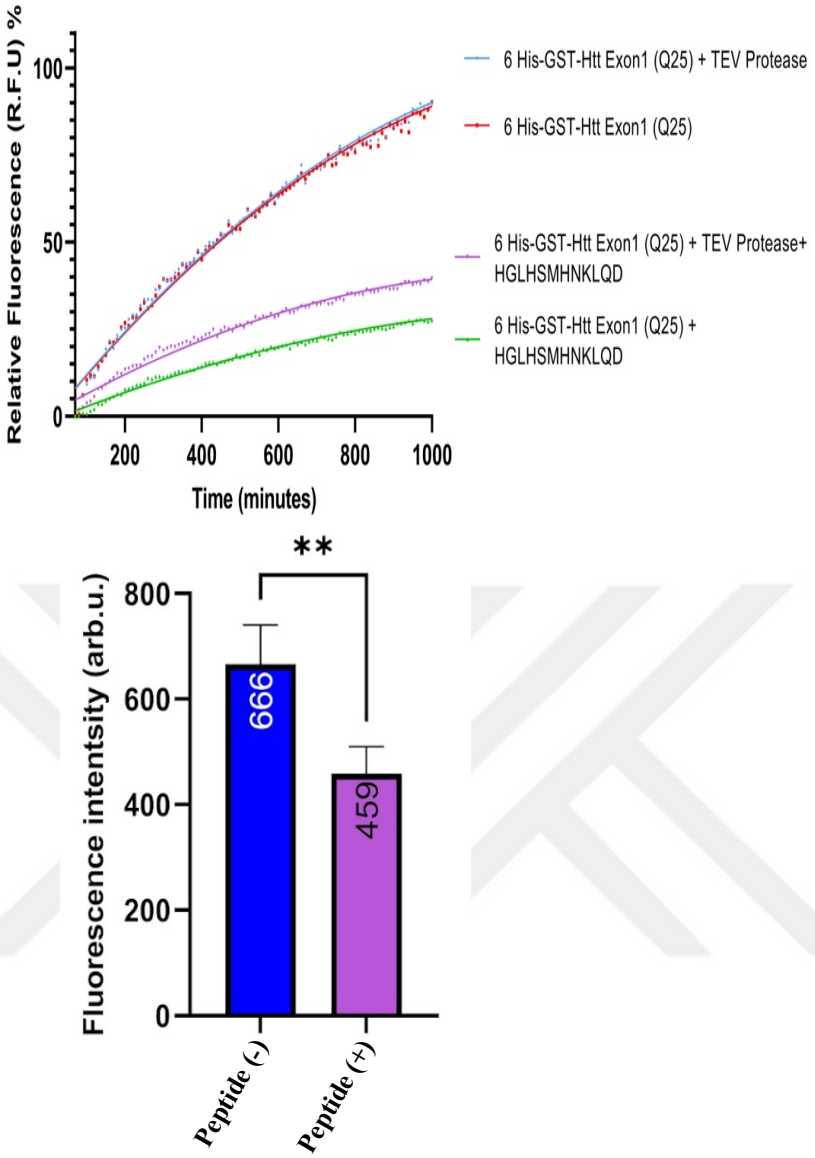

Figure25. Aggregation kinetics for Htt-(Q25) with the addition of peptide HGLHSMHNKLQD shown in real time by tht assay.

a) The fluorescence intensity was normalized against GST cleaved Htt-(Q25) and plotted as a standard curve.

b) The fluorescence decreased by 31% in GST cleaved Htt-(Q25) in the presence of the peptide. The bar represents mean fluorescence intensity of the end point fluorescence value and the error bars show the standard deviation of the triplicates. Student t-test was performed to check the significance in the fluorescence difference between the groups. (p= <0.0001).

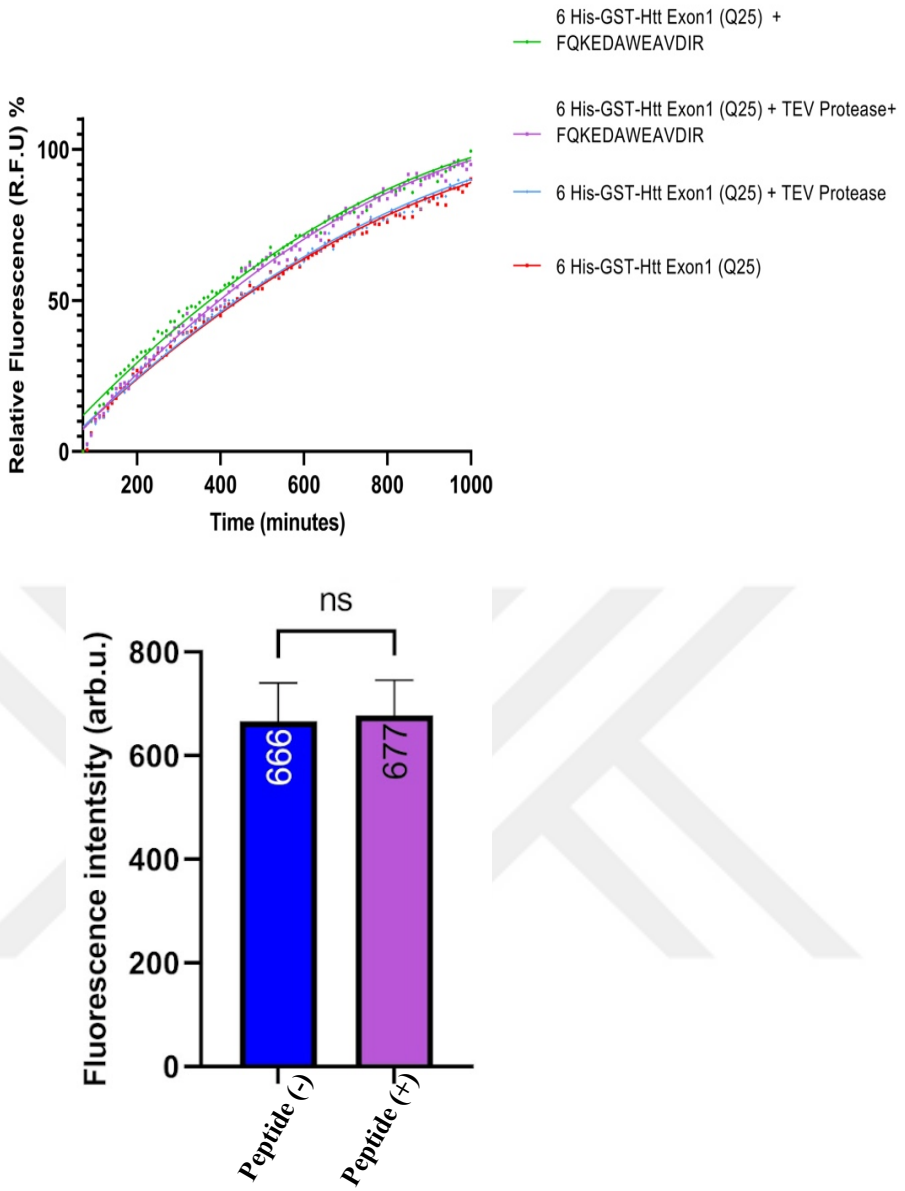

Figure 26. Aggregation kinetics for Htt-(Q25) with the addition of peptide FQKEDAWEADIR shown in real time by tht assay.

a) The fluorescence intensity was normalized against GST cleaved Htt-(Q25) and plotted as a standard curve.

b) The fluorescence increased by 1.7% in GST cleaved Htt-(Q25) in the presence of the peptide. The bar represents mean fluorescence intensity of the end point fluorescence value and the error bars show the standard deviation of the triplicates. Student t-test was performed to check the significance in the fluorescence difference between the groups. (p= <0.0001).

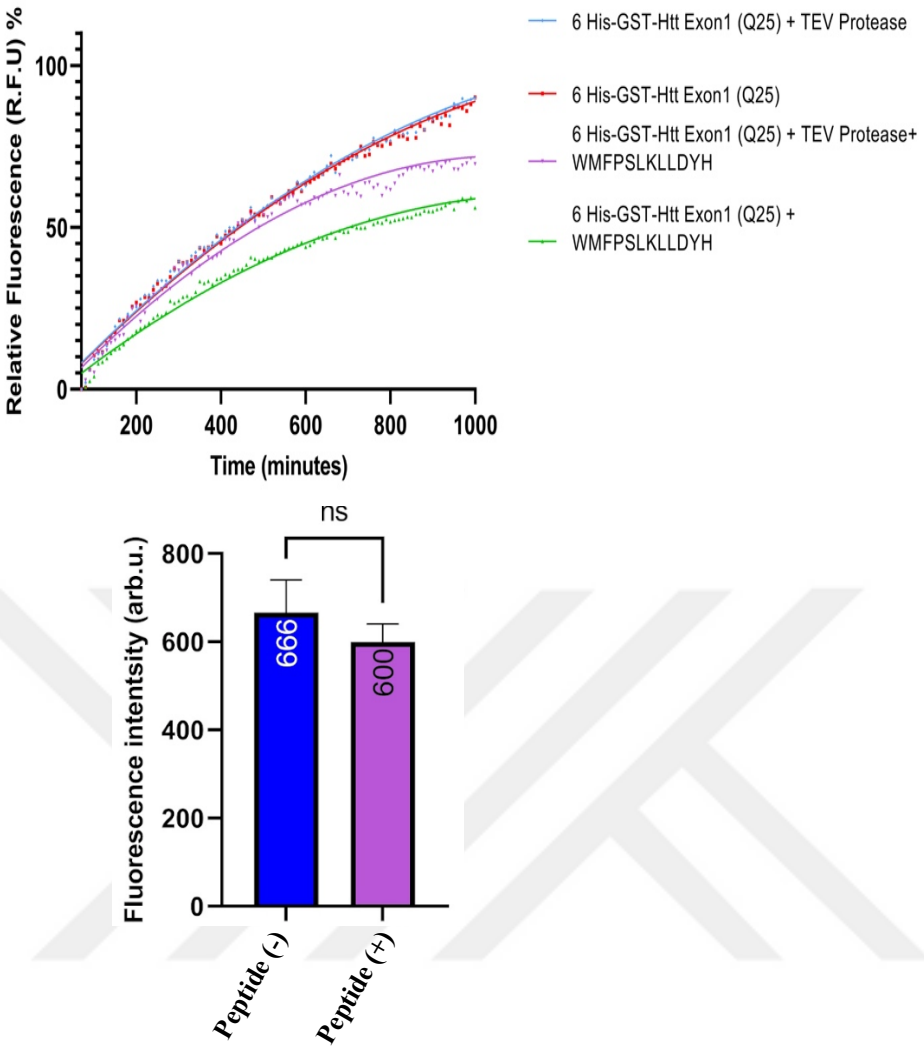

Figure 27. Aggregation kinetics for Htt-(Q25) with the addition of peptide WMFPSLKLLDYH shown in real time by tht assay.

a) The fluorescence intensity was normalized against GST cleaved Htt-(Q25) and plotted as a standard curve.

b) The fluorescence decreased by 10% in GST cleaved Htt-(Q25) in the presence of the peptide. The bar represents mean fluorescence intensity of the end point fluorescence value and the error bars show the standard deviation of the triplicates. Student t-test was performed to check the significance in the fluorescence difference between the groups. (p= <0.0001).

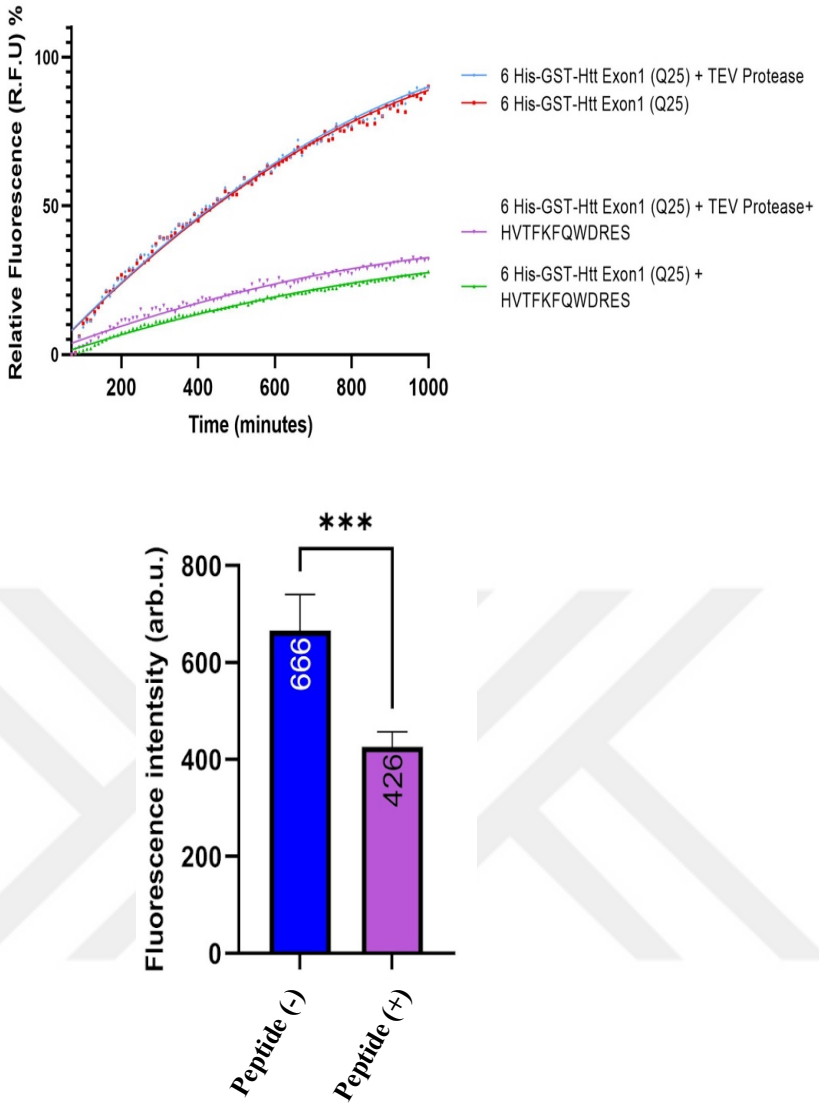

Figure 28. Aggregation kinetics for Htt-(Q25) with the addition of peptide HVTFKFQDRES shown in real time by tht assay.

a) The fluorescence intensity was normalized against GST cleaved Htt-(Q25) and plotted as a standard curve.

b) The fluorescence decreased by 36% in GST cleaved Htt-(Q25) in the presence of the peptide. The bar represents mean fluorescence intensity of the end point fluorescence value and the error bars show the standard deviation of the triplicates. Student t-test was performed to check the significance in the fluorescence difference between the groups. (p= <0.0001).

As the glutamine expansion/ length of polyQ repeats is directly correlated with the increase in the kinetics of aggregation. Highest fluorescence was observed for Htt-Q103, followed by Htt-Q46 and then HttQ25. Fluorescence for both GST fused and GST-Cleaved (real-time reaction) were recorded for the interval of at least 16 hours. It has previously been shown that fusion of GST protein with Htt proteins forms a stable structure. The model proposed by Scherzinger (67) suggests that GST-Htt (exon1) protein are bound to the surface of GST protein as dimers, stabilized by strong hydrogen bonds formed between the antiparallel β strands forming a stable hairpin structure. In this conformation the hairpins are not accessible to one another, therefore the possibility of them interacting is significantly reduced. However as in our construct the site-specific cleavage by tev protease; between the GST tag and the Htt protein; releases the GST bound protein. These Htt- proteins are then able to interact with each other, forming polyQ-comprising β sheet fibrils and thus initiating the aggregation process. This can be seen by increase in the fluorescence signal with time.

Upon addition of peptides, either decrease or increase was observed in the fluorescence signal. The decrease in fluorescence suggests that there was a decrease in fibrillization process and that the inhibitory peptide blocked aggregation in the otherwise highly aggregated protein (in the case of Q103 and Q46). Inhibition in signal of Htt Q25 suggest that the peptide was able to block aggregation even for short polyQ repeats. Therefore, if clinically translated can be used at an early onset of disease progression.

Some peptides caused increase in fluorescence signal. A reason for that could be that the peptide doesn't block aggregation, but is exciting it by binding at some other domain of the Htt protein. Or that the peptide doesn't bind to the protein and during the screening process it might have interacted with Aga2 or the linker region between Aga2 and Htt monomer [69].

After evaluating all Tht assays perfomed, 3 ligand peptides, that caused decrease in fluorescent signal in all three protein were selected for further analysis of their inhibition on Aggregation kinetics by Atomic Force Microscopy

INHIBITORY PEPTIDE	Htt(Q46)	Htt(Q25)	Htt(Q103)
1. HHGANSLSLVSQD	decreases	decreases	decreases
2. SWPLTPVRFMTE	decreases	increases	decreases
3. HGLHSMHNKLTR	decreases	decreases	decreases
4. FKQDAWEAVDIR	decreases	increases	increases
5. WMFPSLKLLDYH	decreases	decreases	decreases
6. HVTFKFQWDRES	increases	decreases	decreases

Table 2. Summarizes the increase or decrease in fluorescence detected after tht assay for all three Htt proteins, in the presence of all 6 peptides. **HHGANSLSLVSQD, HGLHSMHNKLTR, WMFPSLKLLDYH** caused decrease in fluorescence in all three Htt proteins.

Atomic Force Microscopy

The effect of the inhibitory peptides on the Aggregation kinetics of both wildtype Htt-Q25 and mutant Htt-Q46 and HttQ103 were studied by Atomic Force Microscopy.

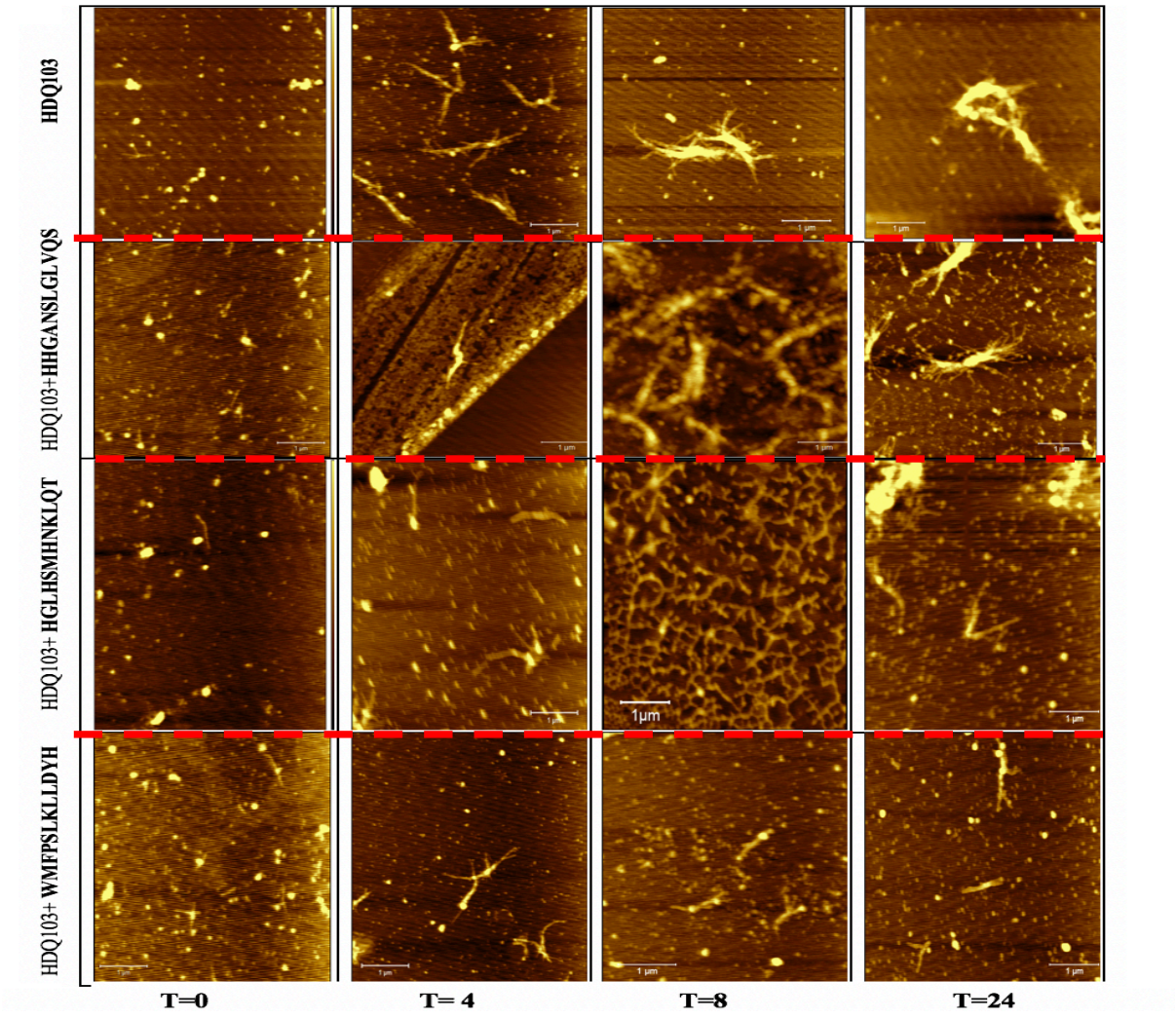

Figure 29. Shows the aggregation kinetics of HttQ103, both in absence and presence of inhibitory peptides. The AFM images show samples obtained at 0 hour, 4 hours, 8 hours, and 24 hours. Imges A through D correspond to fibril growth kinetic of of HttQ103 protein. Images E through H correspond to fibril growth kinetics of HttQ103 in the presence of inhibitory peptide **HHGANSLLGLVQS** Images I through L correspond to fibril growth kinetics of HttQ103 in the presence of inhibitory peptide **HGLHSMHNKLLQT** and Images M through P correspond to fibril growth kinetics of of HttQ103 in the presence of inhibitory peptide **WMFPSLKLLDYH. Scale bar is 1um.**

To initiate the aggregation process, Site specific cleavage of GST was done by the addition of tev protease. The fibrils were allowed to grow for two hours after which peptides was added. This was noted as hour t=0. As shown in the figure above samples were collected every 4 hours for AFM imaging. For Htt(Q103), at t=0, small round Oligomers and individual fibrils are visible. These are expected to be observed at early stages of fibrillization kinetics, as reported before by (Dahlgren et.al). At t=4, we observed an increase in length of fibrils and branching. Branched morphology is a well-established characteristic of Htt protein with polyQ> 36, and this was observed for t=4, t=8 and t=24. The branching and aggregation increased with time and more clustering was observed. The Length of 100 different fibrils at each time point was measured. The length of fibrils at individual time points are graphed below in figure 30. observed a decrease in length at t=24. This could be due to degradation of Htt(Q103) in tev cleavage buffer.

While comparing the fibril kinetics of peptide treated proteins, a significant decrease in fibril length was observed for all time points. A decrease in clustering and branching was also seen. This decrease was quantified by measuring 100 fibrils at all time points and plotting the mean length in the figure below. Even at early stages of aggregation kinetic the inhibitory effect of peptide is visible. Less branching and even individual fibrils are observed at t=4 and t=8. This gives clear evidence that the peptide applied inhibit the aggregation of otherwise aggregated HttQ103 protein with well-defined branching and clustering. These decrease in the length of the fibrils indicate inhibition of fibril formation at an early stage.

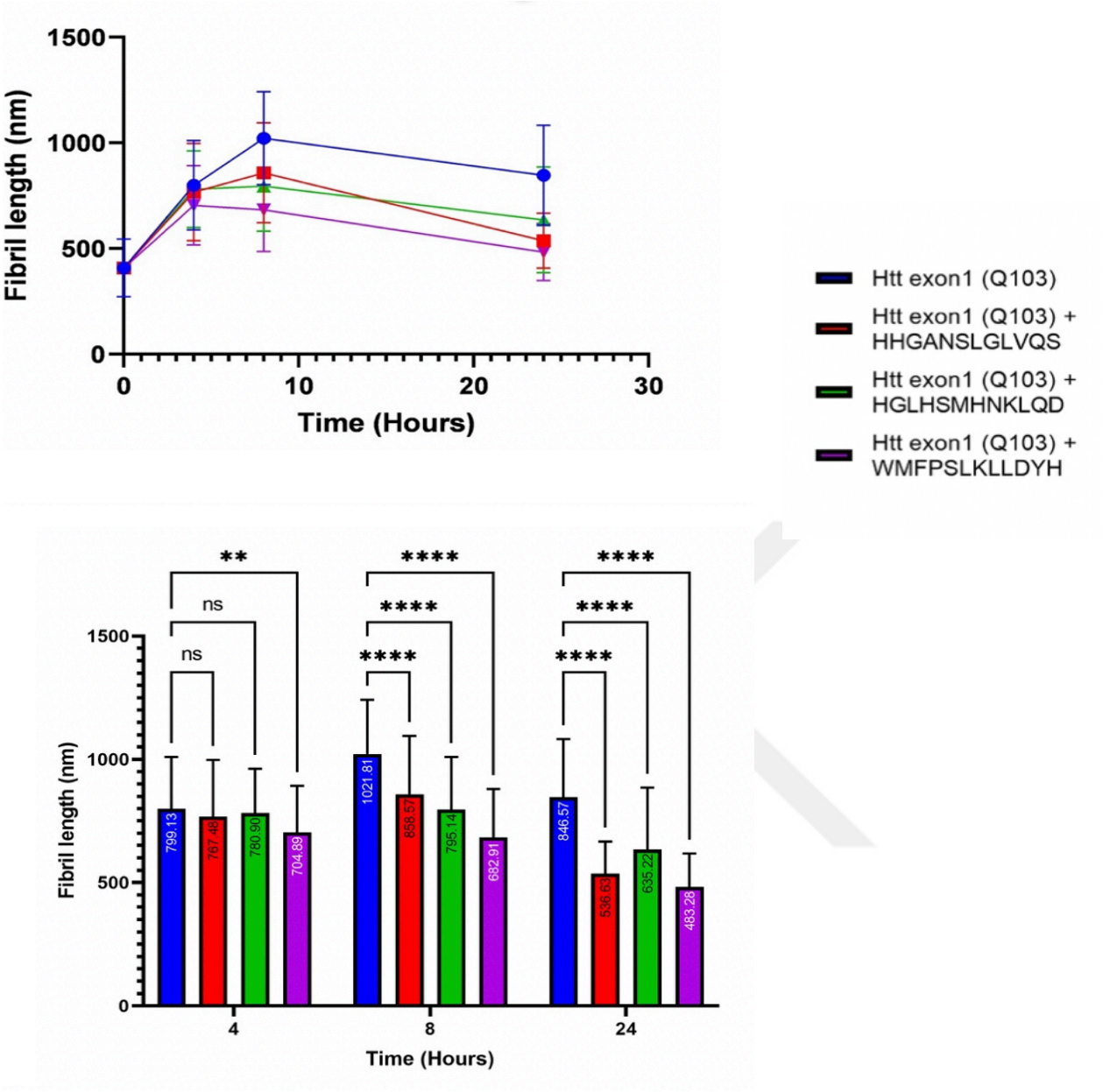

Figure30 . Shows change in fibril length of the peptide treated Htt(exon1) Q103 respect to time. The mean and standard deviation of 100 fibrils are plotted. From the data above it was seen that

HHGANSLGLVQS= 36.5% Percentage decrease in fibril length after 24 hours

HGLHSMHNKLQD= 24.91% Percentage decrease in fibril length 24 hours

WMPSLKLLLDYH= 42.87% Percentage decrease in fibril length after 24 hours

The effect of the peptides were then checked on Htt-Q46.

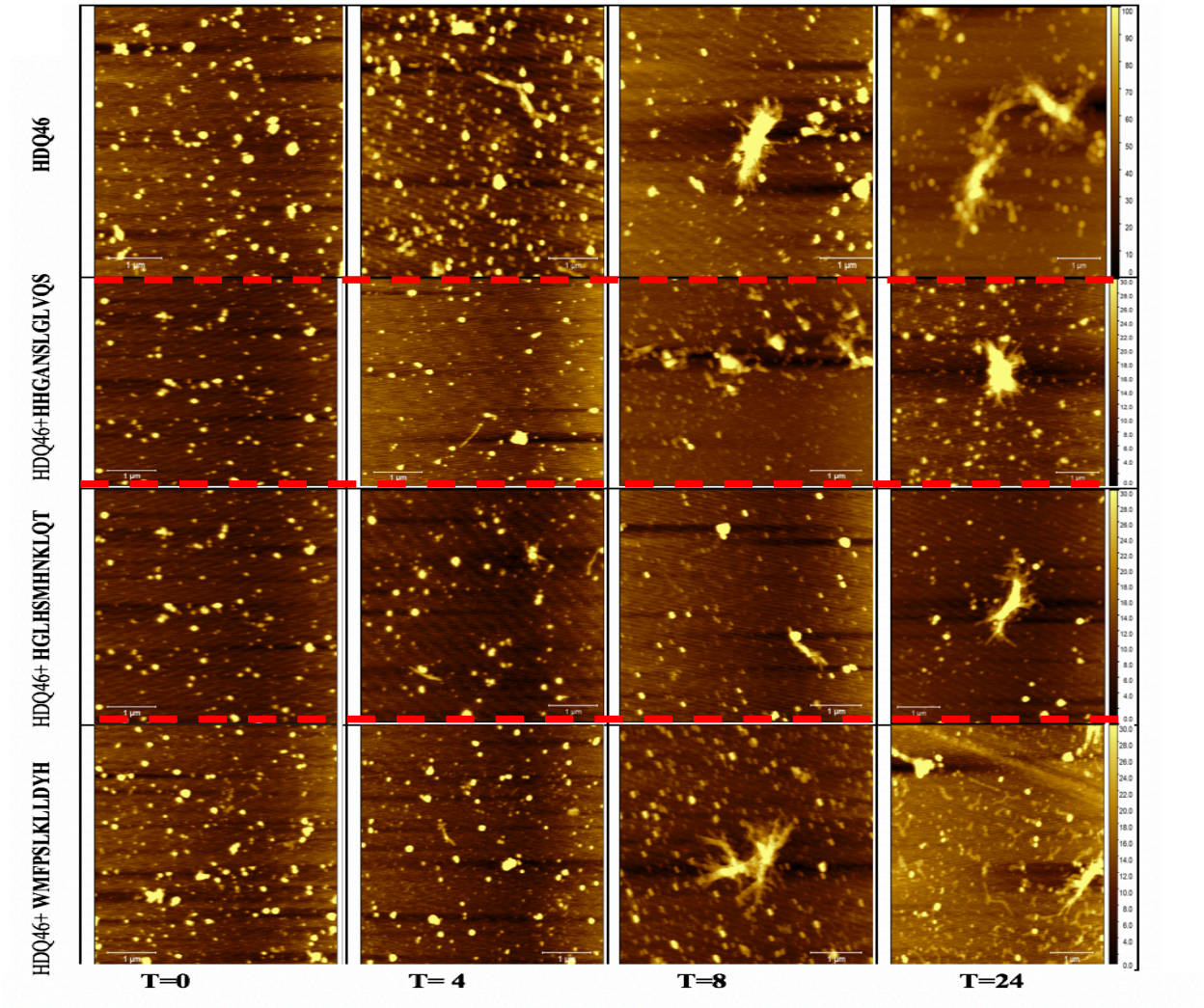

Figure31. Shows the aggregation kinetics of HttQ46, both in absence and presence of inhibitory peptides. The AFM images show samples obtained at 0 hour, 4 hours, 8 hours, and 24 hours. Images A through D correspond to fibril growth kinetic of of HttQ46 protein. Images E through H correspond to fibril growth kinetics of of Htt Q46 in the presence of inhibitory peptide **HHGANSLLGLVQS** Images I through L correspond to fibril growth kinetics of $Htt_{(exon1)}$ Q46 in the presence of inhibitory peptide **HGLHSMHNKLLQT** and Images M through P correspond to fibril growth kinetics of Htt Q46 in the presence of inhibitory peptide **WMFPSLKLLDYH. Scale bar is 1um.**

To initiate the aggregation kinetic in HttQ46 of , Site specific cleavage of GST was done by the addition of tev protease, As described in material and methods chapter. The fibrils were allowed to grow for two hours after which peptides was added in equimolar ratio. This was noted as hour t=0. As shown in the figure above samples were collected every 4 hours for AFM imaging. For HttQ46 (protein only) at t=0, small round Oligomers are visible. These are expected to be observed at early stages of fibrillization kinetics, for shorter polyQ repeats. At t=4, we the oligomeric aggregates dominated as shown previously by beasly et al. At this point fibrillar structures of ~400nm in length are also observed. As Branched morphology is a well-established characteristic of Htt protein with polyQ> 36, ar t=8 and t=24, more branched morphology with clusters was visible. The branching and aggregation increased with time and more clustering was observed. The Length of 100 different fibrils at each time point was measured. The length of fibrils at individual time points are graphed below in figure 32. observed a decrease in length at t=24 and degradation of the protein could be seen. This could possibly be explained the alkaline pH of tev reaction buffer (pH 8.0) these proteins were desalted in for the cleavage reaction.

While comparing the fibril kinetics of peptide treated proteins, a significant decrease in fibril length was observed for all time points. At times 4 and 8 more oligomeric clusters are seen as compared to fibrils. A decrease in clustering and branching was also seen at t=24 and for peptide **WMPSLKLLLDYH** at t=24, thin individual fibrils are visible. This decrease was quantified by measuring 100 fibrils at all time points and plotting the mean length in the figure below. Even at early stages of aggregation kinetic the inhibitory effect of peptide is visible. This gives clear evidence that the peptide applied inhibit the aggregation of otherwise aggregated Htt Q46 protein with well-defined branching and clustering and reduced number of oligomeric aggregates.

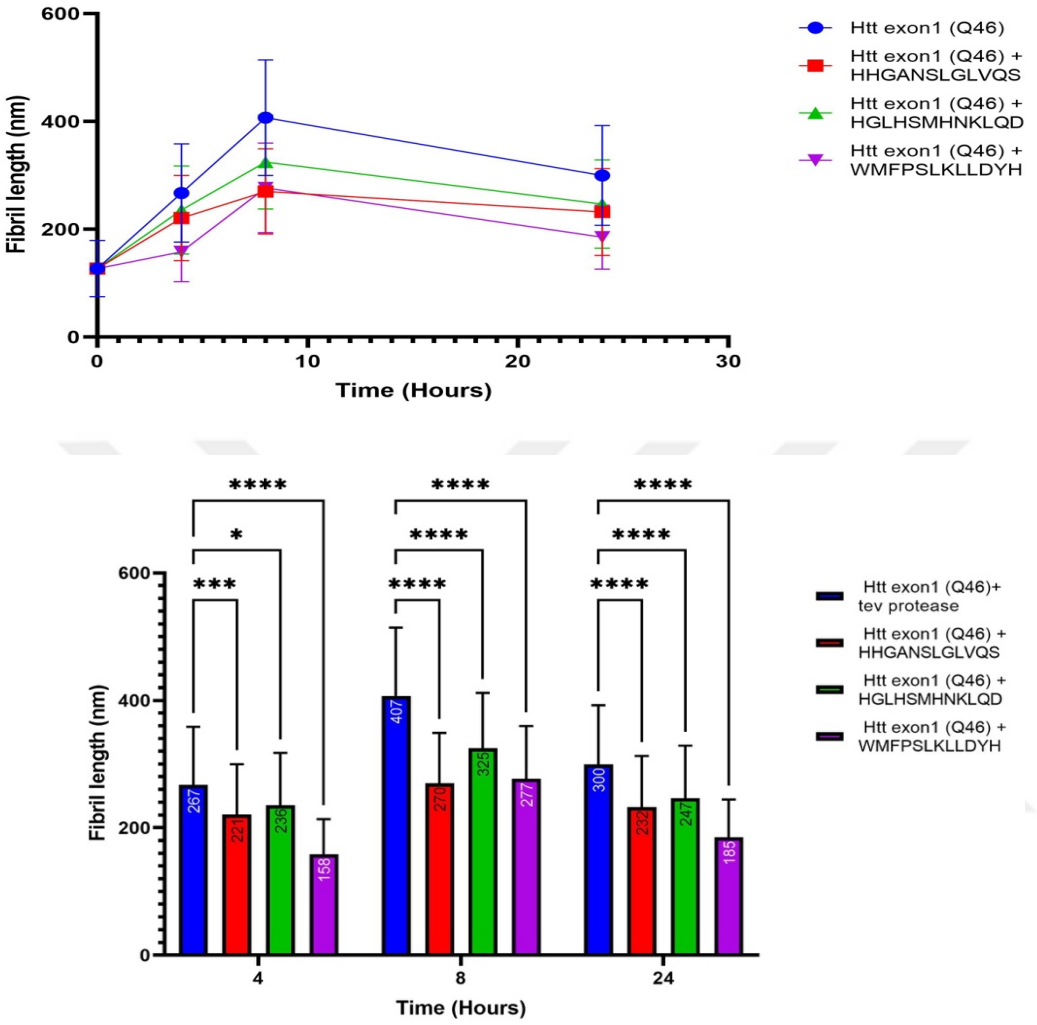

Figure 32 . Shows change in fibril length of the peptide treated Htt(exon1) Q46 respect to time. The mean and standard deviation of 100 fibrils are plotted. From the data above it was seen that

HHGANSLGLVQS= 22.67% Percentage decrease in fibril length after 24 hours
HGLHSMHNKLQD= 17.67% Percentage decrease in fibril length 24 hours
WMPSLKLLLDYH= 38.33% Percentage decrease in fibril length after 24 hours

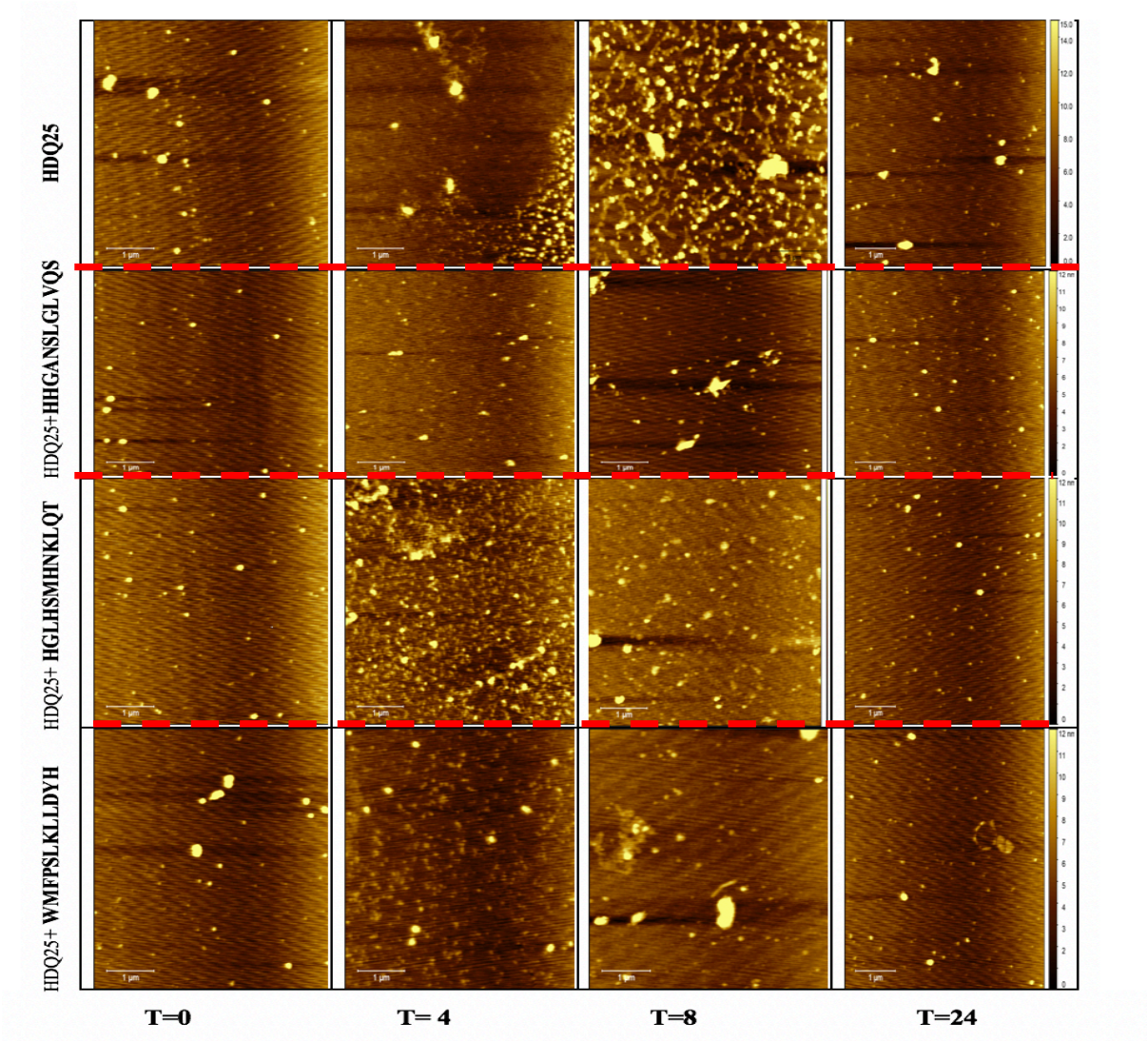

Figure33. Shows the fibrillation kinetics of HttQ25, both in absence and presence of inhibitory peptides. The AFM images show samples obtained at 0 hour, 4 hours, 8 hours, and 24 hours. Images A through D correspond to fibril growth kinetic of of HttQ25 protein. Images E through H correspond to fibril growth kinetics of of HttQ25 in the presence of inhibitory peptide **HHGANSLLGLVQS** Images I through L correspond to fibril growth kinetics of HttQ25 in the presence of inhibitory peptide **HGLHSMHNKLLQT** and Images M through P correspond to fibril growth kinetics of HttQ25 in the presence of inhibitory peptide **WMFPSLKLLDYH. Scale bar is 1um.**

As done previously, Site specific cleavage of GST fused HttQ46 was done by the addition of tev protease, described in material and methods chapter. Two hours after the tev reaction, peptides was added in equimolar ratio. This was noted as hour t=0. As shown in the figure above samples were collected every 4 hours for AFM imaging. For HttQ25 (protein only) at t=0, small round Oligomers with a diameter of 80-100nm were visible. These were as expected. Since HttQ25 do not form insoluble aggregates, small oligomers were seen predominately in t=4 samples as well with very few small individual fibrils. These fibrils were significantly smaller in length than the mutant Htt exon1 proteins discussed above. At t=8 for HttQ25, protein only small individual fibrils ranging from 100-140nm were observed and at t=24 again small oligomers were observed. The diameters of these oligomers were measured. To eliminate any impurity present in SiO2 wafer, only oligomers above 5nm in height were accounted for. The diameters of 100 different fibrils/ oligomers at each time point was measured. The length these fibrils at individual time points are graphed below in figure 34. observed a decrease in length at t=24 and degradaration of the protein could be seen. This could possibly be explained the alkaline pH of tev reaction buffer (pH 8.0) these proteins were desalted in for the cleavage reaction.

While comparing the fibril kinetics of peptide treated proteins, a significant decrease in fibril length was observed for all time points. At times 4 and 8 and 24 we did not see any individual fibers but only oligomers were visible in case of all peptides. These results give clear evidence that the inhibitory peptides are very specific and show inhibition of fibri formatio even for short ployQ stretches.

This along with tht data suggests that the inhibitory peptides are highly efficient in blocking aggregation process in all Huntington repeats.

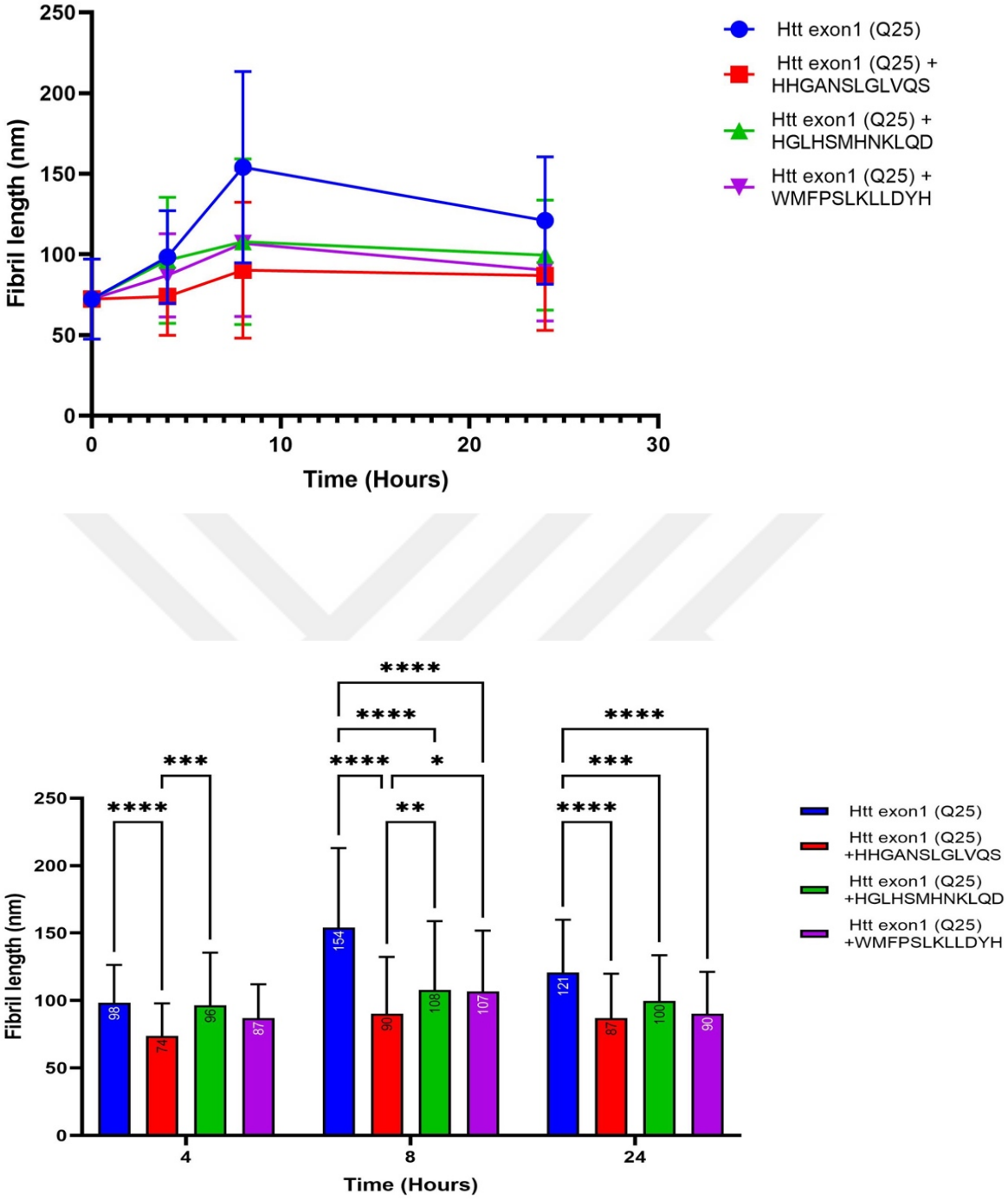

Figure34 . Shows change in fibril length of the peptide treated Htt(exon1) Q46 respect to time. The mean and standard deviation of 100 fibrils are plotted. From the data above it was seen that

HHGANSLGLVQS= 28% Percentage decrease in fibril length after 24 hours
HGLHSMHNKLQD= 17.3% Percentage decrease in fibril length 24 hours
WMPSLKLLLDYH= 25.6% Percentage decrease in fibril length after 24 hours

The AFM results and the THT Assay results complement each other. It gives us a strong evidence that the inhibitory peptides efficiently blocked the aggregation in both the wildtype and mutant Htt fibrils *in-vitro*. For these experiments the exon1 of both mutant and wildtype htt was focused on. It has been previously shown that the N-terminal HTT peptides exhibit exceptional pathogenicity [69]. The increment in the poly-Q stretch in exon1 lead to unique structural and biophysical changes in the Htt proteins that result in misfolded monomers, which polymerize rapidly to form toxic oligomers. These oligomers then form inclusion bodies in the basal ganglia region of the brain disrupting the neuronal function, leading to neural degeneration [56]. Wildtype Htt was included in all the aggregation kinetics studies, this is mainly due to the fact that HD is an autosomal dominant disorder. One mutant allele is sufficient for the formation of the pathological aggregates. Moreover, it has been shown that mutant httQ46 seeds can cause the formation of insoluble aggregates on httQ25[71] *in vitro*. Therefore, we wanted to see if our peptides had an effect on soluble aggregate formation by Htt Q25 and if our peptide therapy will be effective in heterozygous HD variants.

The utilization of peptides that act to prevent this aggregation in Htt protein by interacting with polyQ stretches provide a promising platform for drug development. The low potential toxicity and the ability of these peptides to target the mHtt at the very initial steps in the aggregation make them an ideal candidate for peptide-based therapeutics. Considering this potential of peptide therapeutics for HD; several therapeutic peptides have been developed such as P42, P42TAT [70], Bivalent Htt-binding peptide [72], Polyglutamine-binding peptide 1 (QBP1) [73]. However, these peptides mainly focus on inhibiting aggregation at later stage in the cascade of htt polymerization and aggregate development.

The inhibitory peptides tested in this study, were screened against the monomeric units of Htt proteins. These monomeric units were expressed on the yeast surface, which allowed for

proper eukaryotic folding/misfolding. The peptides were introduced by Phage display library. The ligand peptides were selected by biopanning without immobilizing yeast cells[74].

The ability of peptide to bind monomeric htt fragments allows blocking of aggregation at a very early stage of disease progression. This gives novelty to our proposed peptides which were used in this study .

The future studies will be focused on assessing the toxicity of these selected peptides in mammalian cells; this would be done by both *in vitro* and *in vivo* experiments.

In-vitro studies will be carried out by utilizing HT22 (mouse hippocampal) cell line. And the toxicity will be evaluated by MTT (3–(4,5-dimethylthiazol-2-yl)-2,5-diphenyltetrazolium bromide) colorimetric test for viability assay. The peptides will be tested individually on Ht22 cells, and in combination with Htt proteins in equimolar ratio by co-transfection. This will allow us to evaluate two things; 1. Whether The peptide has any toxic effect on the neurons and 2. Whether the peptide is decreasing the toxicity of the mHtt aggregates in the neurons. After this the peptides that poses least to no toxicity will be selected for *in vivo* experiments in animal models.

To this date several HD animals' models are available. These include Drosophila polyQ model ELAV-Gal4; UAS-MJDtr-78Q [75], Mice model Full-length hHtt-97Q BACHD [76]. Mouse models will be ideal for this study since we can study the effect of peptides both on a molecular level and we can also closely monitor the behavioral changes on the mice post treatment. Mice transgenic for human huntingtin exon 1 (strain R6/2) [70] can be used for this study. In order to overcome the issues encompassing the limitations of cell membrane penetration, peptide degradation and the delivery of the therapeutic peptides to the central nervous system especially basal ganglia by non-invasive methods, we can adapt the mode of delivery previously described by Arribat et.al[70]. For studies involving animal models, it is imperative to focus on the pharmacokinetic characteristics of ligand peptide and optimize it's

half-life in serum and its distribution profile in CNS. As reported previously by Arribat et.al a water-in-oil microemulsion drug delivery vector named Aonys®, developed by Medesis Pharma (France) in a non-invasive strategy and proved to be a promising delivery vector for the delivery of peptide p42, in both the cortex and striatum[70]. The delivery vector was engineered by combining the properties of the cell penetrating peptide TAT from HIV with a nanostructure-based drug delivery system [70]. Building on these studies we can optimize the microemulsion formulation of our peptides in Aonys® and deliver them by transmucosal (buccal/rectal) administration. In R6/2 HD mouse model the symptoms appear at week 6. We can perform daily administration at pre-symptomatic stage in these mice. We can then perform both brain atrophy evaluation by T2-FLAIR scans and behavioral studies focusing on motor performances in both peptides treated and non-treated mice.

The success of these animal model studies can then allow our peptide therapy to translated into clinical studies.

Conclusion

Huntington's disease is one of the most common hereditary disorder of the nervous system. It is a progressive, autosomal dominant neurodegenerative disease caused by dramatic increase of polyQ repeats in Exon 1 of Htt gene. Theses mutant HTT(mHtt) fragments result in misfolded proteins which leads to aggregation of the mutant protein in neurons. These result in formation of fibrils that interfere with cellular function and causes neural degeneration. Since formation of aggregates is a critical point in the pathology of HD, targeting and inhibiting the aggregation can be an effective therapeutic strategy to halt the disease progression. Peptide Based therapeutics can provide such platform.

In this study, previously screened candidate ligand peptides were characterised and were evaluated for their inhibitory effect against three Htt proteins (Q25)(Q46)(Q103).

In vitro characterisation of peptides on aggregation kinetics was studied by thioflavin T Assay and Atomic Force Microscopy.

3 of the 6 selected peptides (HHGANSLSLVSQD),(HGLHSMHNKLTR) and (WMFPSLKLLDYH) showed a decrease in florescence signal indicating inhibition in fibril formation for all three proteins. AFM images for these peptides showed less aggregation in mHtt proteins. These studies show that the selected peptides are affective for inhibiting the aggregation of fibrils in mHTT proteins and are promising candidates for peptide therapy for HD.

BIBLIOGRAPHY

1. Roos, Raymund AC. "Huntington's disease: a clinical review." *Orphanet journal of rare diseases* 5.1 (2010): 1-8.
2. Margolis, R. L., & Ross, C. A. (2003). Diagnosis of Huntington disease. *Clinical chemistry*, *49*(10), 1726-1732.
3. Huntington, G. On chorea. Med Surg Rep 1872; 26: 320 321
4. Margolis, R. L., O'Hearn, E., Rosenblatt, A., Willour, V., Holmes, S. E., Franz, M. L., & Ross, C. A. (2001). A disorder similar to Huntington's disease is associated with a novel CAG repeat expansion. *Annals of Neurology: Official Journal of the American Neurological Association and the Child Neurology Society*, *50*(3), 373-380.
5. Gusella, J. F., Wexler, N. S., Conneally, P. M., Naylor, S. L., Anderson, M. A., Tanzi, R. E., & Martin, J. B. (1983). A polymorphic DNA marker genetically linked to Huntington's disease. *Nature*, *306*(5940), 234-238.
6. Tabrizi, S. J., Scahill, R. I., Owen, G., Durr, A., Leavitt, B. R., Roos, R. A., & TRACK-HD Investigators. (2013). Predictors of phenotypic progression and disease onset in premanifest and early-stage Huntington's disease in the TRACK-HD study: analysis of 36-month observational data. *The Lancet Neurology*, *12*(7), 637-649.
7. Hersch, S. M., & Rosas, H. D. (2008). Neuroprotection for Huntington's disease: ready, set, slow. *Neurotherapeutics*, *5*(2), 226-236.
8. Díaz-Hernández, M., Torres-Peraza, J., Salvatori-Abarca, A., Morán, M. A., Gómez-Ramos, P., Alberch, J., & Lucas, J. J. (2005). Full motor recovery despite striatal neuron

loss and formation of irreversible amyloid-like inclusions in a conditional mouse model of Huntington's disease. *Journal of Neuroscience*, *25*(42), 9773-9781.

9. Yamamoto, A., Lucas, J. J., & Hen, R. (2000). Reversal of neuropathology and motor dysfunction in a conditional model of Huntington's disease. *Cell*, *101*(1), 57-66.
10. MacDonald, M. E., Ambrose, C. M., Duyao, M. P., Myers, R. H., Lin, C., Srinidhi, L., & Harper, P. S. (1993). A novel gene containing a trinucleotide repeat that is expanded and unstable on Huntington's disease chromosomes. *Cell*, *72*(6), 971-983.
11. Persichetti, F., Ambrose, C. M., Ge, P., McNeil, S. M., Srinidhi, J., Anderson, M. A., & Orkin, S. H. (1995). Normal and expanded Huntington's disease gene alleles produce distinguishable proteins due to translation across the CAG repeat. *Molecular Medicine*, *1*(4), 374-383.
12. Rubinsztein, D. C., Leggo, J., Coles, R., Almqvist, E., Biancalana, V., Cassiman, J. J., & Hayden, M. R. (1996). Phenotypic characterization of individuals with 30–40 CAG repeats in the Huntington disease (HD) gene reveals HD cases with 36 repeats and apparently normal elderly individuals with 36–39 repeats. *American journal of human genetics*, *59*(1), 16.
13. Sathasivam, K., Amaechi, I., Mangiarini, L., & Bates, G. (1997). Identification of an HD patient with a (CAG) 180 repeat expansion and the propagation of highly expanded CAG repeats in lambda phage. *Human genetics*, *99*(5), 692-695.
14. Wells, R. D. (1996). Molecular Basis of Genetic Instability of Triplet Repeats (∗). *Journal of Biological Chemistry*, *271*(6), 2875-2878.
15. Santhana Mariappan, S. V., Silks III, L. A., Chen, X., Springer, P. A., Wu, R., Moyzis, R. K., & Gupta, G. (1998). Solution structures of the Huntington's disease DNA triplets,(CAG) n. *Journal of Biomolecular Structure and Dynamics*, *15*(4), 723-744.

16. Duyao, M., Ambrose, C., Myers, R., Novelletto, A., Persichetti, F., Frontali, M., & MacDonald, M. (1993). Trinucleotide repeat length instability and age of onset in Huntington's disease. *Nature genetics*, *4*(4), 387-392.
17. Trottier, Y., Lutz, Y., Stevanin, G., Imbert, G., Devys, D., Cancel, G., ... & Mandel, J. L. (1995). Polyglutamine expansion as a pathological epitope in Huntington's disease and four dominant cerebellar ataxias. *Nature*, *378*(6555), 403-406.
18. Ikeda, H., Yamaguchi, M., Sugai, S., Aze, Y., Narumiya, S., & Kakizuka, A. (1996). Expanded polyglutamine in the Machado–Joseph disease protein induces cell death in vitro and in vivo. *Nature genetics*, *13*(2), 196-202.
19. Bates, G. P., Mangiarini, L., Mahal, A., & Davies, S. W. (1997). Transgenic models of Huntington's disease. *Human molecular genetics*, *6*(10), 1633-1637.
20. Reddy, P. S., & Housman, D. E. (1997). The complex pathology of trinucleotide repeats. *Current opinion in cell biology*, *9*(3), 364-372.
21. David, G., Abbas, N., Stevanin, G., Dürr, A., Yvert, G., Cancel, G., ... & Brice, A. (1997). Cloning of the SCA7 gene reveals a highly unstable CAG repeat expansion. *Nature genetics*, *17*(1), 65-70.
22. Davies SW, Beardsall K, Turmaine M, DiFiglia M, Aronin N, Bates GP (1998): Are neuronal intranuclear inclusions the common neuropathology of triplet-repeat disorders with polyglutaminerepeat expansions? Lancet 351:131–132.
23. Arning, L., & Nguyen, H. P. (2022). Huntington disease update.
24. Rawlins, M. D., Wexler, N. S., Wexler, A. R., Tabrizi, S. J., Douglas, I., Evans, S. J., & Smeeth, L. (2016). The prevalence of Huntington's disease. *Neuroepidemiology*, *46*(2), 144-153.

25. Pringsheim, T., Wiltshire, K., Day, L., Dykeman, J., Steeves, T., & Jette, N. (2012). The incidence and prevalence of Huntington's disease: a systematic review and meta-analysis. *Movement Disorders*, *27*(9), 1083-1091.

26. Galts, C. P., Bettio, L. E., Jewett, D. C., Yang, C. C., Brocardo, P. S., Rodrigues, A. L. S., & Gil-Mohapel, J. (2019). Depression in neurodegenerative diseases: Common mechanisms and current treatment options. *Neuroscience & Biobehavioral Reviews*, *102*, 56-84.

27. Dorsey, E. R., Beck, C. A., Darwin, K., Nichols, P., Brocht, A. F., Biglan, K. M., & Huntington Study Group COHORT Investigators. (2013). Natural history of Huntington disease. *JAMA neurology*, *70*(12), 1520-1530.

28. Lanska, D. J., Lavine, L., Lanska, M. J., & Schoenberg, B. S. (1988). Huntington's disease mortality in the United States. *Neurology*, *38*(5), 769-769.

29. Lee, J. M., Wheeler, V. C., Chao, M. J., Vonsattel, J. P. G., Pinto, R. M., Lucente, D., & Myers, R. H. (2015). Identification of genetic factors that modify clinical onset of Huntington's disease. *Cell*, *162*(3), 516-526.

30. Kay, C., Collins, J. A., Wright, G. E., Baine, F., Miedzybrodzka, Z., Aminkeng, F., & Hayden, M. R. (2018). The molecular epidemiology of Huntington disease is related to intermediate allele frequency and haplotype in the general population. *American Journal of Medical Genetics Part B: Neuropsychiatric Genetics*, *177*(3), 346-357.

31. Rawlins, M. D., Wexler, N. S., Wexler, A. R., Tabrizi, S. J., Douglas, I., Evans, S. J., & Smeeth, L. (2016). Neuroepidemiology. *The prevalence of Huntington's disease*, *46*, 144-153.

32. Fisher, E. R., & Hayden, M. R. (2014). Multisource ascertainment of Huntington disease in Canada: prevalence and population at risk. *Movement Disorders*, *29*(1), 105-114.

33. Ochaba, J., Lukacsovich, T., Csikos, G., Zheng, S., Margulis, J., Salazar, L., & Steffan, J. S. (2014). Potential function for the Huntingtin protein as a scaffold for selective autophagy. *Proceedings of the National Academy of Sciences*, *111*(47), 16889-16894.
34. Liu, J. P., & Zeitlin, S. O. (2017). Is huntingtin dispensable in the adult brain?. *Journal of Huntington's disease*, *6*(1), 1-17.
35. Semaka, A., Kay, C., Doty, C., Collins, J. A., Bijlsma, E. K., Richards, F., & Hayden, M. R. (2013). CAG size-specific risk estimates for intermediate allele repeat instability in Huntington disease. *Journal of Medical Genetics*, *50*(10), 696-703.
36. Aziz, N. A., Jurgens, C. K., Landwehrmeyer, G. B., Van Roon-Mom, W. M. C., Van Ommen, G. J. B., Stijnen, T., & EHDN Registry Study Group. (2009). Normal and mutant HTT interact to affect clinical severity and progression in Huntington disease. *Neurology*, *73*(16), 1280-1285.
37. Arning, L., Kraus, P. H., Valentin, S., Saft, C., Andrich, J., & Epplen, J. T. (2005). NR2A and NR2B receptor gene variations modify age at onset in Huntington disease. *Neurogenetics*, *6*(1), 25-28.
38. Wexler, N. S., Lorimer, J., Porter, J., Gomez, F., Moskowitz, C., Shackell, E., & Landwehrmeyer, B. (2004). US-Venezuela Collaborative Research Project. Venezuelan kindreds reveal that genetic and environmental factors modulate Huntington's disease age of onset. *Proc Natl Acad Sci USA*, *101*(10), 3498-3503.
39. Rüb, U., Seidel, K., Heinsen, H., Vonsattel, J. P., Den Dunnen, W. F., & Korf, H. W. (2016). H untington's disease (HD): The Neuropathology of a Multisystem Neurodegenerative Disorder of the Human Brain. *Brain Pathology*, *26*(6), 726-740.
40. Papoutsi, M., Labuschagne, I., Tabrizi, S. J., & Stout, J. C. (2014). The cognitive burden in Huntington's disease: pathology, phenotype, and mechanisms of compensation. *Movement Disorders*, *29*(5), 673-683.

41. Rüb, U., Hentschel, M., Stratmann, K., Brunt, E., Heinsen, H., Seidel, K., & den Dunnen, W. (2014). H untington's D isease (HD): Degeneration of Select Nuclei, Widespread Occurrence of Neuronal Nuclear and Axonal Inclusions in the Brainstem. *Brain pathology*, *24*(3), 247-260.
42. Kim, A., Lalonde, K., Truesdell, A., Gomes Welter, P., Brocardo, P. S., Rosenstock, T. R., & Gil-Mohapel, J. (2021). New avenues for the treatment of Huntington's disease. *International Journal of Molecular Sciences*, *22*(16), 8363.
43. Kanazawa, I. (2006). Therapeutic strategies in Huntington's disease. *Journal of Clinical Neurology*, *2*(4), 213-224.
44. O'Suilleabhain, P., & Dewey Jr, R. B. (2003). A randomized trial of amantadine in Huntington disease. *Archives of neurology*, *60*(7), 996-998.
45. Puri, B. K., Leavitt, B. R., Hayden, M. R., Ross, C. A., Rosenblatt, A., Greenamyre, J. T., ... & Murck, H. (2005). Ethyl-EPA in Huntington disease: a double-blind, randomized, placebo-controlled trial. *Neurology*, *65*(2), 286-292.
46. Narabayashi, H. (1973). Experience with stereotactic surgery on choreic movements with some physiological interpretations. *Advances in neurology*, *1*, 789-793.
47. Kazantsev, A., Walker, H. A., Slepko, N., Bear, J. E., Preisinger, E., Steffan, J. S., ... & Thompson, L. M. (2002). A bivalent Huntingtin binding peptide suppresses polyglutamine aggregation and pathogenesis in Drosophila. *Nature genetics*, *30*(4), 367-376.
48. Nagai, Y., Tucker, T., Ren, H., Kenan, D. J., Henderson, B. S., Keene, J. D., ... & Burke, J. R. (2000). Inhibition of polyglutamine protein aggregation and cell death by novel peptides identified by phage display screening. *Journal of Biological Chemistry*, *275*(14), 10437-10442.

49. Nagai, Y., Fujikake, N., Ohno, K., Higashiyama, H., Popiel, H. A., Rahadian, J., ... & Toda, T. (2003). Prevention of polyglutamine oligomerization and neurodegeneration by the peptide inhibitor QBP1 in Drosophila. *Human molecular genetics*, *12*(11), 1253-1259.

50. Derossi, D., Joliot, A. H., Chassaing, G., & Prochiantz, A. (1994). The third helix of the Antennapedia homeodomain translocates through biological membranes. *Journal of Biological Chemistry*, *269*(14), 10444-10450.

51. Khafagy, E. S., & Morishita, M. (2012). Oral biodrug delivery using cell-penetrating peptide. *Advanced drug delivery reviews*, *64*(6), 531-539.

52. Popiel, H. A., Nagai, Y., Fujikake, N., & Toda, T. (2007). Protein transduction domain-mediated delivery of QBP1 suppresses polyglutamine-induced neurodegeneration in vivo. *Molecular Therapy*, *15*(2), 303-309.

53. Popiel, H. A., Nagai, Y., Fujikake, N., & Toda, T. (2009). Delivery of the aggregate inhibitor peptide QBP1 into the mouse brain using PTDs and its therapeutic effect on polyglutamine disease mice. *Neuroscience letters*, *449*(2), 87-92.

54. Aharony, I., Ehrnhoefer, D. E., Shruster, A., Qiu, X., Franciosi, S., Hayden, M. R., & Offen, D. (2015). A Huntingtin-based peptide inhibitor of caspase-6 provides protection from mutant Huntingtin-induced motor and behavioral deficits. *Human molecular genetics*, *24*(9), 2604-2614.

55. Dietz, H. (1998). Polishing the cutting edge of gems. *Nature genetics*, *20*(4), 321-322.

56. Heiser, V., Scherzinger, E., Boeddrich, A., Nordhoff, E., Lurz, R., Schugardt, N., ... & Wanker, E. E. (2000). Inhibition of huntingtin fibrillogenesis by specific antibodies and small molecules: implications for Huntington's disease therapy. *Proceedings of the National Academy of Sciences*, *97*(12), 6739-6744.

57. Baig, M. H., Ahmad, K., Saeed, M., Alharbi, A. M., Barreto, G. E., Ashraf, G. M., & Choi, I. (2018). Peptide based therapeutics and their use for the treatment of neurodegenerative and other diseases. *Biomedicine & Pharmacotherapy*, *103*, 574-581.

58. Yadav, A., Pandey, D., & Ashraf, G. M. (2021). Peptide Based Therapy for Neurological Disorders. *Current Protein and Peptide Science*, *22*(9), 656-665.

59. Schellenberg, G. D. (1995). Genetic dissection of Alzheimer disease, a heterogeneous disorder. *Proceedings of the National Academy of Sciences*, *92*(19), 8552-8559.

60. Pike, C. J., Burdick, D., Walencewicz, A. J., Glabe, C. G., & Cotman, C. W. (1993). Neurodegeneration induced by beta-amyloid peptides in vitro: the role of peptide assembly state. *Journal of Neuroscience*, *13*(4), 1676-1687.

61. Jarrett, J. T., & Lansbury Jr, P. T. (1993). Seeding "one-dimensional crystallization" of amyloid: a pathogenic mechanism in Alzheimer's disease and scrapie?. *Cell*, *73*(6), 1055-1058.

62. Blow, D. M., Chayen, N. E., Lloyd, L. F., & Saridakis, E. (1994). Control of nucleation of protein crystals. *Protein Science*, *3*(10), 1638-1643.

63. Eaton, W. A., & Hofrichter, J. (1995). The biophysics of sickle cell hydroxyurea therapy. *Science*, *268*(5214), 1142-1143.

64. Scherzinger, E., Sittler, A., Schweiger, K., Heiser, V., Lurz, R., Hasenbank, R., ... & Wanker, E. E. (1999). Self-assembly of polyglutamine-containing huntingtin fragments into amyloid-like fibrils: implications for Huntington's disease pathology. *Proceedings of the National Academy of Sciences*, *96*(8), 4604-4609.

65. Zhong, C., Gurry, T., Cheng, A. *et al.* Strong underwater adhesives made by self-assembling multi-protein nanofibres. *Nature Nanotech* **9**, 858–866 (2014).

66. rid, P., Anisimov, S. V., & Popovic, N. (2006, September 7). *Congo red and protein aggregation in Neurodegenerative Diseases*. Brain Research Reviews.

67. Eberhard Scherzinger, Rudi Lurz, Mark Turmaine, Laura Mangiarini, Birgit Hollenbach, Renate Hasenbank, Gillian P Bates, Stephen W Davies, Hans Lehrach, Erich E Wanker,Huntingtin-Encoded Polyglutamine Expansions Form Amyloid-like Protein Aggregates In Vitro and In Vivo,Cell,Volume 90, Issue 3,1997,Pages 549-558

68. Xi, W., Wang, X., Laue, T. M., & Denis, C. L. (2016). Multiple discrete soluble aggregates influence polyglutamine toxicity in a Huntington's disease model system. *Scientific reports*, *6*, 34916. https://doi.org/10.1038/srep34916

69. Barbaro, Brett A et al. "Comparative study of naturally occurring huntingtin fragments in Drosophila points to exon 1 as the most pathogenic species in Huntington's disease." *Human molecular genetics* vol. 24,4 (2015): 913-25. doi:10.1093/hmg/ddu504

70. Arribat, Y., Talmat-Amar, Y., Paucard, A. *et al.* Systemic delivery of P42 peptide: a new weapon to fight Huntington's disease. *acta neuropathol commun* **2**, 86 (2014). https://doi.org/10.1186/s40478-014-0086-

71. Busch, Anne et al. "Mutant huntingtin promotes the fibrillogenesis of wild-type huntingtin: a potential mechanism for loss of huntingtin function in Huntington's disease." *The Journal of biological chemistry* vol. 278,42 (2003): 41452-61. doi:10.1074/jbc.M303354200

72. Kazantsev, Aleksey et al. "A bivalent Huntingtin binding peptide suppresses polyglutamine aggregation and pathogenesis in Drosophila." *Nature genetics* vol. 30,4 (2002): 367-76. doi:10.1038/ng864

73. Popiel, H Akiko et al. “Inhibition of protein misfolding/aggregation using polyglutamine binding peptide QBP1 as a therapy for the polyglutamine diseases.” *Neurotherapeutics : the journal of the American Society for Experimental NeuroTherapeutics* vol. 10,3 (2013): 440-6. doi:10.1007/s13311-013-0184-7

74. Özçelik, Cemile Elif. “Peptide Drug Candidates for Pathogenic Amyloids.” *BUIR Home*, Bilkent University, 24 Jan. 2020, repository.bilkent.edu.tr/handle/11693/52847.

75. Popiel HA, Nagai Y, Fujikake N, Toda T. Protein transduction domain-mediated delivery of QBP1 suppresses polyglutamine-induced neurodegeneration in vivo. *Mol Ther J Am Soc Gene Ther.* 2007;**15**:303–309. doi: 10.1038/sj.mt.6300045.

76. Popiel HA, Nagai Y, Fujikake N, Toda T. Protein transduction domain-mediated delivery of QBP1 suppresses polyglutamine-induced neurodegeneration in vivo. *Mol Ther J Am Soc Gene Ther.* 2007;**15**:303–309. doi: 10.1038/sj.mt.6300045.

Appendix A

Maps of plasmids used for the expression of Htt proteins

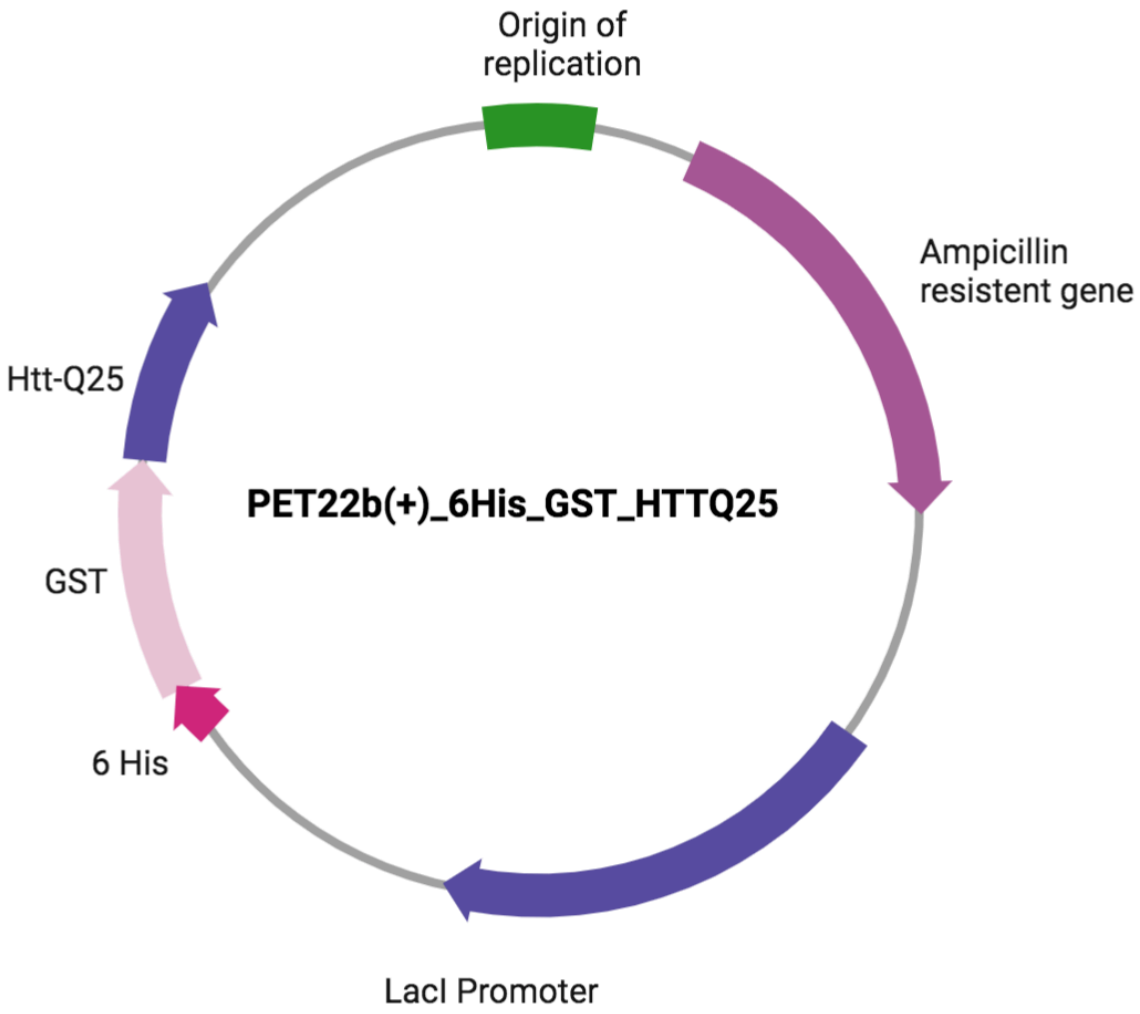

Figure A.1: Plasmid map of PET22b(+) vector with GST-Htt(Q25) construct

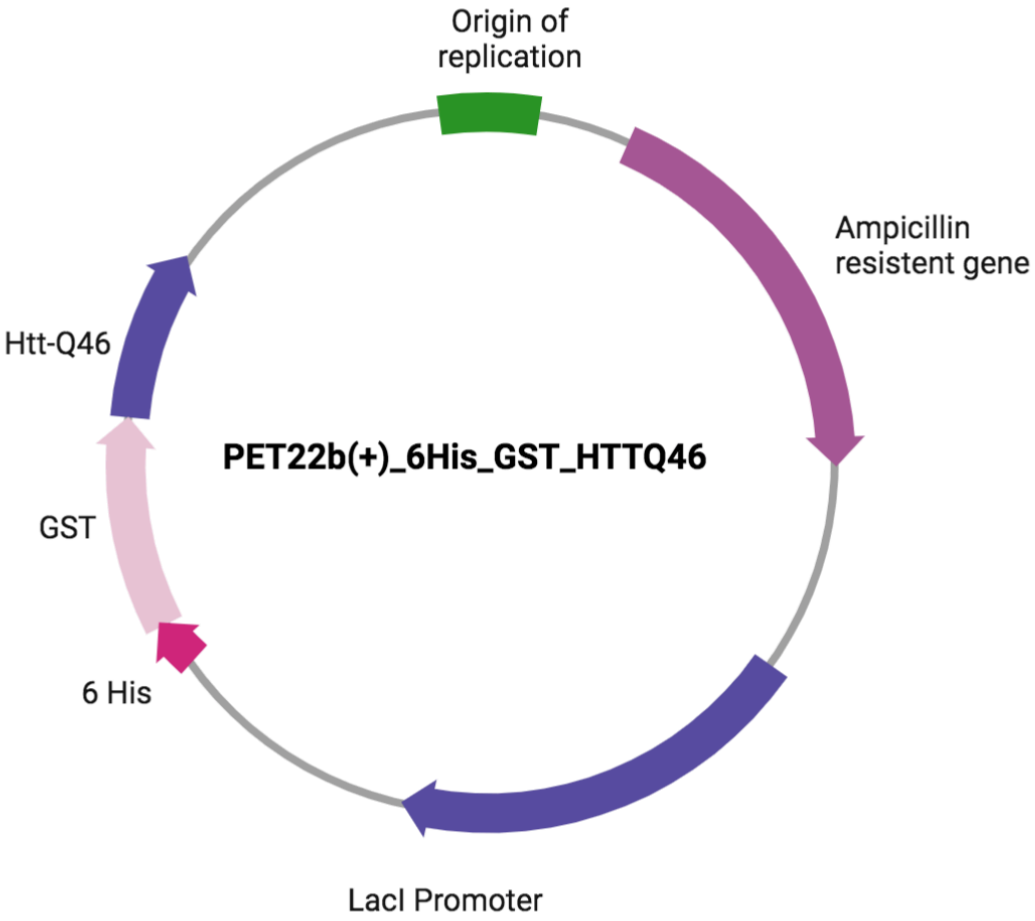

Figure A.2: Plasmid map of PET22b(+) vector with GST-Htt(Q46) construct

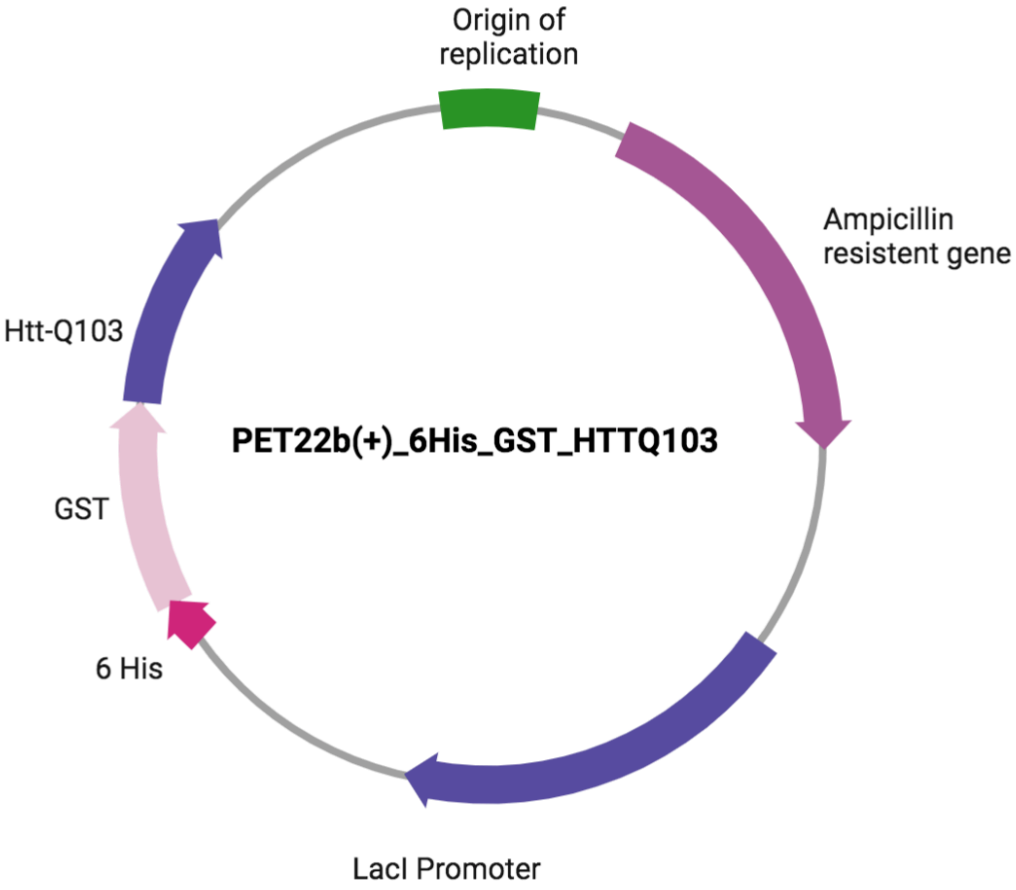

Figure A.3: Plasmid map of PET22b(+) vector with GST-Htt(Q103) construct

Appendex B

DNA segment of Htt and peptide alignment

Peptide alignment results

25Q Htt
AGGTCGGTGCAGAGGCTCCTCAGCCACAGCTGGGCCTGGAGGAGGTGGAGGTGGAGGT
GGAGGAGGTTGTGGCTGAGGCAGCAGAGGCTGTGCCTGTGGAGGAGGTTGAGGAAGTT
GAGGAGGTGGGGGTGGAGGGGGAGGTGGTGGCGGTTGTTGCTGTTGCTGCTGTTGTTGC
TGTTGCTGCTGTTGTTGCTGTTGCTGCTGTTGTTGCTGTTGCTGCTGTTGGAAGCTTTTGAG
GGACTCGAAGGCCTTCATCAGCTTTTCCAGGGTCGCCAT

Peptide 1:
WMFPSLKLLDYH
Peptide 1 Codon optimised:
TGGATGTTCCCTAGCCTGAAGCTCCTTGACTACCAC

> No significant similarity found

Peptide 2:
HSWLGEVLVQNT
Peptide 2 Codon optimised:
CACAGCTGGCTGGGCGAGGTGCTCGTCCAGAACACC

> No significant similarity found

Peptide 3:
HVTFKFQWDRES
Peptide 3 Codon optimised:
CACGTGACCTTTAAGTTCCAGTGGGACAGAGAGAGC

> No significant similarity found

Peptide 4:
TITSSGERVSFM
Peptide 4 Codon optimised:
ACAATCACCTCCTCTGGCGAGAGGGTGAGCTTCATG

> No significant similarity found

Peptide 5:
LQTHSITYRHER
Peptide 5 Codon optimised:
CTGCAGACCCACAGCATCACATACAGGCATGAGAGA

> No significant similarity found

46Q Htt
AGGTCGGTGCAGAGGCTCCTCAGCCACAGCTGGGCCTGGAGGAGGTGGAGGTGGAGGT
GGAGGAGGTTGTGGCTGAGGCAGCAGAGGCTGTGCCTGTGGAGGAGGTTGAGGAAGTT
GAGGAGGTGGGGGTGGAGGGGGAGGTGGTGGCGGTTGTTGCTGTTGCTGCTGTTGTTGC
TGTTGCTGCTGTTGTTGCTGTTGCTGCTGTTGTTGCTGTTGCTGCTGTTGCTGCTGTTGTTG
CTGTTGCTGCTGTTGTTGCTGTTGCTGCTGTTGTTGCTGTTGCTGCTGTTGGAAGCTTTTGA
GGGACTCGAAGGCCTTCATCAGCTTTTCCAGGGTCGCCAT

Peptide 1:
NHHYTYHQYTVG
Peptide 1 Codon optimised:
AACCACCATTACACCTACCACCAGTATACAGTGGGC

> No significant similarity found

Peptide 2:
APTTWFNSDSIT
Peptide 2 Codon optimised:
GCCCCTACTACCTGGTTCAACTCCGACAGCATCACA

> No significant similarity found

Peptide 3:
DMHGRYMMTTRE
Peptide 3 Codon optimised:
GACATGCACGGCAGATACATGATGACCACAAGGGAG

> No significant similarity found

Peptide 4:
FKQDAWEAVDIR
Peptide 4 Codon optimised:
TTCAAGCAGGACGCCTGGGAGGCTGTGGATATCAGG

> No significant similarity found

Peptide 5:
HGLHSMHNKLQD
Peptide 5 Codon optimised:
CACGGCCTCCATAGCATGCACAACAAGCTGCAGGAC

> No significant similarity found

103Q Htt
AGGTCGGTGCAGAGGCTCCTCAGCCACAGCTGGGCCTGGAGGAGGTGGAGGTGGAGGT
GGAGGAGGTTGTGGCTGAGGCAGCAGAGGCTGTGCCTGTGGAGGAGGTTGAGGAAGTT
GAGGAGGTGGGGGTGGAGGGGGAGGTGGTGGCGGTTGTTGCTGTTGCTGCTGTTGTTGC
TGTTGCTGCTGTTGTTGCTGTTGCTGCTGTTGTTGCTGTTGCTGCTGTTGCTGCTGTTGTTG
CTGTTGCTGCTGTTGTTGCTGTTGCTGCTGTTGTTGCTGTTGCTGCTGTTGGAAGCTTTTGA
GGGACTCGAAGGCCTTCATCAGCTTTTCCAGGGTCGCCAT

Peptide 1:
WDMWPSMDWKAE
Peptide 1 codon optimised:
TGGGATATGTGGCCTAGCATGGACTGGAAGGCCGAG

> No significant similarity found

Peptide 2:
KVWELDRYYASH
Peptide 2 codon optimised:
AAGGTGTGGGAGCTGGACAGGTACTATGCCAGCCAC

> No significant similarity found

Peptide 3:
HHGANSLGLVQSs
Peptide 3 codon optimised:
CACCATGGAGCCAACAGCCTCGGCCTGGTGCAGTCC

> No significant similarity found

Peptide 4:
SLELKRSDVQHA
Peptide 4 codon optimised:
AGCCTGGAGCTCAAGAGATCCGACGTGCAGCACGCC

> No significant similarity found

Peptide 5:
SWPLTPVRFMTE
Peptide 5 codon optimised:
AGCTGGCCCCTGACACCTGTGAGATTCATGACCGAG

> No significant similarity found

Appendex C

Buffers AND Media

LB

Lysogeny Broth media (LB)	**1 Litre**
Tryptone	**10g**
Yeast Exctract	**5g**
NaCl	**5g**

Table C1

Autoinduction ZYM5052

ZYM5052 (Autoinduction media)	**1L**
Yeast Extract	**5g**
Monopotassium Phosphate (KH2PO4)	**3,4g**
Disodium Phosphate (Na2HPO4)	**3,5g**
Ammonium Chloride (NH4Cl)	**2,67g**
Magnesium Sulfate Heptahydrate (MgSO4x7H2O)	**0,49g**
Sodium Sulfate (Na2SO4)	**0,71g**
Glucose Monohydrate	**0,5g**
Glycerol	**5ml**

Lactose	**2g**
Trace Metals (50.000x)	**20ul**

Table C2

BUFFERS FOR PROTEIN PURIFICATION

10 mM Imidazole (pH 7.4) binding buffer for Hispur Cobalt resin.

50mM Sodium Phosphate
300mM NaCl
10mM Imidazole

150 mM Imidazole (pH 7.4) elution buffer for HisPur Cobalt Resin.

50mM Sodium Phosphate
300mM NaCl
150mM Imidazole

Table C3 Binding and elution buffer for HisPur Cobalt resin

20mM Imidazole (pH 7.4) binding buffer for Ni-NTA column.

20mM Sodium Phosphate
0.5M NaCl
10mM Imidazole

500 mM Imidazole (pH 7.4) elution buffer Ni-NTA column.

20mM Sodium Phosphate
0.5M NaCl
150mM Imidazole

Table C4 Table C3 Binding and elution buffer for Histag Ni-NTA column

TEV REACTION BUFFER

50 mM Tris-HCl (pH 8.0
0.5 mM EDTA
1mM DTT

Table C5. Tev reaction buffer

Appendex D

Tht concentration optmisation with Htt Q103

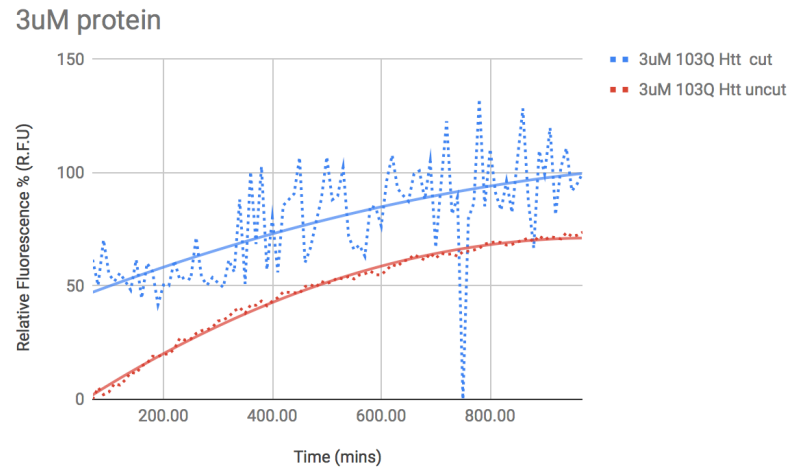

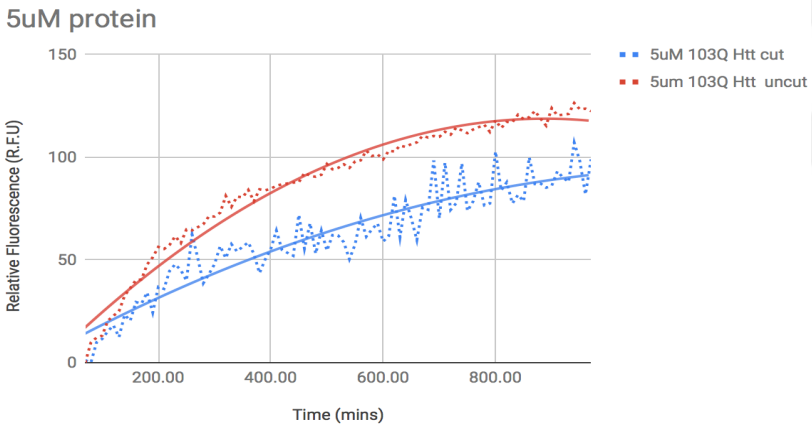

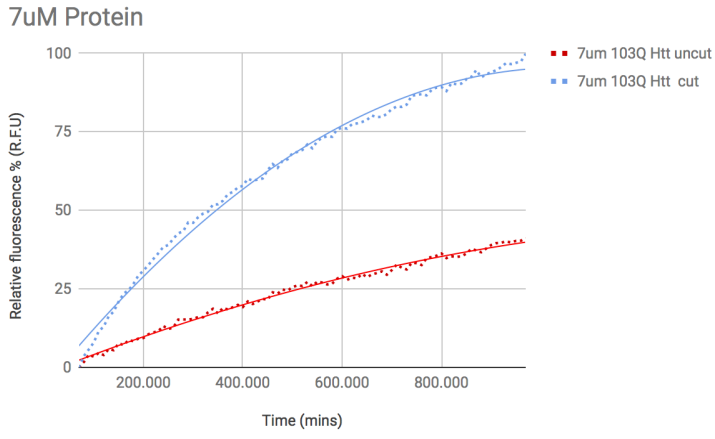

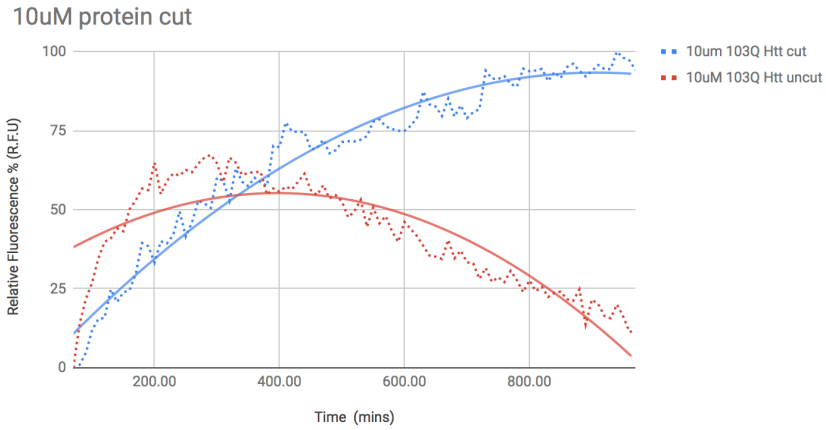
10uM protein cut
100
75
50
25
0
Relative Fluorescence % (R.F.U)
200.00
400.00
600.00
800.00
Time (mins)
10um 103Q Htt cut
10uM 103Q Htt uncut

Appendex E

AFM concentration optmisation for HttQ46

46Qhtt – 2uM protein (18hours)

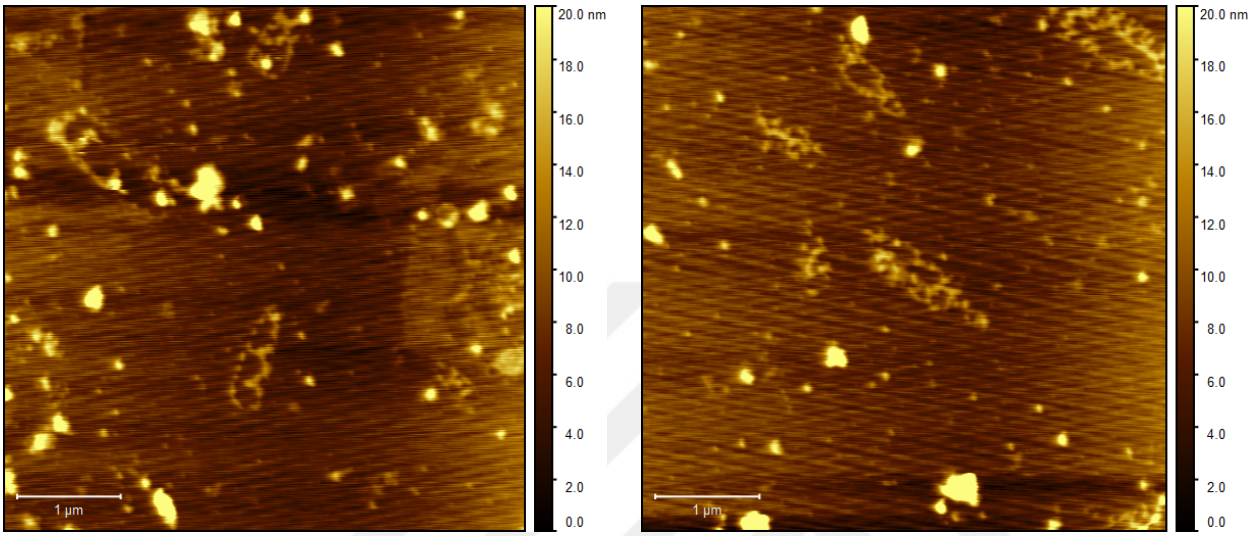

46Qhtt – 10uM protein (18hours)

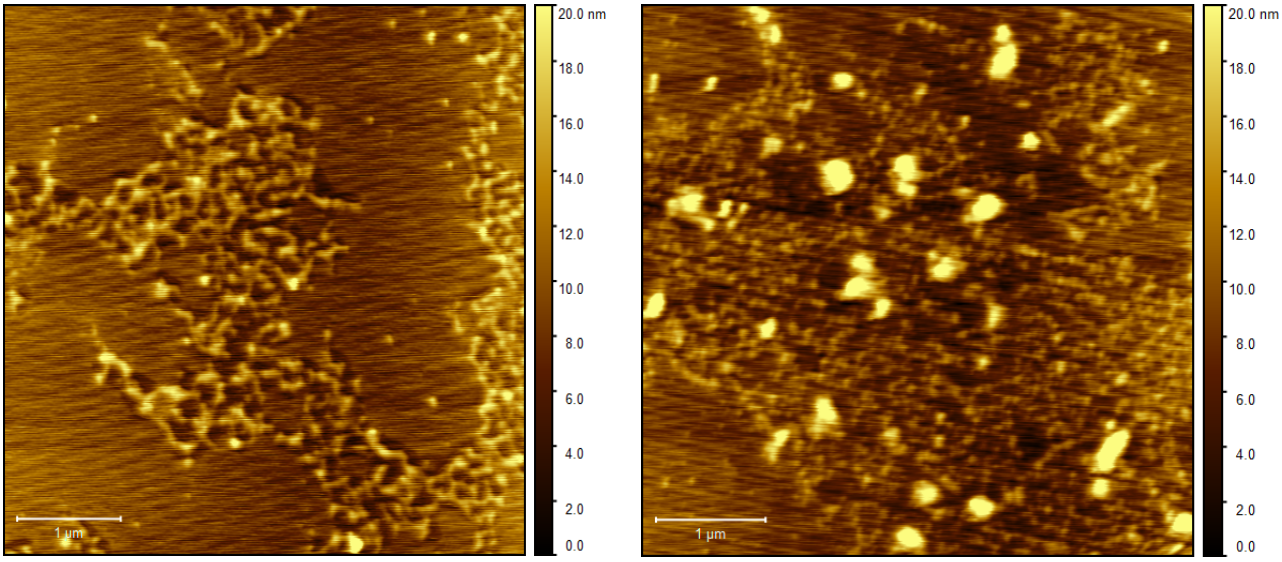

46Qhtt – 30uM protein (18hours)